Transcriptome analysis of islets from diabetes-resistant and diabetes-prone obese mice reveals novel gene regulatory networks involved in beta cell compensation and failure.

Short/running title: **Transcriptomic changes in islets during obesity**

Jeng Yie Chan[1,2,6], Mohammed Bensellam[1,3,6], Ruby C. Y. Lin[2,4,5,6], Cassandra Liang[1], Kailun Lee[1], Jean-Christophe Jonas[3] and D. Ross Laybutt[1,2]

[1]Garvan Institute of Medical Research, Sydney, NSW, Australia

[2]School of Medical Sciences, University of New South Wales, NSW, Australia

[3]Université catholique de Louvain, Institut de recherche expérimentale et clinique, Pôle d'endocrinologie, diabète et nutrition, Brussels, Belgium

[4]Centre for Infectious Diseases and Microbiology, Westmead Institute for Medical Research, Sydney, Australia

[5]Sydney Medical School, The University of Sydney, NSW, Australia

[6]Jeng Yie Chan, Mohammed Bensellam and Ruby C. Y. Lin contributed equally to this work

Corresponding author:

D. Ross Laybutt

Garvan Institute of Medical Research

384 Victoria St, Darlinghurst, NSW 2010, Australia.

Tel: 61-2-9295-8228; Fax: 61-2-9295-8201

Email: r.laybutt@garvan.org.au

Abbreviations

AA: Amino acid. DE: Differentially expressed. ELISA: Enzyme-linked immunosorbent assay. ER: Endoplasmic reticulum. FA. Fatty acid. FDR: False discovery rate. GPCR: G protein-coupled receptor. GPL: Glycerophospholipid. GO: Gene ontology. GSEA: Gene set enrichment analysis. GSIS: Glucose-stimulated insulin secretion. HCL: Hierarchical clustering analysis. HTRF: Homogeneous time resolved fluorescence. KEGG: Kyoto encyclopedia of genes and genomes. KO: Knockout. MHC: Major histocompatibility. MODY: Maturity-onset diabetes of the young. PCA: Principal component analysis. PDI: Protein disulfide isomerase. ROS: Reactive oxygen species. siRNA: Small-interfering RNA. SLR: Signal log ratio. SREBP: Sterol regulatory element binding protein. T2D: Type 2 diabetes. TG: Triglyceride. UPR: Unfolded protein response. ZDF: Zucker diabetic fatty.

Abstract

The mechanisms underpinning beta cell compensation for obesity-associated insulin resistance and beta cell failure in type 2 diabetes remain poorly understood. We used a large-scale strategy to determine the time-dependent transcriptomic changes in islets of diabetes-prone *db/db* and diabetes-resistant *ob/ob* mice at 6 and 16 weeks of age. Differentially expressed genes were subjected to cluster, gene ontology, pathway and gene set enrichment analyses. A distinctive gene expression pattern was observed in 16 wk *db/db* islets in comparison to the other groups with alterations in transcriptional regulators of islet cell identity, upregulation of glucose/lipid metabolism and various stress response genes, and downregulation of specific amino acid transport and metabolism genes. In contrast, *ob/ob* islets displayed a coordinated downregulation of metabolic and stress response genes at 6 weeks of age, suggestive of a preemptive reconfiguration in these islets to lower the threshold of metabolic activation in response to increased insulin demand thereby preserving beta cell function and preventing cellular stress. In addition, amino acid transport and metabolism genes were upregulated in *ob/ob* islets, suggesting an important role of glutamate metabolism in beta cell compensation. Gene set enrichment analysis of differentially expressed genes identified enrichment of binding motifs for transcription factors, FOXO4, NFATC1 and MAZ. siRNA-mediated knockdown of these genes in MIN6 cells altered cell death, insulin secretion and stress gene expression. In conclusion, these data revealed novel gene regulatory networks involved in beta cell compensation and failure. Preemptive metabolic reconfiguration in diabetes-resistant islets may dampen metabolic activation and cellular stress during obesity.

Keywords: Beta cell compensation; Beta cell failure; Type 2 diabetes; Islets; Obesity

1. Introduction

The failure of pancreatic beta cells to adequately adapt to increased insulin demand is fundamental to the development of type 2 diabetes (T2D). Normally, an adaptation in beta cell mass and secretion maintains normoglycemia in the face of the increased demand imposed by insulin resistance and obesity. In susceptible individuals, the failure to sustain this process results in the development of T2D [1-3]. However, the underlying mechanisms that are responsible for the progression from successful beta cell compensation to beta cell failure remain poorly understood.

Obese mice with opposite propensity for the development of diabetes offer valuable models to interrogate these mechanisms [4-6]. The *ob/ob* and *db/db* mouse models of deficient leptin signaling display hyperphagia, obesity and insulin resistance. However, while *ob*/*ob* mice on the C57BL/6J genetic background are resistant to diabetes development owing to robust beta cells and sustained insulin secretion, *db*/*db* mice on the C57BL/KsJ genetic background display a progressive age-dependent beta cell decompensation and development of diabetes [6,7].

Our previous studies using islets from diabetes-resistant *ob/ob* and diabetes-prone *db/db* mice uncovered novel mechanisms of beta cell compensation and failure [6]. Our and others evidence suggested an important role of the adaptive unfolded protein response (UPR) in the maintenance of the beta cell differentiated phenotype and protection against gene expression alterations that accompany beta cell failure and development of diabetes [6,8,9]. However, a comprehensive large-scale strategy in these models is necessary to decipher the molecular events and signaling pathways involved in the transition from successful beta cell compensation to beta cell failure, including those involved in the modulation of the adaptive UPR.

Here, we utilized genome-wide Affymetrix Microarrays to determine the changes in the islet transcriptomic landscape that mediate the processes of beta cell compensation and failure in *ob/ob* and *db/db* mice [6]. The findings could be exploited to inform therapeutic interventions aimed at restoring functional beta cell mass in T2D.

2. Methods

2.1. Mice

Male C57BL/KsJ *db/db* and C57BL/6J *ob/ob* mice, and their age-matched lean control mice (C57BL/KsJ or C57BL/6J, respectively) were taken from the Garvan Institute breeding colonies. Animals were kept under conventional conditions with free access to a standard chow diet and water. All procedures were approved by the Garvan Institute/St.Vincent's Hospital Animal Experimentation Ethics Committee, following guidelines issued by the National Health and Medical Research Council of Australia. Whole islets were isolated from *db/db* and *ob/ob* mice, and their age-matched lean control mice at 6 and 16 weeks of age for RNA extraction as previously described [6]. The metabolic characteristics of these mouse models were previously described [6].

2.2. Transcriptome analysis

Total RNA was interrogated using Affymetrix MoGene 2.0/2.1 ST v1.0 gene arrays according to manufacturer's instructions (Ramaciotti Centre for Genomics, UNSW Sydney, Australia) on the following groups: 6 wk C57BL/KsJ control (n=2) and *db/db* (n=2), 16 wk C57BL/KsJ control (n=3) and *db/db* (n=3), 6 wk C57BL/6J control (n=2) and *ob/ob* (n=2) and 16 wk C57BL/6J control (n=2) and *ob/ob* (n=2). Interrogating probes were imported and normalised using RMA algorithm and RMA background corrected (Partek Genome Suite v6.151022). Quantile normalisation was used and median polish was used for probeset summarisation in log 2 space. Batch difference was considered. Changes in gene expression in 6 wk *db/db*, 16 wk *db/db*, 6 wk *ob/ob* and 16 wk *ob/ob* mice were quantitated as fold change of their respective age-matched control mice. Principal component analysis (PCA) was used to examine the overall gene expression changes for each genotype (Figure 1A). One way ANOVA for the effect of age and strain (6 wk *db/db* vs 16 wk

db/db, 6 wk *ob/ob* vs 16 wk *ob/ob*, 16 wk *db/db* vs 16 wk *ob/ob*, 6 wk *db/db* vs 6 wk *ob/ob*) was carried out where at unadjusted $P < 0.05$, genes were considered differentially expressed (DE). Post-hoc analysis i.e., False discovery rate (FDR) based on Benjamini-Hochberg was considered. Hierarchical clustering analysis (HCL) was carried out where expression normalisation was undertaken by shifting genes to mean of zero and scaled to standard deviation of one. Of note, visualisation of gene profiles between 6 wk *db/db* vs 16 wk *db/db*, 6 wk *ob/ob* vs 16 wk *ob/ob*, 16 wk *db/db* vs 16 wk *ob/ob*, 6 wk *db/db* vs 6 wk *ob/ob* reflected differences observed in the initial PCA survey.

DE genes were subjected to pathway and gene set enrichment analysis (GSEA) analyses to investigate an age effect as well as metabolic status i.e., diabetes vs obesity. The criteria were set for age or metabolic status respectively with 1000 permutations and we restricted analysis to functional groups with more than 15 genes as well as functional groups with fewer than 500 genes for pathway analysis. GO functional classification of DE genes was determined using DAVID database (https://david-d.ncifcrf.gov/, last accessed 20 August 2020). The generated biological process categories were manually curated to ensure correct belonging of each gene to a given category based on the available information in the databases MGI (http://www.informatics.jax.org/), OMIM (https://www.ncbi.nlm.nih.gov/omim), Uniprot (https://ebi16.uniprot.org/) and Pubmed (https://pubmed.ncbi.nlm.nih.gov/). Based on this information, they were then further subdivided into subcategories to shed light on the specific metabolic and signaling pathways affected. The different categories were presented in the form of heatmaps displaying the normalised mean signal to log ratio of each gene in the islets of 6 wk *db/db* vs. 6 wk control, 16 wk *db/db* vs. 16 wk control, 6 wk *ob/ob* vs. 6 wk control and 16 wk *ob/ob* vs. 16 wk control.

For identification of potential therapeutic targets, these DE genes were subjected to GSEA using the C3 list in the Molecular Signatures Database (MSigDB v5.1) to identify enriched transcription factor binding motifs [10,11]. Gene sets that contain genes with a cis-regulatory motif that is conserved across the human, mouse, rat and dog genomes were catalogued. The top enriched motifs identified at $P < 0.05$ (FDR adjusted) were considered significant and can be linked to a conserved putative cis-regulatory element from our transcriptome dataset. Predicted target mRNAs from these enriched transcription factor families were analysed further using Gene Ontology and Pathway enrichment to elucidate affected regulatory pathways.

2.3. Human islet single-cell RNA-seq analysis from public data

To verify the key changes in human beta cells, we used a human islet single-cell RNA-seq data set from ArrayExpress (E-MTAB-5061) [12]. We used the RPKM matrix and the cell type annotation provided to extract and visualize gene expression in beta cells and alpha cells from 6 non-diabetic donors and 4 type 2 diabetic donors.

2.4 Immunostaining

Immunostaining was performed as previously described [13] with the following antibodies: ID3, 1:50 (BCH-4/17-3, Biocheck, Foster City, CA, USA) and INSULIN, 1:1000 (I2018, Sigma-Aldrich, St Louis, MO, USA); STAT3, 1:100 (610189, BD Biosciences, San Jose, CA, USA) and INSULIN, 1:50 (ab7842, Abcam, Cambridge, MA, USA). Images were acquired using a Leica DM5500 fluorescent microscope.

2.5. Cell culture

MIN6 cells were maintained in DMEM (ThermoScientific, Carlsbad, CA, USA) containing 25 mM glucose, 10 mM HEPES, 10% FCS, 100 U/mL penicillin and 100 μg/mL streptomycin. Either 2 x 10^5 or 4 x 10^5 cells were seeded per well in a 24-well or 12-well plate, respectively. MIN6 cells were transfected with Foxo4, Nfatc1, and Maz ON-TARGETplus SMARTpool siRNA or Non-Targeting siRNA using DharmaFECT 3 (Dharmacon, Millennium Science, Mulgrave, VIC, Australia) according to the manufacturer's instruction.

2.6. Insulin secretion and cell death measurements

For insulin secretion assay, cells were incubated for 1 h at 37°C in Krebs-Ringer HEPES buffer containing 2.8 or 25 mM glucose. Insulin was measured in an aliquot of the buffer by HTRF (Cisbio, Codolet, France).

Cell death was determined with the use of a Cell Death Detection ELISA (Roche Diagnostics) [14], which measures cytoplasmic histone-associated-DNA-fragments. Cells were lysed in 0.5 mL of the supplied lysis buffer, incubated for 30 min at room temperature, and the lysate was spun at 200xg for 10 min. The ELISA assay was then performed according to manufacturers' instructions and the results were corrected for DNA content.

2.7. Quantitative PCR (qPCR)

Total RNA was extracted from cultured cells using RNeasy Mini Kit, respectively (Qiagen, Doncaster, Australia). cDNA was synthesised using the QuantiTect Reverse Transcription Kit (Qiagen, Victoria, Australia). Real-time PCR were performed on a 7900HT Real-Time PCR System (Applied Biosystems, Foster City, CA) using *Power* SYBR Green PCR Master Mix (Applied Biosystems), respectively. Primer details are provided in Supplementary Table 1. The value obtained for each specific product was normalised to control gene (cyclophilin A) as

previously described for these genes [14] and expressed as a fold-change of the value in control extracts.

3. Results and discussion

3.1. Data analysis and gene clustering

Differentially expressed (DE) genes were identified by comparing the following genotypes and ages: 6 wk *db/db* vs 6 wk *ob/ob*, 6 wk vs 16 wk *db/db*, 6 wk vs 16 wk *ob/ob* and 16 wk *db/db* vs 16 wk *ob/ob*. Using the criteria unadjusted $P < 0.05$ and fold change >2 and <-2, we identified 6887 DE genes that are significantly affected in at least one of the comparisons. PCA revealed distinctive gene expression profiles for *db/db* and *ob/ob* islets at 6 and 16 weeks of age respectively. Interestingly, 6 wk *db/db* and *ob/ob* islets displayed a similar gene expression pattern. At 16 weeks of age, *ob/ob* islets displayed a closer pattern to 6 wk *db/db* and *ob/ob* islets, while 16 wk *db/db* islets presented a completely distinctive pattern from the three other groups (Figure 1A). This finding was further confirmed and illustrated by HCL of DE genes generated from genotype comparison (Figure 1B).

DE genes in both genotypes were compared in 2 manners in Venn diagrams – disease effect: changes that occurred with time in the same genotype as compared to the other genotype (Figure 1C), or age effect: changes that occurred between genotypes at either the 6 or 16 week time point (Figure 1D). Venn diagrams indicated that most changes were related to the advanced diabetes state in 16 wk *db/db* islets.

DE genes were then subjected to functional gene (GO) and pathway analyses to gain insight into the molecular mechanisms underlying beta cell compensation and failure. It is important to note that the use of whole islets is a limitation of the model. However, the proportion of beta cells within

islets was similar in 16-week-old C57BL/6J control and *ob/ob* mice (control: 86.3 ± 1.2%; *ob/ob*: 86.3 ± 4.3%; n=3 in each group), in close alignment with findings in 16-week-old C57BL/KsJ control (86.4 ± 2.0%) and *db/db* (88.6 ± 0.9%) mice [6]. Thus, the changes in gene expression observed in islets are not due to changes in the proportion of beta cells within islets

3.2. GO and pathway analyses

3.2.1. Transcriptional regulation

Transcriptional regulators are the primary drivers of the beta cell differentiated phenotype and their dysregulation marks states of metabolic stress and altered beta cell identity [15]. Transcriptional regulation category was enriched with 192 DE genes presenting two different clusters: (1) those specifically upregulated in 16 wk *db/db* islets and unaffected or downregulated in the three other groups and (2) those specifically downregulated in 16 wk *db/db* islets and unaffected or upregulated in the three other groups (Figure 2A). A further analysis of this category revealed four major subcategories of transcriptional regulators: those involved in islet cell identity, stress regulators, epigenetic regulators and transcriptional repressors (Figure 2A). In the first subcategory, *Neurog3* (also known as *Ngn3*) and *Hnf4g* mRNA levels were the most strongly upregulated in diabetic 16 wk *db/db* islets in comparison to the other groups (Figure 2A, B). *Neurog3* is an important transcription factor that is transiently expressed in pre-endocrine progenitor cells while its expression in adult beta cells is a marker of dedifferentiation [16,17]. Conversely, the role of *Hnf4g* in beta cells is unclear. Previous evidence has shown that *Hnf4g*-KO mice displayed improved glucose tolerance. This effect has been attributed to increased expression and release of GLP-1 by enteroendocrine L-cells. *Hnf4g* deletion was also associated with increased islet size, beta cell area and islet cell proliferation [18]. However, whether this was

entirely due to the incretin effect or involved other effects of *Hnf4g* deletion on beta cells is unknown. To a lesser extent, *Maf*, *Sox4* and *Onecut2* mRNA levels were also upregulated in 16 wk *db/db* islets vs the other groups (Figure 2A). *Sox4* has previously been identified as a T2D risk gene [19] and its upregulation has been shown to impair insulin granule exocytosis [20]. Noteworthy, while the mRNA levels of three alpha cell markers *Mafb*, *Irx1* and *Irx2* were unchanged in 16 wk *db/db* islets, they were markedly downregulated in 16 wk *ob/ob* islets (Figure 2A, C). This coordinated and consistent downregulation suggests a potential change in alpha cell identity in the islets of compensating *ob/ob* mice. On the other hand, *Pax2*, *Pax3*, *Pax7*, *Onecut1* (also known as *Hnf6*) and *Ptf1a* were specifically downregulated in 16 wk *db/db* islets while upregulated, or unchanged in the other groups (Figure 2A). Paired box transcription factors are known for their important roles in lineage specification and maintenance of progenitor cells in different tissues, including the endocrine pancreas. Evidence has also revealed their role in the maintenance of maturity, proliferation and survival of adult beta and alpha cells while their mutations have been associated with diabetes [21-24]. A potential driver of these changes is islet cell identity could be metabolic stress.

Indeed, the second subcategory enclosed various stress response transcriptional regulators. Noteworthy, most of them were upregulated in 16 wk *db/db* islets in comparison to the other groups (Figure 2A). Among them, *Hif2α* (also known as *Epas1*) mRNA levels were the most strongly upregulated (Figure 2A). Upregulation of hypoxia-inducible transcription factors and downstream target genes may result from altered islet vasculature [25] and hyperglycemia-induced increase in O_2 consumption and subsequent hypoxic stress within beta cells [26-28]. *Creb3l3* was also markedly upregulated in 6 wk *db/db* islets and furthermore in 16 wk *db/db* islets while it was downregulated in 6 wk *ob/ob* islets and unchanged in 16 wk *ob/ob* islets (Figure 2A). This gene

encodes a single-pass membrane protein localized in the endoplasmic reticulum (ER) and activated by regulated intramembrane proteolysis similarly to SREBPs and ATF6 transcription factors. It has been involved in lipid and apolipoprotein metabolism, acute phase activation and ER stress [29]. In human islets, *Creb3l3* mRNA levels were upregulated by palmitate and oleate treatment, but reduced in response to chemical inducers of ER stress [30]. Besides, several transcriptional regulators were involved in proinflammatory signaling (*Elf4*, *Nfkb2*, *Bcl6*, *Stat3* and *Irf1*) and others in response to oxidative stress (*Id3*, *Tfam*, *Max*, *Myc*) (Figure 2A, D). In agreement, by immunofluorescence on histological pancreatic sections, we observed increased expression of ID3 and STAT3 in beta cells of diabetic *db/db* mice in comparison with control mice, but not in *ob/ob* mice (Supplementary Figure 1). We have previously identified inhibitor of differentiation proteins (IDs) as novel oxidative stress-responsive genes in beta cells and demonstrated that ID1 and ID3 play an important adaptive role via interaction with the NFE2L2-small MAFs antioxidant pathway [13]. However, since upregulation of IDs also negatively affects the beta cell differentiated phenotype, dedifferentiation could represent an adaptive mechanism to stress at the price of altered cell identity and function [15]. Interestingly, RNA-seq analysis of single islet cells from non-diabetic human donors revealed upregulation of *ID1* and *ID3* in beta cells exhibiting low insulin gene expression (reduced differentiation) and high UPR gene expression (higher stress) [31]. On the other hand, *Bhlha15* (also known as *Mist1*), *Trp73* and *Klf15* were downregulated in 16 wk *db/db* islets and upregulated in 16 wk *ob/ob* islets (Figure 2A). This may reflect a different type of stress in compensating *ob/ob* islets or a potential complex adaptive role of these effectors [32,33].

Besides transcription factors, selective transcriptional regulation also involves epigenetic mechanisms. Thus, several genes involved in histone posttranslational modification (*Morf4l1*, *Mysm1*, *Kdm6a*, *Cdyl2*, *Phc2*, *Msl1*, *Kdm4b*), nuclear DNA modification (*Tet1*, *Tet2*),

mitochondrial DNA modification (*Top1mt*) and DNA/RNA modification (*Mettl4*) were more highly expressed in 16 wk *db/db* islets vs the other groups (Figure 2A). Conversely, another group of genes (*Ezh2*, *Top2a*, *Npm2*, *Uhrf1*, *Kdm5d*) was specifically downregulated in 16 wk *db/db* islets and upregulated in the other groups, most notably in 16 wk *ob/ob* islets (Figure 2A, E). Interestingly, the Polycomb H3K27 methyltransferase gene *Ezh2* has previously been implicated in adaptive beta cell proliferation and restoration of beta cell mass upon injury. Its deletion was associated with reduced beta cell proliferation and mass and development of mild diabetes [34]. Besides, the DNA topoisomerase gene *Top2a* was strongly upregulated in proliferating beta cells [35]. *Uhrf1* is another key epigenetic regulator gene that has been implicated in cell cycle progression and maintenance of histone posttranslational modifications and DNA methylation [36]. Its precise role in beta cell pathophysiology is unclear but its specific expression pattern (upregulation in the compensation context and downregulation in the decompensation context; Figure 2E) implies an adaptive role. Together, these observations infer that compensatory beta cell proliferation is compromised in diabetes-prone mice.

The final subcategory of transcriptional regulators enclosed transcriptional repressors (Figure 2A). Most of these genes were specifically upregulated in 16 wk *db/db* islets vs the other groups. Among them, *Klf10* (also known as *Tieg1*) was the most upregulated gene but its role in beta cell pathophysiology is unclear. In rat islets, it was markedly upregulated by high glucose [37], while the other Kruppel-like gene family member *Klf4* was upregulated by palmitate treatment in human islets [30]. *Klf7* was unchanged in 16 wk *db/db* islets but slightly downregulated in 6 wk *db/db* and *ob/ob* islets and to a stronger extent in 16 wk *ob/ob* islets. Its overexpression in HIT-T15 cells has been shown to reduce glucose-stimulated insulin secretion (GSIS) and insulin gene expression together with other beta cell-enriched genes [38]. Moreover, polymorphisms in *Klf7* were linked

with T2D [39]. *Tle4* has been identified as a T2D risk gene [40]. It encodes a homologue of Groucho that binds to TCF transcription factors, including TCF7L2, to repress transcriptional activation by canonical Wnt signaling [41]. On the other hand, *Bcl6* has been shown to be induced by serum and glucose deprivation in MIN6 cells and to inhibit proliferation by repressing *Ccnd2* [42]. Other evidence has also proposed a complex dual adaptive anti-inflammatory/proapoptotic role of *Bcl6* in beta cells [43].

Collectively, these novel findings highlighted that in comparison to diabetes resistant mice, islets from diabetes prone mice are more sensitive to metabolic stress and activate a complex adaptive/deleterious response at the epigenetic, transcriptional activation and transcriptional repression level. These molecular changes contribute to the alteration of islet cell identity and functional beta cell mass possibly by altering various metabolic and signaling pathways.

3.2.2. Signaling

In this category, we found a strong enrichment in genes belonging to olfactory transduction, including different olfactory receptor genes (268), vomeronasal receptor genes (87) and *Omp* (Supplementary Figure 2A). In agreement, olfactory transduction was the top significantly enriched KEGG pathway when comparing 6 vs 16 wk *db/db* islets (Supplementary Table 2) and 16 wk *db/db* vs 16 wk *ob/ob* islet (Supplementary Table 3). Strikingly, most of these genes were specifically downregulated in 16 wk *db/db* islets vs the other groups. Interestingly, evidence has shown that several olfactory receptor genes are expressed in MIN6 cells and mouse islets and revealed a role of *Olfr15* in octanoic acid-mediated potentiation of GSIS [44,45]. *Olfr15* expression was also reduced in *db/db* islets and islets of mice fed a high fat diet [44]. While *Olfr15* was not differentially affected in our study, dysregulation of the other receptors may contribute to

beta cell decompensation and impaired insulin secretion in response to glucose and other nutrients/substrates. Of note, we reported a hint of olfactory transduction signaling in chronic high-fat diet and metabolic dysfunction in the islet [46], in the retroperitoneal white adipose tissue [47] and in diabetic vascular disease [48]. Further studies are needed to determine the mechanism underlying the downregulation of this pathway in diabetic islets.

Several components of the Wnt signaling pathway were upregulated in 16 wk *db/db* islets vs the other groups, except for *Wnt5b* that was upregulated in 6 and 16 wk *ob/ob* islets (Supplementary Figure 2A, B). Canonical Wnt signaling is important for pancreas development and beta cell proliferation, survival and function while its dysregulation is associated with the onset of T2D [41]. Upregulation of Wnt signaling pathway components has been reported in the islets of obese mice and human T2D donors [49-51]. Non-canonical *Wnt4*-encoded ligand may repress canonical Wnt signaling in pancreatic islets and beta cell lines [50] and upregulation of peripheral and plasma WNT4 levels has been proposed to contribute to beta cell decompensation [52]. In agreement with our findings, upregulation of non-canonical *Wnt5b* has been reported in hyperplastic islets from prediabetic mice [51]. The potential implication of *Wnt5b* in compensatory beta cell proliferation is unclear, but polymorphisms in this gene have been associated with T2D [53].

Moreover, different genes belonging to the Notch signaling pathway were also upregulated in 16 wk *db/db* islets vs the other groups (Supplementary Figure 2A). This cell-to-cell communication pathway is involved in pancreas development as well as adult beta cell homeostasis [54,55]. Among the four Notch receptor genes, *Notch3* was specifically upregulated in *db/db* islets, but not in *ob/ob* islets (Supplementary Figure 2A, C).

Another important developmental pathway that was activated in 16 wk *db/db* islets was the BMP/TGFβ pathway, including a marked upregulation of *Tgfbr2* (Supplementary Figure 2A, D). Besides developmental roles, TGFβ signaling has been shown to play both adaptive and maladaptive roles in adult beta cells [56-58].

We also found few genes involved in the circadian rhythm pathway to be upregulated in 16 wk vs 6 wk *db/db* islets. Indeed, this pathway was significantly enriched in the comparisons 6 vs 16 wk *db/db* islets (Supplementary Table 2) and 16 wk *db/db* vs 16 wk *ob/ob* islets (Supplementary Table 3). In *ob/ob* islets, *Ror2*, *Cry1* and to a lesser extent *Hif2α* were also upregulated while *Per1*, *Csnk1e* and *Nrip1* were downregulated in 16 wk *ob/ob* islets vs 16 wk *db/db* islets. In contrast, *Timeless* was markedly upregulated in 16 wk *ob/ob* islets vs 16 wk *db/db* islets (Supplementary Figure 2A). Fine-tuned circadian rhythm pathway is necessary for proper alpha and beta cell function [59,60]. Therefore, upregulation of circadian rhythm genes in 16 wk *db/db* islets is perhaps adaptive. On the other hand, the role of *Timeless* in islet biology is unknown. It has been proposed as a link between the circadian pathway and cell cycle DNA-damage check points and its knockdown in NHF1 cells impaired replication and intra-S checkpoints [61]. Thus, a potential role of *Timeless* in compensatory beta cell proliferation in *ob/ob* islets could be proposed.

Besides olfactory receptors, *Fzd6* and *Fzd7*, the Signaling category was enriched in other genes involved in G protein-coupled receptor (GPCR) signaling, including various receptors and regulatory proteins (Supplementary Figure 2A). GPCRs play key roles in the regulation of hormone secretion from islet cells and are important drug targets for T2D therapy [62]. Within the subgroup of genes with higher expression in 16 wk *db/db* islets vs the other groups, we found receptors that have been shown to positively regulate insulin secretion such as *Ednra*, *Ednrb*, *Gpr119*, *Gpr68*, *P2ry6* and *Gcgr* [63]. Upregulation of some of these receptors could be adaptive

to the loss of other signaling routes in diabetic islets. Indeed, *Gpr119* expression was upregulated in the islets of mice lacking *Glp1r* and *Gcgr* and has been suggested to contribute to improved oral glucose tolerance and beta cell function in this model [64]. In contrast, other receptors have been shown to negatively regulate insulin secretion, including *Gabbr2* and *Ghsr* [63]. The marked downregulation of the latter gene in 16 wk *ob/ob* islets may be an important adaptive mechanism to maintain adequate insulin secretion [65]. On the other hand, other genes exhibited lower expression in 16 wk *db/db* islets vs the other groups, in particular in comparison to 16 wk *ob/ob* islets. While the role of some of them is uncertain, others may play a role in beta cell compensation, including *Cckar* [66] and *Drd2* (Supplementary Figure 2A, E) [67].

Together, these changes reveal the complex landscape of signaling pathways that may contribute to beta cell sensitivity or resistance in obese mice. Many of the affected genes/pathways represent interesting targets for future developments. Besides signaling, growing evidence indicates a key role of metabolism in the modulation of differentiation and cell identity. Interestingly, we found important changes in genes regulating the metabolism of sugars, lipids and proteins.

3.2.3. Sugar metabolism

Sugar metabolism category comprised 49 DE genes that were mostly upregulated in 16 wk *db/db* islets in comparison to the other groups, thereby indicating an important metabolic activity in these islets (Figure 3A). This category could be subdivided into 3 major subcategories: glucose transport, glycolysis and mitochondrial metabolism in addition to few genes belonging to the pentose phosphate pathway, monocarboxylate transport, gluconeogenesis and sugar hydrolysis (Figure 3A). Upregulation of *Slc5a1* (also known as *Sglt1*) may occur in non-beta cells. In agreement, we found that *SLC5A1* mRNA levels were strongly upregulated in human alpha cells, but not in beta

cells, of T2D donors (Supplementary Figure 3A, B). Indeed, the encoded Na^+-glucose co-transporter has been shown to play a role in the regulation of glucagon secretion by alpha cells [68,69]. In further agreement, *Slc5a1* expression was upregulated in the islets of diabetic *db/db* mice [69]. Moreover, the mRNA levels of *Slc5a1* were upregulated by glucose dose-dependently in αTC cells [69], thereby suggesting the involvement of glucotoxicity. On the other hand, the precise role of the ER inorganic phosphate/glucose-6-phosphate antiporter genes (*Slc37a1*, *Slc37a2*) or other glucose transporter genes (*Slc2a7*, *Slc2a9*) in islet biology remains unknown.

Most glycolytic genes were specifically upregulated in 16 wk *db/db* islets vs the other groups (Figure 3A). These changes, together with upregulation of *Hif2α* (Figure 2A) and other hypoxia-response genes (also discussed in the section "Response to stress") may reflect a metabolic adaption to hyperglycemia-related hypoxia within the islets of decompensating diabetic mice [27,70], and may be responsible for glucose hypersensitivity and impaired GSIS [37,71]. *Aldob* was the most strongly affected gene in this subgroup (Figure 3A, B). We have previously shown that *Aldob* was the gene most affected by glucose in rat islets transcriptome [37]. This finding was confirmed in human islets and a negative correlation between *ALDOB* expression and insulin secretion has been proposed, although the precise molecular mechanism remains elusive [72]. *Idh1* has been suggested to negatively regulate GSIS [73] and IDH1 activity was elevated in islets from T2D donors [74].

In parallel, several genes involved in mitochondrial metabolism were upregulated in 16 wk *db/db* islets, including a marked upregulation of *Ucp2* (Figure 3A, C). A tendency toward upregulation of *UCP2* was observed in human beta cells of T2D donors opposed to downregulation in alpha cells (Supplementary Figure 3E, F). The upregulation of UCP2 has been shown to involve the glucolipotoxic diabetic environment and to negatively regulate GSIS [75]. On the other hand,

upregulation of *Ucp2* has also been suggested to confer protection against oxidative stress [76]. In contrast, a few genes involved in oxidative phosphorylation were upregulated in 16 wk *ob/ob* islets vs 16 wk *db/db* islets, including *Atp5c1* (ATP synthase subunit), *Ndufb10* (complex I subunit), *Ndufb7* (complex I subunit) and *Cox6a2* (cytochrome c oxidase subunit) (Figure 3A). Moreover, *ATP5C1* and *NDUFB7* mRNA levels were reduced in human beta cells of T2D donors (Supplementary Figure 3G, I). Upregulation of these genes may contribute to enhance mitochondrial function, which is key to sustain adequate insulin secretion.

Noteworthy, most glucose metabolism genes belonging to these 3 subgroups were downregulated (some of them strongly) in 6 wk *ob/ob* islets vs 6 wk *db/db* islets. Intriguingly, in 16 wk *ob/ob* islets, many of these genes were upregulated vs 6 wk *ob/ob* islets, but their expression levels remained lower in comparison to 16 wk *db/db* islets. The pentose phosphate pathway genes *Pgd* and *H6pd* also displayed a similar pattern. This is an interesting observation that suggests a potential preemptive metabolic reconfiguration occurring in young *ob/ob* islets that may play an important adaptive role, perhaps by lowering the threshold of metabolic activation in response to increased insulin demand to keep low levels of cellular stress and consequently a lower activation of deleterious stress signaling pathways. This hypothesis is supported by a similar observation with many lipid metabolism genes.

3.2.4. Lipid metabolism

Lipid metabolism category comprised 163 DE genes, most of them were markedly upregulated in 16 wk *db/db* islets vs the other groups, thereby confirming the higher metabolic activity of these islets (Figure 4). Noteworthy, different lipid metabolism related KEGG pathways were significantly enriched in the comparisons 6 vs 16 wk *db/db* islets (Supplementary Table 2), 16 wk

db/db vs 16 wk *ob/ob* islets (Supplementary Table 3) and 6 vs 16 wk *ob/ob* islets (Supplementary Table 4). This category was subdivided into 7 major subcategories: lipid transport, glycerophospholipid/triglyceride (GPL/TG) biosynthesis, steroid biosynthesis, fatty acid (FA) biosynthesis, FA activation, FA oxidation and lipid hydrolysis (Figure 4). Obesity and diabetes states are characterized by dyslipidemia, and corroborative evidence has shown that chronic exposure of islets and beta cells to elevated levels of saturated FAs exerted toxic effects on the beta cell differentiated phenotype [77]. Therefore, the important upregulation of various lipid transport genes, including *Npc1l1*, *Cd36* and *Lrp1* in 16 wk *db/db* islets may enhance lipid uptake and contribute to beta cell lipotoxicity [78-80]. Upregulation of other genes, such as apolipoproteins (*Apob*, *Apoa4*, *Apoa1*, *Apoe*), fatty acid binding proteins (*Fabp2*, *Fabp1*), cholesterol (*Abca1*, *Abcg5*) and phospholipid (*Abca7*) efflux transporters may be adaptive and may also reflect an important intra-islet lipid biosynthetic activity. Indeed, several genes involved in GPL/TG, steroid and very long-chain FA biosynthesis were markedly upregulated in 16 wk *db/db* islets (Figure 4). Previous evidence has shown increased intra-islet TGs in diabetic ZDF male rats [81]. In addition, lipid droplet accumulation has been reported in rat and human islets exposed to glucolipotoxic conditions [82,83] and in the islets of T2D subjects [84]. Importantly, preventing lipogenesis in male ZDF rat islets by estrogen receptor activation prevented beta cell failure and maintained the beta cell differentiated phenotype [85]. Besides the biosynthetic/storage activity, there was a concomitant upregulation of several genes involved in lipid hydrolysis, medium-chain and long-chain FA activation and FA oxidation (Figure 4). Moreover, parallel changes in mRNA levels of several lipid metabolism genes were observed in human beta cells of T2D donors (Supplementary Figure 4). This important lipid metabolism activity within decompensating islets could profoundly impact the beta cell phenotype through the generation of toxic lipid metabolites

and the activation of deleterious stress pathways, including ER stress, oxidative stress, inflammation and altered autophagy [77,86].

Interestingly, many of these genes were downregulated in *ob/ob* islets at 6 weeks of age and restored to near control levels at 16 weeks, but remained much lower in comparison to 16 wk *db/db* islets, in agreement with our observations with glucose metabolism genes. This further supports our hypothesis of a preemptive metabolic reconfiguration in *ob/ob* islets that may contribute to the compensatory phenotype in these mice.

3.2.5. Protein metabolism

We found 224 DE genes in this category that can be divided into two clusters: (1) genes upregulated in 16 wk *db/db* islets vs the other groups and (2) genes downregulated in 16 wk *db/db* islets vs the other groups (Figure 5). Subsequent analysis of this category revealed 8 major subcategories: amino acid transport, amino acid metabolism, urea cycle, translation regulation, ribosomal proteins, lysosomal protease activity, cellular/membrane protease activity and extracellular protease activity (Figure 5). Unsurprisingly, different amino acid related KEGG pathways were significantly enriched in the comparisons 6 vs 16 wk *db/db* islets (Supplementary Table 2), 16 wk *db/db* vs 16 wk *ob/ob* islet (Supplementary Table 3) and 6 vs 16 wk *ob/ob* islets (Supplementary Table 4). Under obesity, beta cells are heavily engaged in proinsulin biosynthesis to meet the metabolic demands of the organism, and therefore an adequate expression of the myriad genes involved in this process is fundamental. Amino acids are protein building blocks that need to be supplied and metabolised appropriately to fuel the hyperactive biosynthetic machinery. In addition, earlier and recent evidence supports an important role of specific amino acids in beta cell signaling and insulin secretion [87-89]. Thus, several amino acid transporter genes were

upregulated in 16 wk *db/db* islets vs the other groups. The known amino acids transported by the product of each specific gene are indicated on the right of the AA transport heatmap (Figure 5). Interestingly, as for glucose and lipid metabolism genes, many of these transporter genes were markedly downregulated in 6 wk *ob/ob* islets and restored in 16 wk islets, but always to a lower extent vs 16 wk *db/db* islets (Figure 5). Noteworthy, *Ace2* was markedly upregulated in the islets of diabetic 16 wk *db/db* mice and downregulated in the islets of the other compensating groups. In addition to its role in the renin-angiotensin system, ACE2 is involved in the trafficking to the plasma membrane of the neutral amino acid transporter SLC6A19 [90], and is also a receptor for human coronaviruses, including SARS-CoV-2 [91]. In contrast, another group of amino acid transporter genes were downregulated in 16 wk *db/db* islets vs the other groups, including *Slc38a3*, *Slc1a3* and *Slc17a8* (Figure 5 and Supplementary Figure 5A-C). These findings acquire special importance when analyzed in the light of the observed changes in amino acid metabolism genes. Strikingly, most of amino acid metabolism genes were strongly downregulated in 16 wk *db/db* islets while upregulated to different extents in 16 wk *ob/ob* islets, including a marked upregulation of *Gls2* and *Bcat2* (Figure 5 and Supplementary Figure 5D, E). These two genes are important traits of adult differentiated human beta cells since their expression is markedly downregulated in fetal beta cells (Supplementary Figure 6A, B) [92]. There was also a tendency toward downregulation of protein metabolism genes in human beta cells of T2D donors (Supplementary Figure 7). In addition to a similar pattern of the lysosomal protease gene *Ggh* (Figure 5 and Supplementary Figure 5F), these novel findings draw an interesting mechanism centered around glutamate that may play a key compensatory role (Supplementary Figure 5G). Indeed, the high affinity transporter SLC1A3 mediates the uptake of glutamate, and SLC38A3 mediates the uptake of glutamine which is metabolized by GLS2 to generate glutamate. Moreover, BCAT2 metabolizes

leucine, isoleucine and valine to produce glutamate. Furthermore, the lysosomal protease GGH hydrolyses the polyglutamate side chains of polyglutamate-folate to generate free glutamate. These mechanisms converge to increase cytosolic glutamate levels. Interestingly, the vesicular transporter SLC17A8 mediates the transport of glutamate into insulin granules. The latter event has been shown to be required for incretin-induced potentiation of insulin secretion. On the other hand, glutamate transport into granules required incretin-downstream signaling (Supplementary Figure 5G) [88]. Previous evidence already supported a role of glutamate in GSIS and suggested uptake of glutamate into the secretory granules [93]. In addition, evidence has also suggested a role for glutamate in insulin granule exocytosis via inhibition of protein phosphatase activity (Supplementary Figure 5G) [94]. Altogether, these findings unveil a novel compensatory mechanism involving a coordinated regulation of specific amino acid transport and metabolism gene networks and incretin signaling that is defective in diabetic islets.

We also found a specific upregulation of urea cycle genes in 16 wk *db/db* islet vs the other groups (Figure 5). Besides being the only endogenous source of arginine, ornithine and citrulline, the urea cycle is the primary pathway for the clearance of surplus nitrogen. Therefore, its activation may reflect an important protein turnover, as inferred by the clear protease gene expression signature in 16 wk *db/db* islets (Figure 5). Additionally, it has been proposed to protect islets from cytokine cytotoxicity by reducing arginine usage for nitric oxide production [95]. Many of these genes were downregulated in 6 wk *ob/ob* islets and restored to near basal levels at 16 weeks. Together with observations with glucose and lipid metabolism genes, these cumulative results further support the hypothesis of a reconfiguration in *ob/ob* islets to lower the metabolic threshold.

Our evidence also implicated a compromised translational regulation in decompensating islets. Thus, several negative regulators of translation were upregulated in 16 wk *db/db* islets vs the other

groups, including *Zfp36*, *Eif4enif1*, *Zfp36l2*, *Cyfip1* and *Pum1*, whereas several positive regulators of translation were downregulated in these islets, including *Dazl*, *Eif1ax*, *Eif4a2*, *Eif2s3y*, *Mknk1* and *Ddx3y* (Figure 5). Strikingly, all DE ribosomal protein genes were downregulated in 16 wk *db/db* islets vs the other groups (Figure 5). Likewise, the ribosomal protein genes were universally downregulated in human beta cells of T2D donors whereas they were either unchanged or mildly increased in alpha cells (Supplementary Figure 8, 9). Together, this evidence further supports an impaired translational activity. This may lead to ER stress in these metabolically hyperactive islets. Alternatively, ER stress resulting from glucolipotoxic and proinflammatory diabetic milieu may negatively impact the translational machinery. Either way, we found that islets from decompensating diabetic mice exhibited an important stress signature.

3.2.6. Response to stress

The 312 genes belonging to this category were generally upregulated in 16 wk *db/db* islets vs the other groups and were classified into 11 major subcategories: inflammatory signaling, cytokines/chemokines, anti-inflammatory signaling, the complement pathway, MHC, hypoxia, oxidative stress, glutathione metabolism, DNA damage, positive regulation of cell death and negative regulation of cell death (Supplementary Figure 10A). Obesity and (pre)diabetic states are characterized by systemic low-grade inflammation, and cumulative evidence indicates an important role of local islet inflammation in beta cell demise [96]. Thus, most inflammatory signaling subcategory genes were markedly upregulated in 16 wk *db/db* islets in comparison to the other groups, including several members of the tumor necrosis factor superfamily (*Tnfrsf23*, *Tnfrsf21* also known as *Dr6*, *Tnfrsf1b*, *Tnfrsf1a*, *Tnfrsf11a*, *Tnfaip8l3* and *Tnfsf13b*), *Lgals3*, *Casp1*, *Nfkb2*, *Tlr3*, *Ifngr1*, *Ifngr2* and different kinases/adapter proteins involved in inflammatory receptor signaling (*Irak3*, *Mlkl*, *Dapk1*, *Irak4* and *Irak1bp*) (Supplementary Figure 10A). Many of

them were also upregulated, although to a lower extent, in 6 wk *db/db* islets but not in *ob/ob* islets (except for *Tnfrsf23*, *Tnfrsf21* and *Irak3*), in agreement with our previous observations [6]. CASP1 plays a key role in inflammasome signaling by cleaving inactive proinflammatory cytokines and regulating pyroptosis [97]. *Casp1* was markedly upregulated in 16 wk *db/db* islets, strongly downregulated in 6 wk *ob/ob* islets and restored to near basal levels in 16 wk *ob/ob* islets (Supplementary Figure 10B). Several genes in this subcategory displayed a similar pattern that paralleled changes in metabolic genes. A second group of genes in this subcategory were downregulated in 16 wk *db/db* islets vs 6 wk *db/db* islet while exhibiting minimal changes in *ob/ob* islets, except for the significant upregulation of *Cxcr1*, *Nlrp4a*, *Nlrp4e* and *Nlrp1b* in 16 wk *ob/ob* islets (Supplementary Figure 10A). While this may reflect a slight activation of inflammatory signaling in these islets, the role of *Nlrp4a* and *Nlrp4e* in islets is unknown.

Cytokine and chemokine genes were overall slightly downregulated in 16 wk *db/db* islets, except for a strong upregulation of *Ccl25*, *Il18* and *Ccl28* (Supplementary Figure 10A). A recent study has shown that exogenous CCL25 inhibited GSIS and promoted cytokine-induced caspase 3/7 activity in mouse and human islets [98]. Moreover, previous evidence has shown the expression and production of functional IL18 by primary mouse islets, and suggested its implication in insulitis and beta cell demise [99]. *Il18* expression pattern resembled that of *Casp1* (Supplementary Figure 10A, B).

Interestingly, parallel to upregulation of proinflammatory signaling in 16 wk *db/db* islets, mRNA levels of several anti-inflammatory signaling genes were increased, including *Il4ra*, *Il13ra1*, *Il6ra* and *Tnfsf10* (also known as *Trail*) (Supplementary Figure 10A). This highlights the coexistence and complex interaction of adaptive and deleterious stress responses within diabetic islets. In addition, various genes belonging to the complement pathway were upregulated in the islets of

decompensating diabetic mice, including complement component C3 (Supplementary Figure 10A). Increased expression of islet C3 has been reported in GK rats, *db/db* mice and T2D donors, and has been proposed to play an adaptive role under stress conditions by regulating cytoprotective autophagy, AKT activation and JNK inhibition [100,101]. It is unclear if the sum of the upregulation of the different complement genes, in addition to C3, is adaptive or cytolytic, but concomitant upregulation of negative regulatory components *Susd4*, *Serping1* and *Cd59b* may tip the scales towards an adaptive function.

Several class I major histocompatibility (MHC) genes were also upregulated in 16 wk *db/db* islets vs the other groups, while another subgroup of these genes was downregulated (Supplementary Figure 10A). Hyperexpression of HLA class I antigens has been reported in islets from type 1 diabetes donors [102]. Whether these changes may contribute to the vulnerability of *db/db* beta cells to T cell destruction is unclear. Importantly, upregulation of MHC-related genes has also been observed in the islets of pancreatectomized rats, thereby suggesting a role of hyperglycemia [103].

A clear hypoxic gene expression signature was found in the islets of 16 wk *db/db* mice (Supplementary Figure 10A), in agreement with our and others previous findings [26,27,70] (discussed in "Transcriptional regulation" and "Sugar metabolism" sections). In addition, these islets also presented an oxidative stress gene expression signature, including a marked upregulation of *Xdh* and *Txnip* and upregulation of different components of the glutathione metabolism pathway (Supplementary Figure 10A, C). Oxidative stress in an important mechanism downstream of glucotoxicity that markedly contributes to the deterioration of the beta cell differentiated phenotype. Importantly, reactive oxygen species (ROS) generated under hyperglycemia can activate other stress responses, such as ER stress, while the activation of various stress responses,

such as inflammation and hypoxia, can result in ROS production, thereby highlighting the cross talk between stress pathways and giving a central place to oxidative stress in the pathogenesis of T2D (reviewed in [15,28,104]). Previous evidence has shown that *Txnip* was strongly upregulated in rat and human islets exposed to elevated glucose levels [37,105], but not palmitate [30]. It was also upregulated in diabetic models and implicated in the inhibition of insulin production and secretion and the stimulation of cell death. These effects were mediated by the negative regulation of the antioxidant protein thioredoxin, regulation of specific microRNAs and activation of the inflammasome [106]. On the other hand, upregulation of glutathione metabolism genes is adaptive and may promote survival and oppose beta cell dedifferentiation [107]. Nevertheless, given the low basal expression of some key antioxidant genes in beta cells, it might be insufficient to face the important ROS generation under chronic hyperglycemia (reviewed in [15,28]).

Oxidative stress can induce important macromolecular damage, including DNA damage. Indeed, we found upregulation of several DNA damage response genes in 16 wk *db/db* islets, including *Cdkn1a* (also known as *p21*), *Gadd45a*, *Parp10* and *Parp4* (Supplementary Figure 10A, D). In parallel, another group of DNA damage response genes were downregulated in 16 wk *db/db* islets and were overall upregulated in the other groups (Supplementary Figure 10A). Interestingly, the latter group comprises various cell cycle checkpoint regulator and DNA replication/repair genes, including *Aunip*, *Chek2*, *Pole*, *Fanca*, and *Chaf1a* (Supplementary Figure 10A, E). Upregulation of these genes in compensating islets may play a role during compensatory proliferation by regulating cell cycle progression and DNA repair [108]. On the other hand, downregulation of these genes in decompensating 16 wk *db/db* islets may negatively impact compensatory proliferation and increase their susceptibility to DNA damage.

An expected consequence of the activated stress signature in diabetic islets is the upregulation of proapoptotic genes, including different caspase genes (*Casp1*, *Casp7*, *Casp8*), *Cideb*, *Mlkl* (necroptosis), *Bak1*, *Bcl2l14*, *Apaf1* and *Fas*. These islets also exhibited upregulation of a few genes shown to play antiapoptotic roles, including *Cck*, *Irs2*, *Tnfsf10* and *Kitl* [109,110] (Supplementary Figure 10A). Together with anti-inflammatory and antioxidant gene changes, it confirms the complex interplay of deleterious and adaptive pathways within diabetic islets. The UPR is another key adaptive pathway activated in response to ER stress. We have previously provided evidence of a link between the failure of the UPR and beta cell decompensation [6]. In the present study, we extend previous findings and explore novel regulatory mechanisms.

3.2.7. ER stress and UPR

This category encompassed 33 genes subdivided into 2 principal clusters: (1) genes with higher expression in 16 wk *db/db* islets vs the other groups, and (2) genes with lower expression in 16 wk *db/db* islets vs the other groups (Figure 6A). The first cluster comprised several adaptive genes involved in protein folding, quality control and trafficking, including a strong upregulation of *Agr2*, *Uggt2*, *Hspa13* and *Chch4d* (Figure 6A). Strong upregulation of *AGR2*, a protein disulfide isomerase (PDI) family member, was also verified in human beta cells of T2D donors (Supplementary Figures 11A). Although the precise role of AGR2 in beta cells has not been explored, a recent study has shown that early treatment of *db/db* mice with an SGLT2 inhibitor maintained glucose homeostasis and preserved beta cell mass in association with a marked upregulation of *Agr2* mRNA and protein levels, thereby suggesting a potential important adaptive function [111]. However, besides other chaperones, co-chaperones and isomerases, this cluster also enclosed the proapoptotic gene *Trib3* (Figure 6A, B). Its implication in beta cell demise under ER stress is well established (reviewed in [28]); although surprisingly, its expression was reduced

in human beta cells of T2D donors (Supplementary Figures 11A). Overall, the results indicated the presence of ER stress in 16 wk *db/d*b islets vs the other groups and the concomitant activation of adaptive and proapoptotic response. Moreover, analysis of cluster 2 revealed the downregulation of an important set of adaptive UPR genes in 16 wk *db/db* islets in comparison to the other groups, including ER-associated degradation genes (*Derl3*, *Serp1*), PDI genes (*Pdia8*, *Pdia2*) and peptidyl-prolyl isomerase genes (*Ppib*, *Ppic*) (Figure 6A, C-E). Downregulation of *PPIB* has also been observed in the islets of T2D donors [112]. Here we found that *PPIB* and *SERP1* were downregulated in human beta cells of T2D donors while unchanged in alpha cells (Supplementary Figures 11G-J). Thus, the maintenance of these UPR genes may promote beta cell compensation by ensuring a robust ER machinery to face the important synthetic load under obesity and avoiding the accumulation of misfolded proteins and ensuing ER stress and alteration of the beta cell differentiated phenotype [9,15]. These results corroborate and extend our previous observations [6]. In addition, GSEA analysis identified a significant enrichment in transcription factor binding motifs and subsequent functional studies indicated a role for novel transcription factors in the regulation of beta cell survival, function and UPR gene expression.

3.2.8. GSEA and effects of siRNA-mediated silencing of *Foxo4*, *Nfatc1*, or *Maz* on MIN6 cell death, glucose-stimulated insulin secretion and gene expression

GSEA of genes that were differentially expressed between *db/db* and *ob/ob* islets highlighted several transcription factors that could be involved in the opposing beta cell responses to obesity-induced insulin resistance. Thus, we found a significant enrichment for binding motifs of the following transcription factors: E12, MAZ, NFAT, SP1, LEF1, FOXO4, AP4 and PAX4. There were two additional binding motifs with unknown targets (Figure 7A). Based on previous reports on their potential involvements in diabetes and beta cell biology, we focused on MAZ, NFATC1

and FOXO4 to further explore their roles in the regulation of beta cell function and the modulation of gene expression. siRNA-mediated knockdown of these transcription factors (*Foxo4*, *Nfatc1*, and *Maz*) was undertaken.

Ablation of *Foxo1-4* in beta cells has previously been shown to cause early-onset, maturity-onset diabetes of the young (MODY)-like diabetes in mice [113]. However, we found that knockdown of *Foxo4* alone in MIN6 beta cells had no significant effect on cell death or GSIS (Figure 7B, C). In addition, knockdown of *Foxo4* did not affect the expression of beta cell enriched genes such as *Kir6.2*, *mGPDH*, *Nkx6.1*, *Slc2a2* (also known as *Glut2*), *Pdx1*, *Neurod1* (also known as *Beta2*) and insulin, despite a slight but significant reduction in the expression of *Mafa* (Figure 7D). Interestingly, the mRNA levels of several important adaptive UPR genes (*Hspa5*, *Hsp90b1*, *Pdia4*, and *Dnajc3*) were increased while others were not (*Xbp1*, *Fkbp11*). The proapoptotic ER stress gene *Atf3* was also unaffected. Similarly, the oxidative stress response genes *Hmox1*, *Cat* and *Sod1* were unchanged (Figure 7D). Thus, while attenuation of *Foxo4* expression had no significant impact on cell death and the expression of some stress response genes, it significantly upregulated the expression of various adaptive UPR genes.

NFAT binding motif was selectively enriched in genes that were altered between *db/db* and *ob/ob* mice at 16 weeks of age. *Nfatc2* has been associated with human diabetes [114], whereas *Nfatc1* overexpression was capable of expanding beta cell mass in mice [115]. Here we found that *Nfatc1* knockdown significantly increased cell death without affecting GSIS (Figure 7B, C). Moreover, *Nfatc1* knockdown reduced the mRNA expression of *Slc2a2* and *Mafa* but had no effect on the mRNA levels of *Nkx6.1*, *Pdx1*, *Neurod1* and insulin. Nevertheless, the mRNA levels of *Kir6.2* and *mGPDH* were significantly increased (Figure 7E). Conversely, the adaptive UPR genes *Xbp1*, *Fkbp11*, *Pdia4* and *Hsp90b1* were downregulated while *Hspa5* and *Dnajc3* remained unaltered

(Figure 7D). On the other hand, *Atf3* and *Hmox1* were downregulated while *Cat* and *Sod1* were unchanged (Figure 7E). These results indicate that under control conditions, *Nfatc1* may play a role in the regulation of adaptive UPR gene expression, which promotes beta cell survival.

Evidence has shown that MAZ is capable of binding to the insulin promoter [116], and was previously identified as potential target transcription factor for T2D hub gene candidates [117]. Interestingly, knockdown of *Maz* led to increases in both cell death and GSIS (Figure 7B, C). These changes were accompanied by a reduction in the mRNA levels of *Mafa*, *Nkx6.1*, and *Atf3* and no observed differences in the expression of *Kir6.2*, *mGPDH*, *Slc2a2*, *Pdx1*, *Neurod1*, insulin, *Xbp1*, *Hspa5*, and *Hmox1*. In contrast, mRNA expression of *Fkbp11*, *Dnajc3*, *Pdia4*, *Hsp90b1*, *Cat*, and *Sod1* were increased following *Maz* depletion (Figure 7F). Upregulation of adaptive UPR genes and antioxidant genes in this case may reflect a change in biosynthetic activity and mitochondrial function and upregulation of GSIS. Overall, these studies reveal novel roles of these transcription factors in beta cell biology. The findings implicate *Foxo4* in the negative regulation and *Nfatc1* in the positive regulation of adaptive UPR gene expression in beta cells.

4. Conclusion

In conclusion, we have used a comprehensive large scale strategy in obese mouse models with different propensity for the development of diabetes and revealed the complex landscape of transcriptional changes that accompany the process of beta cell compensation as well as those involved in beta cell decompensation and development of diabetes (Figure 8). Thus, successful adaptation to the increased metabolic demand under obesity was associated with a normal glucose and lipid metabolism and upregulation of amino acid metabolism, together with the absence of supraphysiological levels of stress and sustained ER homeostasis and machinery. In contrast, beta

cell failure was accompanied by a high glucose and lipid metabolic activity, reduced amino acid metabolism and a high level of stress, including hypoxia, oxidative stress, ER stress and inflammation, despite concomitant upregulation of adaptive responses, and an altered ER homeostasis and translational machinery (Figure 8). Interestingly, analysis of time-dependent gene expression changes in the islets of these models revealed that diabetes resistant mice exhibited a marked downregulation of numerous metabolic and stress genes at 6 weeks of age that were restored to near control levels at 16 weeks, while being much lower in comparison to 16 wk *db/db* islets. We propose that a preemptive metabolic reconfiguration in young *ob/ob* islets lowers the threshold of metabolic activation in response to increased insulin demand, thereby maintaining low levels of cellular stress and activity of deleterious stress signaling pathways.

Acknowledgements

This work was supported by a project grant from the National Health and Medical Research Council (NHMRC) of Australia to D.R.L and an NHMRC Early Career Fellowship to J.Y.C.

Conflict of Interest

The authors declare that they have no conflict of interest.

Author Contributions

J.Y. Chan, M. Bensellam, R.C.Y. Lin and D.R. Laybutt designed and performed research, analyzed data and wrote the paper. C. Liang and K. Lee performed research, analyzed data and revised the paper. J-C Jonas analyzed data and revised the paper.

Figure Legends

Figure 1. Data analysis and gene clustering. (A) Principal component analysis of transcriptome data showing distinctive gene expression of the genotypes at 16 wk and at 6 wk. (B) Hierarchical clustering analysis of differentially expressed genes across the 4 groups showing that islets from 16 wk *db/db* mice have distinctive gene expression in comparison to islets from 6 wk *db/db*, 6 wk *ob/ob* and 16 wk *ob/ob* mice. (C) Venn diagram showing a disease effect where 1649 genes are differentially expressed in *ob/ob* and 3776 genes specifically in *db/db*. There are 559 genes in common between *ob/ob* and *db/db* genotypes. (D) Venn diagram showing an age effect where 4490 genes are differentially expressed in *db/db* islets vs *ob/ob* islets at 16 wk compared to 1371 genes differentially expressed at 6 wk. The common genes (n=602) reflect homeostasis genes.

Figure 2. Changes in the mRNA levels of genes involved in transcriptional regulation in the islets of diabetes-prone and diabetes-resistant mice. (A) A primary heatmap displaying changes in the 192 DE genes involved in transcriptional regulation in the islets of *db/db* mice at 6 and 16 wk and in the islets of *ob/ob* mice at 6 and 16 wk from left to right, respectively. Secondary heatmaps depicting the principal subcategories, including islet cell identity, stress regulators, epigenetic regulators and repressors are shown on the right of the principal heatmap. Each gene in these heatmaps is identified by its array probe set ID and official gene symbol. Examples of key genes belonging to each subcategory are illustrated on the graphics on the right of the secondary heatmaps, including (B) *Neurog3*, (C) *Irx2*, (D) *Id3* and (E) *Uhrf1*. Data are the normalized mean SLR ± SEM for 2 (6 wk *db/db*), 3 (16 wk *db/db*), 2 (6 wk *ob/ob*) and 2 (16 wk *ob/ob*) microarray experiments. *$p<0.05$, **$p<0.01$ for the indicated comparison.

Figure 3. Changes in the mRNA levels of genes involved in sugar metabolism in the islets of diabetes-prone and diabetes-resistant mice. (A) A primary heatmap displaying changes in the 49 DE genes involved in sugar metabolism in the islets of *db/db* mice at 6 and 16 wk and in the islets of *ob/ob* mice at 6 and 16 wk from left to right, respectively. On the right of the principal heatmap, secondary heatmaps are depicting the principal subcategories, including glucose transport, glycolysis, mitochondrial metabolism and few smaller subcategories. Each gene in these heatmaps is identified by its array probe set ID and official gene symbol. Examples of key genes belonging to each subcategory are illustrated on the graphics below the heatmaps, including (B) *Aldob* and (C) *Ucp2*. Data are the normalized mean SLR ± SEM for 2 (6 wk *db/db*), 3 (16 wk *db/db*), 2 (6 wk *ob/ob*) and 2 (16 wk *ob/ob*) microarray experiments. *$p<0.05$, **$p<0.01$ for the indicated comparison.

Figure 4. Changes in the mRNA levels of genes involved in lipid metabolism in the islets of diabetes-prone and diabetes-resistant mice. (A) A primary heatmap displaying changes in the 163 DE genes involved in lipid metabolism in the islets of *db/db* mice at 6 and 16 wk and in the islets of *ob/ob* mice at 6 and 16 wk from left to right, respectively. On the right of the principal heatmap, secondary heatmaps are depicting the principal subcategories, including lipid transport, GPL/TG biosynthesis, steroid biosynthesis, FA biosynthesis, FA activation, FA oxidation and lipid hydrolysis. Each gene in these heatmaps is identified by its array probe set ID and official gene symbol. Data are the normalized mean SLR for 2 (6 wk *db/db*), 3 (16 wk *db/db*), 2 (6 wk *ob/ob*) and 2 (16 wk *ob/ob*) microarray experiments. FA: Fatty acid; GPL: Glycerophospholipid; TG: triglyceride.

Figure 5. Changes in the mRNA levels of genes involved in protein metabolism in the islets of diabetes-prone and diabetes-resistant mice. (A) A primary heatmap displaying changes in the 224

DE genes involved in protein metabolism in the islets of *db/db* mice at 6 and 16 wk and in the islets of *ob/ob* mice at 6 and 16 wk from left to right, respectively. On the right of the principal heatmap, secondary heatmaps are depicting the principal subcategories, including amino acid transport, amino acid metabolism, urea cycle, translation regulation, ribosomal proteins, lysosomal protease activity, cellular/membrane protease activity and extracellular protease activity. Each gene in these heatmaps is identified by its array probe set ID and official gene symbol. Data are the normalized mean SLR for 2 (6 wk *db/db*), 3 (16 wk *db/db*), 2 (6 wk *ob/ob*) and 2 (16 wk *ob/ob*) microarray experiments. AA: amino acid.

Figure 6. Changes in the mRNA levels of genes involved in ER stress and the adaptive UPR in the islets of diabetes-prone and diabetes-resistant mice. (A) Heatmap displaying changes in the 33 DE genes involved in ER stress and the adaptive UPR in the islets of *db/db* mice at 6 and 16 wk and in the islets of *ob/ob* mice at 6 and 16 wk from left to right, respectively. Each gene in this heatmap is identified by its array probe set ID and official gene symbol. Examples of key genes in this category are illustrated on the graphics on the right of the heatmap, including (B) *Trib3*, (C) *Derl3*, (D) *Ppib* and (E) *Ppic*. Data are the normalized mean SLR ± SEM for 2 (6 wk *db/db*), 3 (16 wk *db/db*), 2 (6 wk *ob/ob*) and 2 (16 wk *ob/ob*) microarray experiments. *$p<0.05$, **$p<0.01$, ***$p<0.001$ for the indicated comparison.

Figure 7. GSEA and effects of siRNA-mediated silencing of *Foxo4*, *Nfatc1*, or *Maz* on MIN6 cell death, glucose-stimulated insulin secretion and gene expression. (A) Significant enrichment of specific transcription factor binding motifs after GSEA of DE genes between diabetes-prone *db/db* islets and diabetes-resistant *ob/ob* islets. MIN6 cells were transfected with either negative control non-targeting siRNA (Con) or siRNA against *Foxo4*, *Nfatc1* or *Maz* prior to the assessments of (B) cell death (n=4 experiments performed in triplicates) and (C) GSIS. For secretion experiments,

clear bars represent low glucose condition whereas hatched bars represent high glucose condition. In another set of experiments, changes in key beta cell enriched genes and oxidative stress and ER stress response genes were assessed in MIN6 cells transfected with siRNA against (D) *Foxo4*, (E) *Nfatc1* or (F) *Maz vs* Con. Data are means ± SEM for 4 (cell death; in triplicates), 4-6 (GSIS; in triplicates) or 3-6 (gene expression; in triplicates) independent experiments. *p<0.05, **p<0.01, ***p<0.001 *vs* Con.

Figure 8. The proposed model highlighting the key metabolic and stress pathways altered in the islets of obese mice with a diabetes-prone phenotype in comparison to the islets of obese mice with a diabetes-resistant phenotype. See the text for details. AA: amino acid; ER: endoplasmic reticulum; ERAD: ER-associated degradation.

Supplementary Figure 1. ID3 and STAT3 protein expression is upregulated in islets of diabetic *db/db* mice. Immunostaining of (A) ID3 and (B) STAT3 in pancreas sections of C57BL/KsJ control and *db/db* mice and C57BL/6J control and *ob/ob* mice. Arrows indicate examples of STAT3 positive nuclei in beta cells. Images are representative of 3 animals per group. Scale bar, 40 μm.

Supplementary Figure 2. Changes in the mRNA levels of genes involved in signaling in the islets of diabetes-prone *and* diabetes-resistant mice. (A) A primary heatmap displaying changes in the 428 DE genes involved in signaling in the islets of *db/db* mice at 6 and 16 wk and in the islets of *ob/ob* mice at 6 and 16 wk from left to right, respectively. On the right of the principal heatmap, secondary heatmaps are depicting the principal subcategories, including olfactory transduction, Wnt pathway, Notch pathway, BMP/TGFβ pathway, circadian rhythm pathway and other GPCR signaling. Each gene in these heatmaps is identified by its array probe set ID and official gene symbol. Examples of key genes belonging to each subcategory are illustrated on the graphics on the right of the secondary heatmaps, including (B) *Wnt4*, (C) *Notch3*, (D) *Tgfbr2* and (E) *Drd2*. Data are the normalized mean SLR ± SEM for 2 (6 wk *db/db*), 3 (16 wk *db/db*), 2 (6 wk *ob/ob*) and 2 (16 wk *ob/ob*) microarray experiments. *p<0.05, **p<0.01 for the indicated comparison.

Supplementary Figure 3. Changes in the mRNA levels of the glucose metabolism genes (A,B) *SLC5A1*, (C,D) *LDHA*, (E,F) *UCP2*, (G,H) *ATP5C1* and (I,J) *NDUFB7* in human beta and alpha cells from 6 non-diabetic (ND; green bars) and 4 type 2 diabetic donors (T2D; red bars). Single cell RNA sequencing data were obtained from ArrayExpress database under the accession number E-MTAB-5061. Data are the mean of number of reads per kilo base per million mapped reads (RPKM) ± SEM for 171 (non-diabetic beta), 99 (T2D beta), and 256 (non-diabetic and T2D alpha) single cells. *p<0.05, **p<0.01, ***p<0.001 *vs.* non-diabetic.

Supplementary Figure 4. Changes in the mRNA levels of the lipid metabolism genes (A,B) *ACHE*, (C,D) *ELOVL7*, (E,F) *PLPP1*, (G,H) *ACSM3* and (I,J) *PLCE1* in human beta and alpha cells from 6 non-diabetic (ND; green bars) and 4 type 2 diabetic donors (T2D; red bars). Single cell RNA sequencing data were obtained from ArrayExpress database under the accession number E-MTAB-5061. Data are the mean of reads per kilobase of transcript per million mapped reads (RPKM) ± SEM for 171 (non-diabetic beta), 99 (T2D beta), and 256 (non-diabetic and T2D alpha) single cells. *p<0.05, **p<0.01, ***p<0.001 *vs.* non-diabetic.

Supplementary Figure 5. Changes in the mRNA levels of genes involved in amino acid transport metabolism in the islets of diabetes-prone *and* diabetes-resistant mice. Changes in the mRNA levels of (A) *Slc38a3*, (B) *Slc1a3*, (C) *Slc17a8*, (D) *Gls2*, (E) *Bcat2* and (F) *Ggh* in the islets of *db/db* mice at 6 (pale red bars) and 16 wk (red bars) and in the islets of *ob/ob* mice at 6 (pale green bars) and 16 wk (green bars). (G) The proposed compensatory mechanism involving these amino acid transport and metabolism gene. See the text for details. Data are the normalized mean SLR ± SEM for 2 (6 wk *db/db*), 3 (16 wk *db/db*), 2 (6 wk *ob/ob*) and 2 (16 wk *ob/ob*) microarray experiments. *p<0.05, **p<0.01, ***p<0.001 for the indicated comparison. E: glutamate; I: isoleucine; L: leucine; Q: glutamine; V: valine.

Supplementary Figure 6. Changes in the mRNA levels of human (A) *GLS2* and (B) *BCAT2* in purified fetal and adult alpha and beta cell subsets. RNA sequencing data were obtained from Gene Expression Omnibus database under the accession number GSE67543. Data are the mean of average number of transcripts per million (TPM) ± SEM for 5 (fetal alpha), 6 (adult alpha and fetal beta) and 7 (adult beta) preparations. **p<0.01, ***p<0.001 for the indicated comparison.

Supplementary Figure 7. Changes in the mRNA levels of the protein metabolism genes (A,B) *BCAT2*, (C,D) *SHMT2*, (E,F) *ASL*, (G,H) *GGH* and (I,J) *RPL41* in human beta and alpha cells from 6 non-diabetic (ND; green bars) and 4 type 2 diabetic donors (T2D; red bars). Single cell RNA sequencing data were obtained from ArrayExpress database under the accession number E-MTAB-5061. Data are the mean of reads per kilobase of transcript per million mapped reads (RPKM) ± SEM for 171 (non-diabetic beta), 99 (T2D beta), and 256 (non-diabetic and T2D alpha) single cells. **p*<0.05, ***p*<0.01 *vs.* non-diabetic.

Supplementary Figure 8. Changes in the mRNA levels of the ribosomal protein genes (A,B) *RPS18*, (C,D) *RPL23*, (E,F) *MRPS24*, (G,H) *MRPL20* and (I,J) *RPS20* in human beta and alpha cells from 6 non-diabetic (ND; green bars) and 4 type 2 diabetic donors (T2D; red bars). Single cell RNA sequencing data were obtained from ArrayExpress database under the accession number E-MTAB-5061. Data are the mean of reads per kilobase of transcript per million mapped reads (RPKM) ± SEM for 171 (non-diabetic beta), 99 (T2D beta), and 256 (non-diabetic and T2D alpha) single cells. **p*<0.05, ***p*<0.01, ****p*<0.001 *vs.* non-diabetic.

Supplementary Figure 9. Changes in the mRNA levels of the ribosomal protein genes (A,B) *RPL29*, (C,D) *RPL28*, (E,F) *RPL10A*, (G,H) *RPL31* and (I,J) *MRPL14* in human beta and alpha cells from 6 non-diabetic (ND; green bars) and 4 type 2 diabetic donors (T2D; red bars). Single cell RNA sequencing data were obtained from ArrayExpress database under the accession number E-MTAB-5061. Data are the mean of reads per kilobase of transcript per million mapped reads (RPKM) ± SEM for 171 (non-diabetic beta), 99 (T2D beta), and 256 (non-diabetic and T2D alpha) single cells. **p*<0.05, ***p*<0.01, ****p*<0.001 *vs.* non-diabetic.

Supplementary Figure 10. Changes in the mRNA levels of genes involved in response to stress in the islets of diabetes-prone and diabetes-resistant mice. (A) A primary heatmap displaying changes in the 312 DE genes involved in response to stress in the islets of *db/db* mice at 6 and 16 wk and in the islets of *ob/ob* mice at 6 and 16 wk from left to right, respectively. On the right of the principal heatmap, secondary heatmaps are depicting the principal subcategories, including inflammatory signaling, cytokines/chemokines, anti-inflammatory signaling, the complement pathway, MHC, hypoxia, oxidative stress, glutathione metabolism, DNA damage, positive regulation of cell death and negative regulation of cell death. Each gene in these heatmaps is identified by its array probe set ID and official gene symbol. Examples of key genes belonging to each subcategory are illustrated on the graphics below the heatmaps, including (B) *Casp1*, (C) *Txnip*, (D) *Cdkn1a* and (E) *Aunip*. Data are the normalized mean SLR ± SEM for 2 (6 wk *db/db*), 3 (16 wk *db/db*), 2 (6 wk *ob/ob*) and 2 (16 wk *ob/ob*) microarray experiments. *$p<0.05$, **$p<0.01$ for the indicated comparison.

Supplementary Figure 11. Changes in the mRNA levels of the ER stress and UPR genes (A,B) *AGR2*, (C,D) *TRIB3*, (E,F) *FOXRED2*, (G,H) *SERP1* and (I,J) *PPIB* in human beta and alpha cells from 6 non-diabetic (ND; green bars) and 4 type 2 diabetic donors (T2D; red bars). Single cell RNA sequencing data were obtained from ArrayExpress database under the accession number E-MTAB-5061. Data are the mean of reads per kilobase of transcript per million mapped reads (RPKM) ± SEM for 171 (non-diabetic beta), 99 (T2D beta), and 256 (non-diabetic and T2D alpha) single cells. *$p<0.05$ *vs.* non-diabetic.

REFERENCES

[1] Pratley, R.E., Weyer, C., 2002. Progression from IGT to type 2 diabetes mellitus: the central role of impaired early insulin secretion. Curr Diab Rep 2(3):242-248.

[2] Kahn, S.E., 2003. The relative contributions of insulin resistance and beta-cell dysfunction to the pathophysiology of Type 2 diabetes. Diabetologia 46(1):3-19.

[3] Hulman, A., Simmons, R.K., Brunner, E.J., Witte, D.R., Faerch, K., Vistisen, D., et al., 2017. Trajectories of glycaemia, insulin sensitivity and insulin secretion in South Asian and white individuals before diagnosis of type 2 diabetes: a longitudinal analysis from the Whitehall II cohort study. Diabetologia 60(7):1252-1260.

[4] Shafrir, E., Ziv, E., Mosthaf, L., 1999. Nutritionally induced insulin resistance and receptor defect leading to beta-cell failure in animal models. Ann N Y Acad Sci 892:223-246.

[5] Kluth, O., Matzke, D., Schulze, G., Schwenk, R.W., Joost, H.G., Schurmann, A., 2014. Differential transcriptome analysis of diabetes-resistant and -sensitive mouse islets reveals significant overlap with human diabetes susceptibility genes. Diabetes 63(12):4230-4238.

[6] Chan, J.Y., Luzuriaga, J., Bensellam, M., Biden, T.J., Laybutt, D.R., 2013. Failure of the adaptive unfolded protein response in islets of obese mice is linked with abnormalities in beta-cell gene expression and progression to diabetes. Diabetes 62(5):1557-1568.

[7] Kjorholt, C., Akerfeldt, M.C., Biden, T.J., Laybutt, D.R., 2005. Chronic hyperglycemia, independent of plasma lipid levels, is sufficient for the loss of beta-cell differentiation and secretory function in the db/db mouse model of diabetes. Diabetes 54(9):2755-2763.

[8] Omikorede, O., Qi, C., Gorman, T., Chapman, P., Yu, A., Smith, D.M., et al., 2013. ER stress in rodent islets of Langerhans is concomitant with obesity and beta-cell compensation but not with beta-cell dysfunction and diabetes. Nutr Diabetes 3:e93.

[9] Herbert, T.P., Laybutt, D.R., 2016. A reevaluation of the role of the unfolded protein response in islet dysfunction: maladaptation or a failure to adapt? Diabetes 65(6):1472-1480.

[10] Cheng, Y.Y., Wright, C.M., Kirschner, M.B., Williams, M., Sarun, K.H., Sytnyk, V., et al., 2016. KCa1.1, a calcium-activated potassium channel subunit alpha 1, is targeted by miR-17-5p and modulates cell migration in malignant pleural mesothelioma. Mol Cancer 15(1):44.

[11] Ooi, J.Y.Y., Bernardo, B.C., Singla, S., Patterson, N.L., Lin, R.C.Y., McMullen, J.R., 2017. Identification of miR-34 regulatory networks in settings of disease and antimiR-therapy: Implications for treating cardiac pathology and other diseases. RNA Biol 14(5):500-513.

[12] Segerstolpe, A., Palasantza, A., Eliasson, P., Andersson, E.M., Andreasson, A.C., Sun, X., et al., 2016. Single-Cell Transcriptome Profiling of Human Pancreatic Islets in Health and Type 2 Diabetes. Cell Metab 24(4):593-607.

[13] Bensellam, M., Montgomery, M.K., Luzuriaga, J., Chan, J.Y., Laybutt, D.R., 2015. Inhibitor of differentiation proteins protect against oxidative stress by regulating the antioxidant-mitochondrial response in mouse beta cells. Diabetologia 58(4):758-770.

[14] Chan, J.Y., Cooney, G.J., Biden, T.J., Laybutt, D.R., 2011. Differential regulation of adaptive and apoptotic unfolded protein response signalling by cytokine-induced nitric oxide production in mouse pancreatic beta cells. Diabetologia 54(7):1766-1776.

[15] Bensellam, M., Jonas, J.C., Laybutt, D.R., 2018. Mechanisms of beta-cell dedifferentiation in diabetes: recent findings and future research directions. J Endocrinol 236(2):R109-R143.

[16] Talchai, C., Xuan, S., Lin, H.V., Sussel, L., Accili, D., 2012. Pancreatic beta cell dedifferentiation as a mechanism of diabetic beta cell failure. Cell 150(6):1223-1234.

[17] Jennings, R.E., Berry, A.A., Strutt, J.P., Gerrard, D.T., Hanley, N.A., 2015. Human pancreas development. Development 142(18):3126-3137.

[18] Baraille, F., Ayari, S., Carriere, V., Osinski, C., Garbin, K., Blondeau, B., et al., 2015. Glucose Tolerance Is Improved in Mice Invalidated for the Nuclear Receptor HNF-4gamma: A Critical Role for Enteroendocrine Cell Lineage. Diabetes 64(8):2744-2756.

[19] Ragvin, A., Moro, E., Fredman, D., Navratilova, P., Drivenes, O., Engstrom, P.G., et al., 2010. Long-range gene regulation links genomic type 2 diabetes and obesity risk regions to HHEX, SOX4, and IRX3. Proc Natl Acad Sci U S A 107(2):775-780.

[20] Collins, S.C., Do, H.W., Hastoy, B., Hugill, A., Adam, J., Chibalina, M.V., et al., 2016. Increased Expression of the Diabetes Gene SOX4 Reduces Insulin Secretion by Impaired Fusion Pore Expansion. Diabetes 65(7):1952-1961.

[21] Zaiko, M., Estreicher, A., Ritz-Laser, B., Herrera, P., Favor, J., Meda, P., et al., 2004. Pax2 mutant mice display increased number and size of islets of Langerhans but no change in insulin and glucagon content. Eur J Endocrinol 150(3):389-395.

[22] Brun, T., Hu He, K.H., Lupi, R., Boehm, B., Wojtusciszyn, A., Sauter, N., et al., 2008. The diabetes-linked transcription factor Pax4 is expressed in human pancreatic islets and is activated by mitogens and GLP-1. Hum Mol Genet 17(4):478-489.

[23] Gosmain, Y., Cheyssac, C., Heddad Masson, M., Dibner, C., Philippe, J., 2011. Glucagon gene expression in the endocrine pancreas: the role of the transcription factor Pax6 in alpha-cell differentiation, glucagon biosynthesis and secretion. Diabetes Obes Metab 13 Suppl 1:31-38.

[24] Gosmain, Y., Katz, L.S., Masson, M.H., Cheyssac, C., Poisson, C., Philippe, J., 2012. Pax6 is crucial for beta-cell function, insulin biosynthesis, and glucose-induced insulin secretion. Mol Endocrinol 26(4):696-709.

[25] Nakamura, M., Kitamura, H., Konishi, S., Nishimura, M., Ono, J., Ina, K., et al., 1995. The endocrine pancreas of spontaneously diabetic db/db mice: microangiopathy as revealed by transmission electron microscopy. Diabetes Res Clin Pract 30(2):89-100.

[26] Sato, Y., Endo, H., Okuyama, H., Takeda, T., Iwahashi, H., Imagawa, A., et al., 2011. Cellular hypoxia of pancreatic beta-cells due to high levels of oxygen consumption for insulin secretion in vitro. J Biol Chem 286(14):12524-12532.

[27] Bensellam, M., Duvillie, B., Rybachuk, G., Laybutt, D.R., Magnan, C., Guiot, Y., et al., 2012. Glucose-induced O(2) consumption activates hypoxia inducible factors 1 and 2 in rat insulin-secreting pancreatic beta-cells. PLoS ONE 7(1):e29807.

[28] Bensellam, M., Laybutt, D.R., Jonas, J.C., 2012. The molecular mechanisms of pancreatic beta-cell glucotoxicity: Recent findings and future research directions. Mol Cell Endocrinol 364(1-2):1-27.

[29] Sampieri, L., Di Giusto, P., Alvarez, C., 2019. CREB3 Transcription Factors: ER-Golgi Stress Transducers as Hubs for Cellular Homeostasis. Front Cell Dev Biol 7:123.

[30] Cunha, D.A., Gurzov, E.N., Naamane, N., Ortis, F., Cardozo, A.K., Bugliani, M., et al., 2014. JunB protects beta-cells from lipotoxicity via the XBP1-AKT pathway. Cell Death Differ 21(8):1313-1324.

[31] Xin, Y., Dominguez Gutierrez, G., Okamoto, H., Kim, J., Lee, A.H., Adler, C., et al., 2018. Pseudotime Ordering of Single Human beta-Cells Reveals States of Insulin Production and Unfolded Protein Response. Diabetes 67(9):1783-1794.

[32] Fazio, E.N., Everest, M., Colman, R., Wang, R., Pin, C.L., 2005. Altered Glut-2 accumulation and beta-cell function in mice lacking the exocrine-specific transcription factor, Mist1. J Endocrinol 187(3):407-418.

[33] Jung, D.Y., Chalasani, U., Pan, N., Friedline, R.H., Prosdocimo, D.A., Nam, M., et al., 2013. KLF15 is a molecular link between endoplasmic reticulum stress and insulin resistance. PLoS ONE 8(10):e77851.

[34] Chen, H., Gu, X., Su, I.H., Bottino, R., Contreras, J.L., Tarakhovsky, A., et al., 2009. Polycomb protein Ezh2 regulates pancreatic beta-cell Ink4a/Arf expression and regeneration in diabetes mellitus. Genes Dev 23(8):975-985.

[35] Klochendler, A., Caspi, I., Corem, N., Moran, M., Friedlich, O., Elgavish, S., et al., 2016. The Genetic Program of Pancreatic beta-Cell Replication In Vivo. Diabetes 65(7):2081-2093.

[36] Bostick, M., Kim, J.K., Esteve, P.O., Clark, A., Pradhan, S., Jacobsen, S.E., 2007. UHRF1 plays a role in maintaining DNA methylation in mammalian cells. Science 317(5845):1760-1764.

[37] Bensellam, M., Van Lommel, L., Overbergh, L., Schuit, F.C., Jonas, J.C., 2009. Cluster analysis of rat pancreatic islet gene mRNA levels after culture in low-, intermediate- and high-glucose concentrations. Diabetologia 52(3):463-476.

[38] Kawamura, Y., Tanaka, Y., Kawamori, R., Maeda, S., 2006. Overexpression of Kruppel-like factor 7 regulates adipocytokine gene expressions in human adipocytes and inhibits glucose-induced insulin secretion in pancreatic beta-cell line. Mol Endocrinol 20(4):844-856.

[39] Kanazawa, A., Kawamura, Y., Sekine, A., Iida, A., Tsunoda, T., Kashiwagi, A., et al., 2005. Single nucleotide polymorphisms in the gene encoding Kruppel-like factor 7 are associated with type 2 diabetes. Diabetologia 48(7):1315-1322.

[40] Voight, B.F., Scott, L.J., Steinthorsdottir, V., Morris, A.P., Dina, C., Welch, R.P., et al., 2010. Twelve type 2 diabetes susceptibility loci identified through large-scale association analysis. Nat Genet 42(7):579-589.

[41] Stanojevic, V., Habener, J.F., 2015. Evolving function and potential of pancreatic alpha cells. Best Pract Res Clin Endocrinol Metab 29(6):859-871.

[42] Glauser, D.A., Schlegel, W., 2009. The FoxO/Bcl-6/cyclin D2 pathway mediates metabolic and growth factor stimulation of proliferation in Min6 pancreatic beta-cells. J Recept Signal Transduct Res 29(6):293-298.

[43] Kharroubi, I., Lee, C.H., Hekerman, P., Darville, M.I., Evans, R.M., Eizirik, D.L., et al., 2006. BCL-6: a possible missing link for anti-inflammatory PPAR-delta signalling in pancreatic beta cells. Diabetologia 49(10):2350-2358.

[44] Leem, J., Shim, H.M., Cho, H., Park, J.H., 2018. Octanoic acid potentiates glucose-stimulated insulin secretion and expression of glucokinase through the olfactory receptor in pancreatic beta-cells. Biochem Biophys Res Commun 503(1):278-284.

[45] Munakata, Y., Yamada, T., Imai, J., Takahashi, K., Tsukita, S., Shirai, Y., et al., 2018. Olfactory receptors are expressed in pancreatic beta-cells and promote glucose-stimulated insulin secretion. Sci Rep 8(1):1499.

[46] Ng, S.F., Lin, R.C., Laybutt, D.R., Barres, R., Owens, J.A., Morris, M.J., 2010. Chronic high-fat diet in fathers programs beta-cell dysfunction in female rat offspring. Nature 467(7318):963-966.

[47] Ng, S.F., Lin, R.C., Maloney, C.A., Youngson, N.A., Owens, J.A., Morris, M.J., 2014. Paternal high-fat diet consumption induces common changes in the transcriptomes of retroperitoneal adipose and pancreatic islet tissues in female rat offspring. FASEB J 28(4):1830-1841.

[48] Cartland, S.P., Lin, R.C.Y., Genner, S., Patil, M.S., Martinez, G.J., Barraclough, J.Y., et al., 2020. Vascular transcriptome landscape of Trail(-/-) mice: Implications and therapeutic strategies for diabetic vascular disease. FASEB J 34(7):9547-9562.

[49] Lee, S.H., Demeterco, C., Geron, I., Abrahamsson, A., Levine, F., Itkin-Ansari, P., 2008. Islet specific Wnt activation in human type II diabetes. Exp Diabetes Res 2008:728763.

[50] Krutzfeldt, J., Stoffel, M., 2010. Regulation of wingless-type MMTV integration site family (WNT) signalling in pancreatic islets from wild-type and obese mice. Diabetologia 53(1):123-127.

[51] Maschio, D.A., Matheus, V.A., Collares-Buzato, C.B., 2019. Islet cells are the source of Wnts that can induce beta-cell proliferation in vitro. J Cell Physiol 234(11):19852-19865.

[52] Kozinski, K., Jazurek, M., Dobrzyn, P., Janikiewicz, J., Kolczynska, K., Gajda, A., et al., 2016. Adipose- and muscle-derived Wnts trigger pancreatic beta-cell adaptation to systemic insulin resistance. Sci Rep 6:31553.

[53] Kanazawa, A., Tsukada, S., Sekine, A., Tsunoda, T., Takahashi, A., Kashiwagi, A., et al., 2004. Association of the gene encoding wingless-type mammary tumor virus integration-site family member 5B (WNT5B) with type 2 diabetes. Am J Hum Genet 75(5):832-843.

[54] Dror, V., Nguyen, V., Walia, P., Kalynyak, T.B., Hill, J.A., Johnson, J.D., 2007. Notch signalling suppresses apoptosis in adult human and mouse pancreatic islet cells. Diabetologia 50(12):2504-2515.

[55] Bartolome, A., Zhu, C., Sussel, L., Pajvani, U.B., 2019. Notch signaling dynamically regulates adult beta cell proliferation and maturity. J Clin Invest 129(1):268-280.

[56] Brown, M.L., Schneyer, A.L., 2010. Emerging roles for the TGFbeta family in pancreatic beta-cell homeostasis. Trends Endocrinol Metab 21(7):441-448.

[57] Blum, B., Roose, A.N., Barrandon, O., Maehr, R., Arvanites, A.C., Davidow, L.S., et al., 2014. Reversal of beta cell de-differentiation by a small molecule inhibitor of the TGFbeta pathway. Elife 3:e02809.

[58] Lee, H., Lee, Y.S., Harenda, Q., Pietrzak, S., Oktay, H.Z., Schreiber, S., et al., 2020. Beta Cell Dedifferentiation Induced by IRE1alpha Deletion Prevents Type 1 Diabetes. Cell Metab 31(4):822-836 e825.

[59] Perelis, M., Ramsey, K.M., Marcheva, B., Bass, J., 2016. Circadian Transcription from Beta Cell Function to Diabetes Pathophysiology. J Biol Rhythms 31(4):323-336.

[60] Petrenko, V., Gandasi, N.R., Sage, D., Tengholm, A., Barg, S., Dibner, C., 2020. In pancreatic islets from type 2 diabetes patients, the dampened circadian oscillators lead to reduced insulin and glucagon exocytosis. Proc Natl Acad Sci U S A 117(5):2484-2495.

[61] Unsal-Kacmaz, K., Mullen, T.E., Kaufmann, W.K., Sancar, A., 2005. Coupling of human circadian and cell cycles by the timeless protein. Mol Cell Biol 25(8):3109-3116.

[62] Persaud, S.J., 2017. Islet G-protein coupled receptors: therapeutic potential for diabetes. Curr Opin Pharmacol 37:24-28.

[63] Amisten, S., Salehi, A., Rorsman, P., Jones, P.M., Persaud, S.J., 2013. An atlas and functional analysis of G-protein coupled receptors in human islets of Langerhans. Pharmacol Ther 139(3):359-391.

[64] Ali, S., Lamont, B.J., Charron, M.J., Drucker, D.J., 2011. Dual elimination of the glucagon and GLP-1 receptors in mice reveals plasticity in the incretin axis. J Clin Invest 121(5):1917-1929.

[65] Yada, T., Damdindorj, B., Rita, R.S., Kurashina, T., Ando, A., Taguchi, M., et al., 2014. Ghrelin signalling in beta-cells regulates insulin secretion and blood glucose. Diabetes Obes Metab 16 Suppl 1:111-117.

[66] Lo, C.M., Obici, S., Dong, H.H., Haas, M., Lou, D., Kim, D.H., et al., 2011. Impaired insulin secretion and enhanced insulin sensitivity in cholecystokinin-deficient mice. Diabetes 60(7):2000-2007.

[67] Garcia-Tornadu, I., Ornstein, A.M., Chamson-Reig, A., Wheeler, M.B., Hill, D.J., Arany, E., et al., 2010. Disruption of the dopamine d2 receptor impairs insulin secretion and causes glucose intolerance. Endocrinology 151(4):1441-1450.

[68] Solini, A., Sebastiani, G., Nigi, L., Santini, E., Rossi, C., Dotta, F., 2017. Dapagliflozin modulates glucagon secretion in an SGLT2-independent manner in murine alpha cells. Diabetes Metab 43(6):512-520.

[69] Suga, T., Kikuchi, O., Kobayashi, M., Matsui, S., Yokota-Hashimoto, H., Wada, E., et al., 2019. SGLT1 in pancreatic alpha cells regulates glucagon secretion in mice, possibly explaining the distinct effects of SGLT2 inhibitors on plasma glucagon levels. Mol Metab 19:1-12.

[70] Bensellam, M., Maxwell, E.L., Chan, J.Y., Luzuriaga, J., West, P.K., Jonas, J.C., et al., 2016. Hypoxia reduces ER-to-Golgi protein trafficking and increases cell death by inhibiting the adaptive unfolded protein response in mouse beta cells. Diabetologia 59(7):1492-1502.

[71] Zehetner, J., Danzer, C., Collins, S., Eckhardt, K., Gerber, P.A., Ballschmieter, P., et al., 2008. PVHL is a regulator of glucose metabolism and insulin secretion in pancreatic beta cells. Genes Dev 22(22):3135-3146.

[72] Gerst, F., Jaghutriz, B.A., Staiger, H., Schulte, A.M., Lorza-Gil, E., Kaiser, G., et al., 2018. The Expression of Aldolase B in Islets Is Negatively Associated With Insulin Secretion in Humans. J Clin Endocrinol Metab 103(12):4373-4383.

[73] Guay, C., Joly, E., Pepin, E., Barbeau, A., Hentsch, L., Pineda, M., et al., 2013. A role for cytosolic isocitrate dehydrogenase as a negative regulator of glucose signaling for insulin secretion in pancreatic ss-cells. PLoS ONE 8(10):e77097.

[74] MacDonald, M.J., Longacre, M.J., Langberg, E.C., Tibell, A., Kendrick, M.A., Fukao, T., et al., 2009. Decreased levels of metabolic enzymes in pancreatic islets of patients with type 2 diabetes. Diabetologia 52(6):1087-1091.

[75] Chan, C.B., Harper, M.E., 2006. Uncoupling proteins: role in insulin resistance and insulin insufficiency. Curr Diabetes Rev 2(3):271-283.

[76] Li, N., Karaca, M., Maechler, P., 2017. Upregulation of UCP2 in beta-cells confers partial protection against both oxidative stress and glucotoxicity. Redox Biol 13:541-549.

[77] Lytrivi, M., Castell, A.L., Poitout, V., Cnop, M., 2020. Recent Insights Into Mechanisms of beta-Cell Lipo- and Glucolipotoxicity in Type 2 Diabetes. J Mol Biol 432(5):1514-1534.

[78] Noushmehr, H., D'Amico, E., Farilla, L., Hui, H., Wawrowsky, K.A., Mlynarski, W., et al., 2005. Fatty acid translocase (FAT/CD36) is localized on insulin-containing granules in human pancreatic beta-cells and mediates fatty acid effects on insulin secretion. Diabetes 54(2):472-481.

[79] Khan, S., Kowluru, A., 2018. CD36 mediates lipid accumulation in pancreatic beta cells under the duress of glucolipotoxic conditions: Novel roles of lysine deacetylases. Biochem Biophys Res Commun 495(3):2221-2226.

[80] Ye, R., Gordillo, R., Shao, M., Onodera, T., Chen, Z., Chen, S., et al., 2018. Intracellular lipid metabolism impairs beta cell compensation during diet-induced obesity. J Clin Invest 128(3):1178-1189.

[81] Lee, Y., Hirose, H., Ohneda, M., Johnson, J.H., McGarry, J.D., Unger, R.H., 1994. Beta-cell lipotoxicity in the pathogenesis of non-insulin-dependent diabetes mellitus of obese rats: impairment in adipocyte-beta-cell relationships. Proc Natl Acad Sci U S A 91:10878-10882.

[82] Vernier, S., Chiu, A., Schober, J., Weber, T., Nguyen, P., Luer, M., et al., 2012. beta-cell metabolic alterations under chronic nutrient overload in rat and human islets. Islets 4(6):379-392.

[83] Dai, C., Kayton, N.S., Shostak, A., Poffenberger, G., Cyphert, H.A., Aramandla, R., et al., 2016. Stress-impaired transcription factor expression and insulin secretion in transplanted human islets. J Clin Invest 126(5):1857-1870.

[84] Tong, X., Dai, C., Walker, J.T., Nair, G.G., Kennedy, A., Carr, R.M., et al., 2020. Lipid Droplet Accumulation in Human Pancreatic Islets Is Dependent On Both Donor Age and Health. Diabetes 69(3):342-354.

[85] Tiano, J.P., Delghingaro-Augusto, V., Le May, C., Liu, S., Kaw, M.K., Khuder, S.S., et al., 2011. Estrogen receptor activation reduces lipid synthesis in pancreatic islets and prevents beta cell failure in rodent models of type 2 diabetes. J Clin Invest 121(8):3331-3342.

[86] Biden, T.J., Boslem, E., Chu, K.Y., Sue, N., 2014. Lipotoxic endoplasmic reticulum stress, beta cell failure, and type 2 diabetes mellitus. Trends Endocrinol Metab 25(8):389-398.

[87] Newsholme, P., Bender, K., Kiely, A., Brennan, L., 2007. Amino acid metabolism, insulin secretion and diabetes. Biochem Soc Trans 35(Pt 5):1180-1186.

[88] Gheni, G., Ogura, M., Iwasaki, M., Yokoi, N., Minami, K., Nakayama, Y., et al., 2014. Glutamate acts as a key signal linking glucose metabolism to incretin/cAMP action to amplify insulin secretion. Cell Rep 9(2):661-673.

[89] Cheng, Q., Beltran, V.D., Chan, S.M., Brown, J.R., Bevington, A., Herbert, T.P., 2016. System-L amino acid transporters play a key role in pancreatic beta-cell signalling and function. J Mol Endocrinol 56(3):175-187.

[90] Kowalczuk, S., Broer, A., Tietze, N., Vanslambrouck, J.M., Rasko, J.E., Broer, S., 2008. A protein complex in the brush-border membrane explains a Hartnup disorder allele. FASEB J 22(8):2880-2887.

[91] Hayashi, T., Abiko, K., Mandai, M., Yaegashi, N., Konishi, I., 2020. Highly conserved binding region of ACE2 as a receptor for SARS-CoV-2 between humans and mammals. Vet Q 40(1):243-249.

[92] Blodgett, D.M., Nowosielska, A., Afik, S., Pechhold, S., Cura, A.J., Kennedy, N.J., et al., 2015. Novel Observations From Next-Generation RNA Sequencing of Highly Purified Human Adult and Fetal Islet Cell Subsets. Diabetes 64(9):3172-3181.

[93] Hori, Y., Rulifson, I.C., Tsai, B.C., Heit, J.J., Cahoy, J.D., Kim, S.K., 2002. Growth inhibitors promote differentiation of insulin-producing tissue from embryonic stem cells. Proc Natl Acad Sci U S A 99(25):16105-16110.

[94] Lehtihet, M., Webb, D.L., Honkanen, R.E., Sjoholm, A., 2005. Glutamate inhibits protein phosphatases and promotes insulin exocytosis in pancreatic beta-cells. Biochem Biophys Res Commun 328(2):601-607.

[95] Fu, A., Alvarez-Perez, J.C., Avizonis, D., Kin, T., Ficarro, S.B., Choi, D.W., et al., 2020. Glucose-dependent partitioning of arginine to the urea cycle protects beta-cells from inflammation. Nat Metab 2(5):432-446.

[96] Boni-Schnetzler, M., Meier, D.T., 2019. Islet inflammation in type 2 diabetes. Semin Immunopathol 41(4):501-513.

[97] Wali, J.A., Masters, S.L., Thomas, H.E., 2013. Linking metabolic abnormalities to apoptotic pathways in Beta cells in type 2 diabetes. Cells 2(2):266-283.

[98] Atanes, P., Lee, V., Huang, G.C., Persaud, S.J., 2020. The role of the CCL25-CCR9 axis in beta-cell function: potential for therapeutic intervention in type 2 diabetes. Metabolism 113:154394.

[99] Frigerio, S., Hollander, G.A., Zumsteg, U., 2002. Functional IL-18 Is produced by primary pancreatic mouse islets and NIT-1 beta cells and participates in the progression towards destructive insulitis. Horm Res 57(3-4):94-104.

[100] Dos Santos, R.S., Marroqui, L., Grieco, F.A., Marselli, L., Suleiman, M., Henz, S.R., et al., 2017. Protective Role of Complement C3 Against Cytokine-Mediated beta-Cell Apoptosis. Endocrinology 158(8):2503-2521.

[101] King, B.C., Kulak, K., Krus, U., Rosberg, R., Golec, E., Wozniak, K., et al., 2019. Complement Component C3 Is Highly Expressed in Human Pancreatic Islets and Prevents beta Cell Death via ATG16L1 Interaction and Autophagy Regulation. Cell Metab 29(1):202-210 e206.

[102] Bowen, A., Kos, K., Whatmore, J., Richardson, S., Welters, H.J., 2016. Wnt4 antagonises Wnt3a mediated increases in growth and glucose stimulated insulin secretion in the pancreatic beta-cell line, INS-1. Biochem Biophys Res Commun 479(4):793-799.

[103] Ebrahimi, A.G., Hollister-Lock, J., Sullivan, B.A., Tsuchida, R., Bonner-Weir, S., Weir, G.C., 2020. Beta cell identity changes with mild hyperglycemia: Implications for function, growth, and vulnerability. Mol Metab 35:100959.

[104] Roma, L.P., Jonas, J.C., 2020. Nutrient Metabolism, Subcellular Redox State, and Oxidative Stress in Pancreatic Islets and beta-Cells. J Mol Biol 432(5):1461-1493.

[105] Shalev, A., Pise-Masison, C.A., Radonovich, M., Hoffmann, S.C., Hirshberg, B., Brady, J.N., et al., 2002. Oligonucleotide microarray analysis of intact human pancreatic islets: identification of glucose-responsive genes and a highly regulated TGFbeta signaling pathway. Endocrinology 143(9):3695-3698.

[106] Thielen, L., Shalev, A., 2018. Diabetes pathogenic mechanisms and potential new therapies based upon a novel target called TXNIP. Curr Opin Endocrinol Diabetes Obes 25(2):75-80.

[107] Zhang, J., An, H., Ni, K., Chen, B., Li, H., Li, Y., et al., 2019. Glutathione prevents chronic oscillating glucose intake-induced beta-cell dedifferentiation and failure. Cell Death Dis 10(4):321.

[108] Lou, J., Chen, H., Han, J., He, H., Huen, M.S.Y., Feng, X.H., et al., 2017. AUNIP/C1orf135 directs DNA double-strand breaks towards the homologous recombination repair pathway. Nat Commun 8(1):985.

[109] Mohanty, S., Spinas, G.A., Maedler, K., Zuellig, R.A., Lehmann, R., Donath, M.Y., et al., 2005. Overexpression of IRS2 in isolated pancreatic islets causes proliferation and protects human beta-cells from hyperglycemia-induced apoptosis. Exp Cell Res 303(1):68-78.

[110] Lavine, J.A., Raess, P.W., Stapleton, D.S., Rabaglia, M.E., Suhonen, J.I., Schueler, K.L., et al., 2010. Cholecystokinin is up-regulated in obese mouse islets and expands beta-cell mass by increasing beta-cell survival. Endocrinology 151(8):3577-3588.

[111] Kanno, A., Asahara, S.I., Kawamura, M., Furubayashi, A., Tsuchiya, S., Suzuki, E., et al., 2019. Early administration of dapagliflozin preserves pancreatic beta-cell mass through a legacy effect in a mouse model of type 2 diabetes. J Diabetes Investig 10(3):577-590.

[112] Bugliani, M., Liechti, R., Cheon, H., Suleiman, M., Marselli, L., Kirkpatrick, C., et al., 2013. Microarray analysis of isolated human islet transcriptome in type 2 diabetes and the role of the ubiquitin-proteasome system in pancreatic beta cell dysfunction. Mol Cell Endocrinol 367(1-2):1-10.

[113] Kim-Muller, J.Y., Zhao, S., Srivastava, S., Mugabo, Y., Noh, H.L., Kim, Y.R., et al., 2014. Metabolic inflexibility impairs insulin secretion and results in MODY-like diabetes in triple FoxO-deficient mice. Cell Metab 20(4):593-602.

[114] Keller, M.P., Paul, P.K., Rabaglia, M.E., Stapleton, D.S., Schueler, K.L., Broman, A.T., et al., 2016. The Transcription Factor Nfatc2 Regulates beta-Cell Proliferation and Genes Associated with Type 2 Diabetes in Mouse and Human Islets. PLoS Genet 12(12):e1006466.

[115] Heit, J.J., Apelqvist, A.A., Gu, X., Winslow, M.M., Neilson, J.R., Crabtree, G.R., et al., 2006. Calcineurin/NFAT signalling regulates pancreatic beta-cell growth and function. Nature 443(7109):345-349.

[116] Kennedy, G.C., Rutter, W.J., 1992. Pur-1, a zinc-finger protein that binds to purine-rich sequences, transactivates an insulin promoter in heterologous cells. Proc Natl Acad Sci U S A 89(23):11498-11502.

[117] Gupta, M.K., Vadde, R., 2019. Identification and characterization of differentially expressed genes in Type 2 Diabetes using in silico approach. Comput Biol Chem 79:24-35.

Figure 1

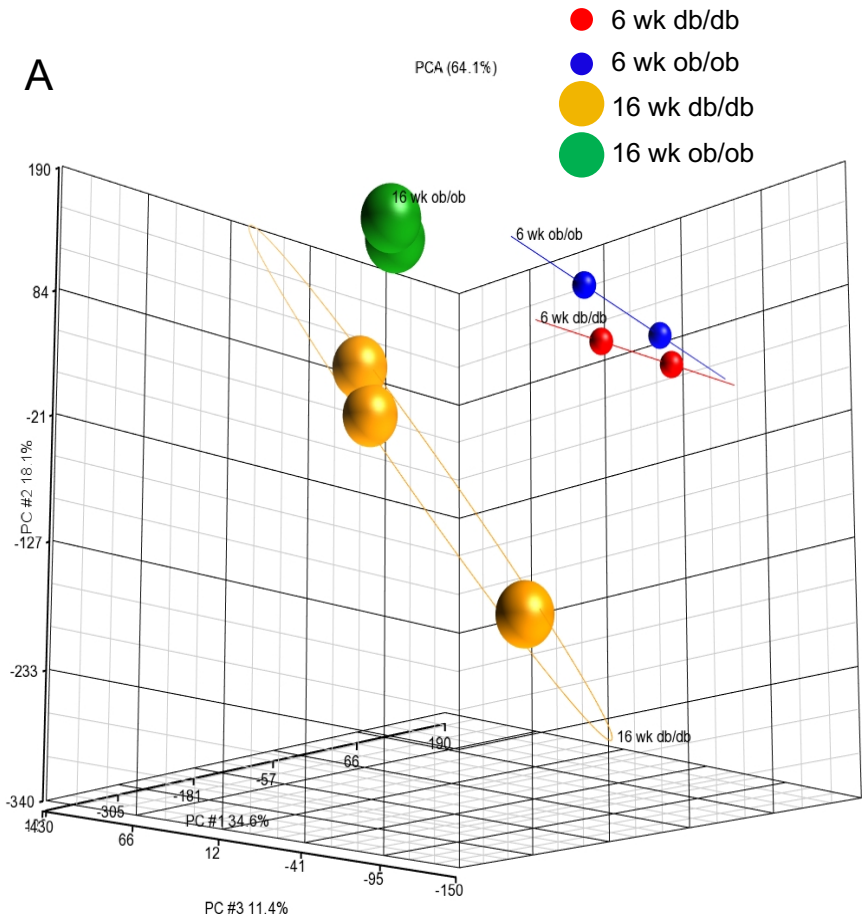
A
PCA (64.1%)
6 wk db/db
6 wk ob/ob
16 wk db/db
16 wk ob/ob
16 wk ob/ob
6 wk ob/ob
6 wk db/db
16 wk db/db
190
84
-21
-127
-233
-340
PC #2 18.1%
1430
66
-305
-181
-57
66
190
PC #1 34.6%
66
12
-41
-95
-150
PC #3 11.4%

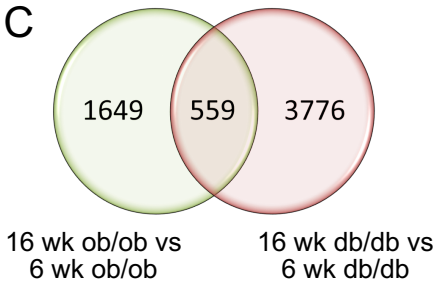
C
1649
559
3776
16 wk ob/ob vs 6 wk ob/ob
16 wk db/db vs 6 wk db/db

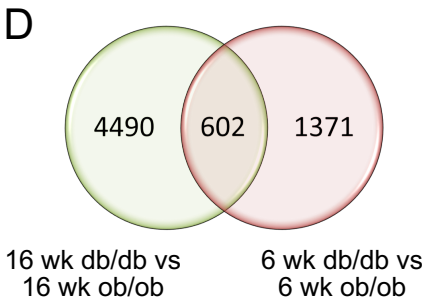
D
4490
602
1371
16 wk db/db vs 16 wk ob/ob
6 wk db/db vs 6 wk ob/ob

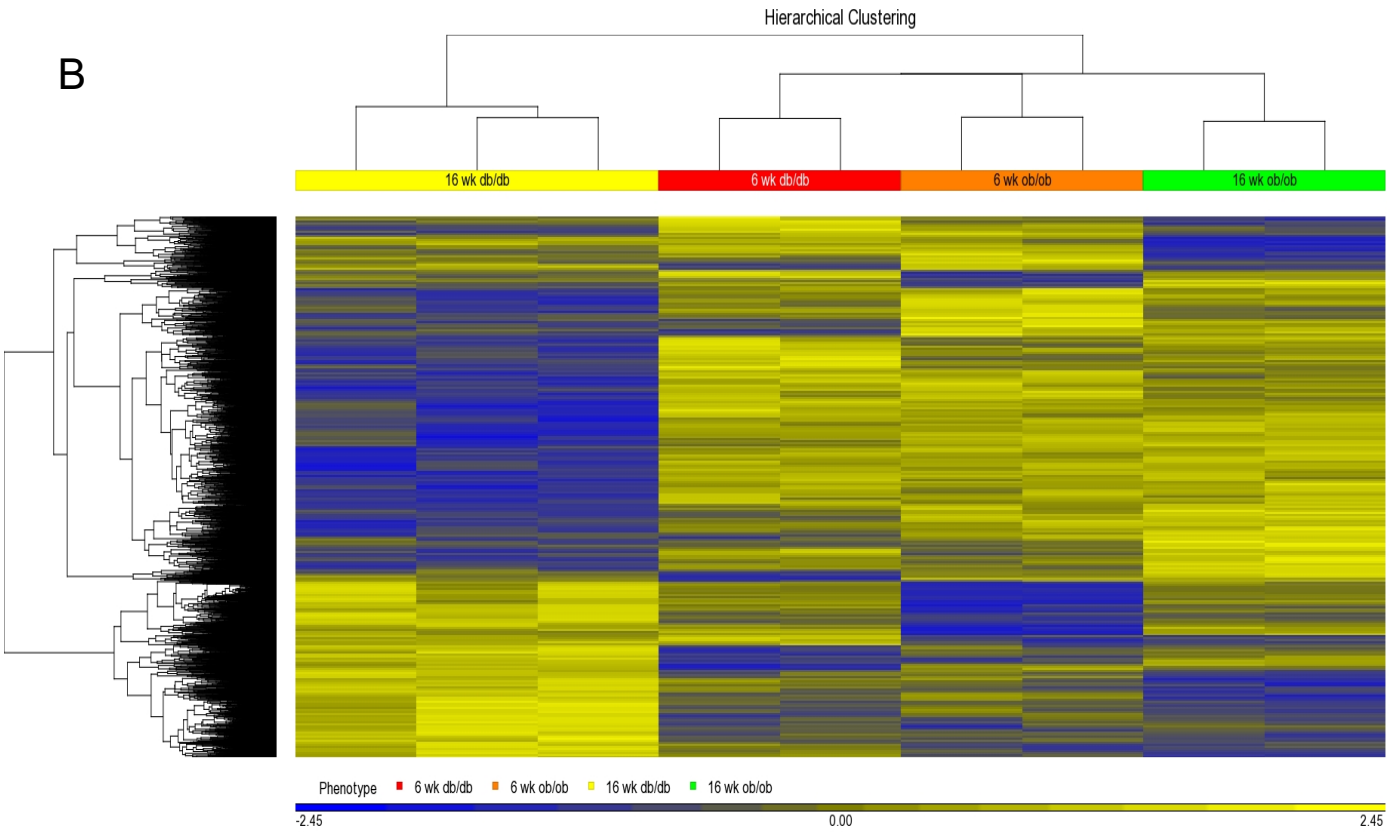
B
Hierarchical Clustering
16 wk db/db
6 wk db/db
6 wk ob/ob
16 wk ob/ob
Phenotype
6 wk db/db
6 wk ob/ob
16 wk db/db
16 wk ob/ob
-2.45
0.00
2.45

Figure 2

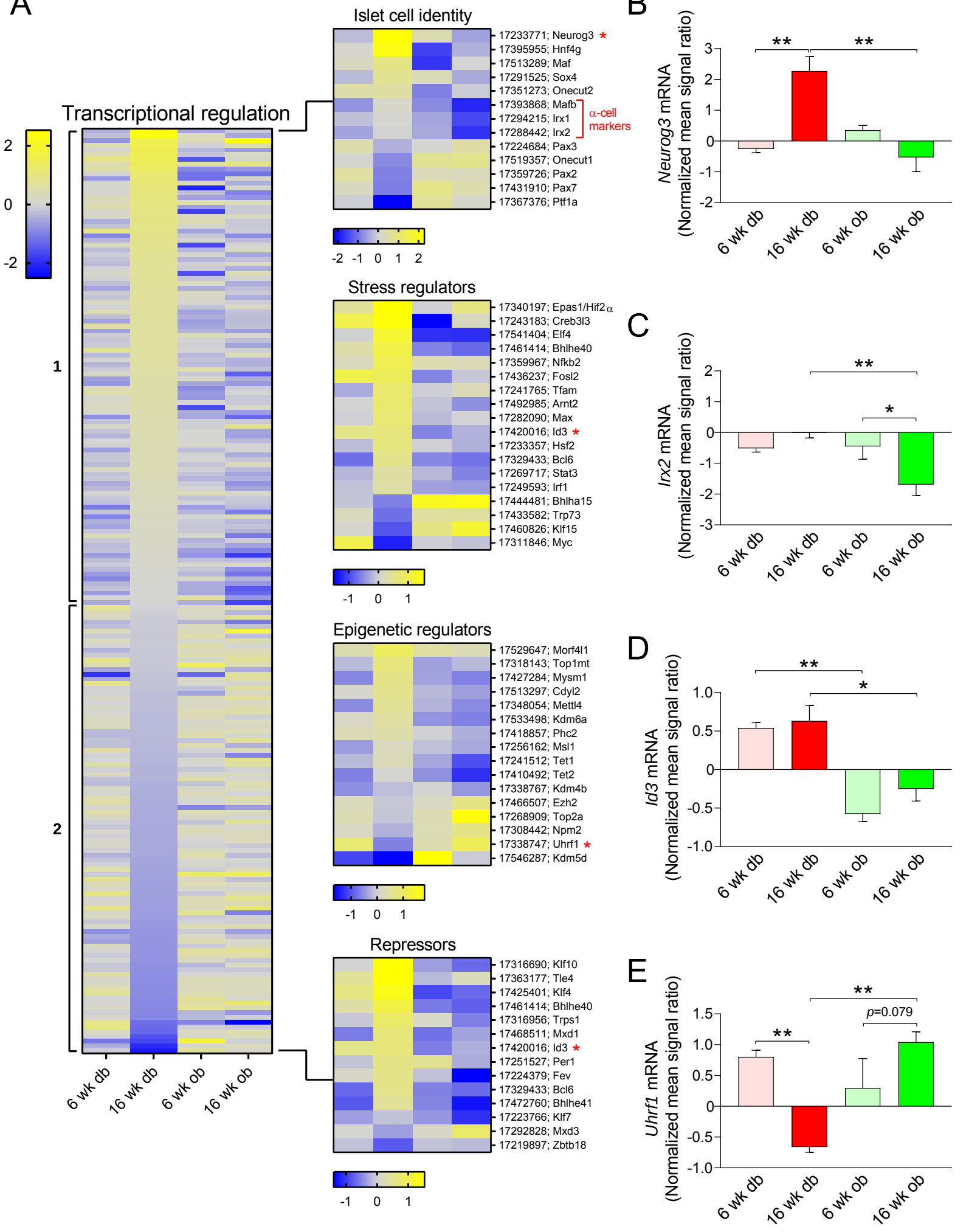
A
Transcriptional regulation
2
0
-2
1
2
6 wk db
16 wk db
6 wk ob
16 wk ob
Islet cell identity
17233771; Neurog3 *
17395955; Hnf4g
17513289; Maf
17291525; Sox4
17351273; Onecut2
17393868; Mafb
17294215; Irx1
17288442; Irx2
α-cell markers
17224684; Pax3
17519357; Onecut1
17359726; Pax2
17431910; Pax7
17367376; Ptf1a
-2 -1 0 1 2
Stress regulators
17340197; Epas1/Hif2α
17243183; Creb3l3
17541404; Elf4
17461414; Bhlhe40
17359967; Nfkb2
17436237; Fosl2
17241765; Tfam
17492985; Arnt2
17282090; Max
17420016; Id3 *
17233357; Hsf2
17329433; Bcl6
17269717; Stat3
17249593; Irf1
17444481; Bhlha15
17433582; Trp73
17460826; Klf15
17311846; Myc
-1 0 1
Epigenetic regulators
17529647; Morf4l1
17318143; Top1mt
17427284; Mysm1
17513297; Cdyl2
17348054; Mettl4
17533498; Kdm6a
17418857; Phc2
17256162; Msl1
17241512; Tet1
17410492; Tet2
17338767; Kdm4b
17466507; Ezh2
17268909; Top2a
17308442; Npm2
17338747; Uhrf1 *
17546287; Kdm5d
-1 0 1
Repressors
17316690; Klf10
17363177; Tle4
17425401; Klf4
17461414; Bhlhe40
17316956; Trps1
17468511; Mxd1
17420016; Id3 *
17251527; Per1
17224379; Fev
17329433; Bcl6
17472760; Bhlhe41
17223766; Klf7
17292828; Mxd3
17219897; Zbtb18
-1 0 1
B
Neurog3 mRNA (Normalized mean signal ratio)
3
2
1
0
-1
-2
**
**
6 wk db
16 wk db
6 wk ob
16 wk ob
C
Irx2 mRNA (Normalized mean signal ratio)
2
1
0
-1
-2
-3
**
*
6 wk db
16 wk db
6 wk ob
16 wk ob
D
Id3 mRNA (Normalized mean signal ratio)
1.0
0.5
0
-0.5
-1.0
**
*
6 wk db
16 wk db
6 wk ob
16 wk ob
E
Uhrf1 mRNA (Normalized mean signal ratio)
1.5
1.0
0.5
0
-0.5
-1.0
**
**
p=0.079
6 wk db
16 wk db
6 wk ob
16 wk ob

Figure 3

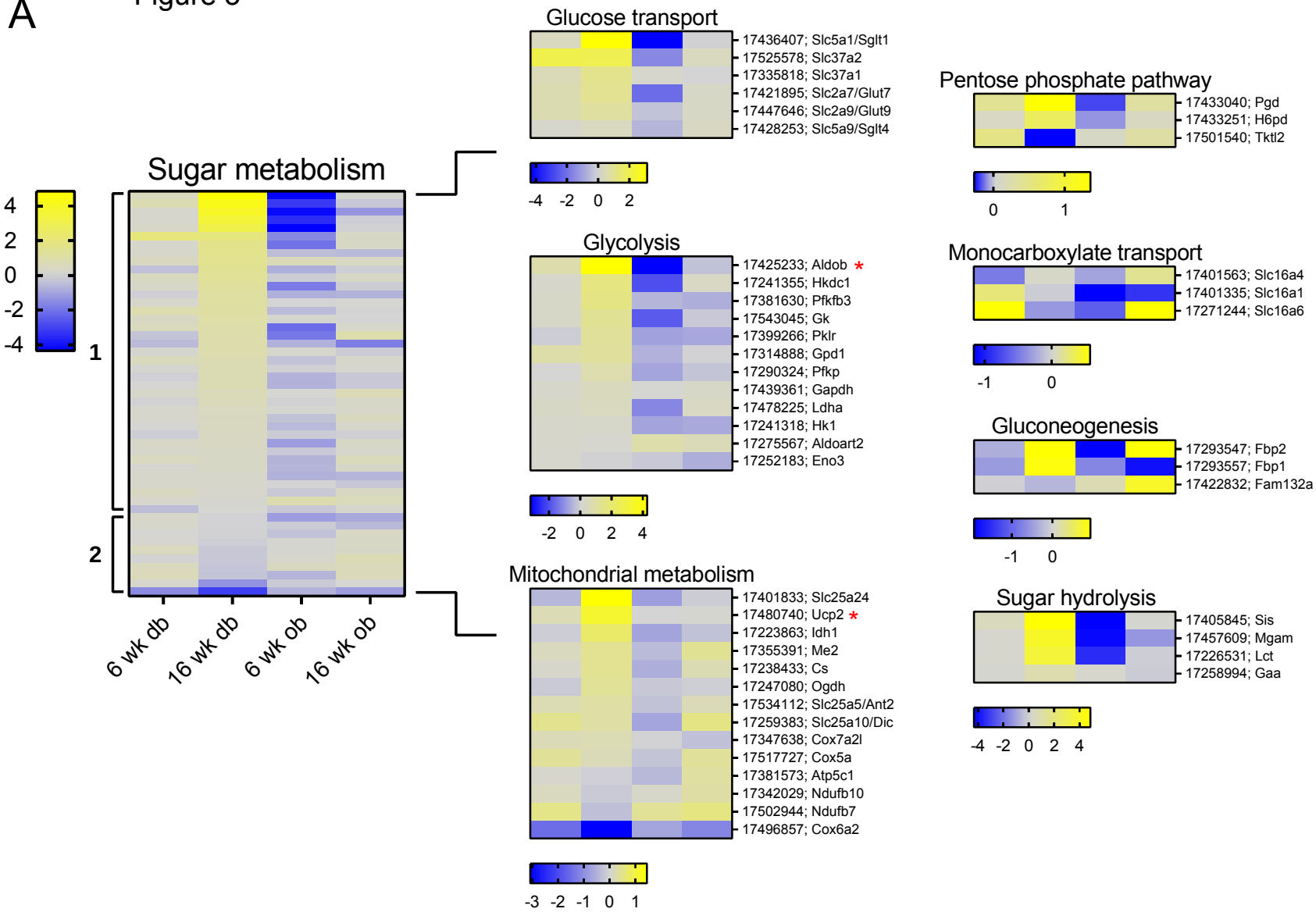
A
Sugar metabolism
4
2
0
-2
-4
1
2
6 wk db
16 wk db
6 wk ob
16 wk ob
Glucose transport
17436407; Slc5a1/Sglt1
17525578; Slc37a2
17335818; Slc37a1
17421895; Slc2a7/Glut7
17447646; Slc2a9/Glut9
17428253; Slc5a9/Sglt4
-4 -2 0 2
Glycolysis
17425233; Aldob *
17241355; Hkdc1
17381630; Pfkfb3
17543045; Gk
17399266; Pklr
17314888; Gpd1
17290324; Pfkp
17439361; Gapdh
17478225; Ldha
17241318; Hk1
17275567; Aldoart2
17252183; Eno3
-2 0 2 4
Mitochondrial metabolism
17401833; Slc25a24
17480740; Ucp2 *
17223863; Idh1
17355391; Me2
17238433; Cs
17247080; Ogdh
17534112; Slc25a5/Ant2
17259383; Slc25a10/Dic
17347638; Cox7a2l
17517727; Cox5a
17381573; Atp5c1
17342029; Ndufb10
17502944; Ndufb7
17496857; Cox6a2
-3 -2 -1 0 1
Pentose phosphate pathway
17433040; Pgd
17433251; H6pd
17501540; Tktl2
0 1
Monocarboxylate transport
17401563; Slc16a4
17401335; Slc16a1
17271244; Slc16a6
-1 0
Gluconeogenesis
17293547; Fbp2
17293557; Fbp1
17422832; Fam132a
-1 0
Sugar hydrolysis
17405845; Sis
17457609; Mgam
17226531; Lct
17258994; Gaa
-4 -2 0 2 4

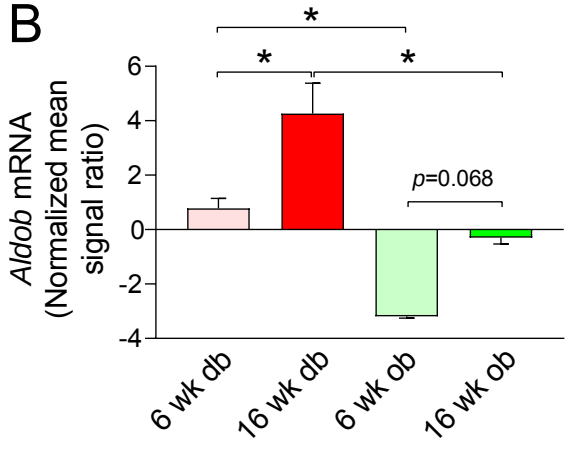
B
Aldob mRNA (Normalized mean signal ratio)
6
4
2
0
-2
-4
*
*
*
p=0.068
6 wk db
16 wk db
6 wk ob
16 wk ob

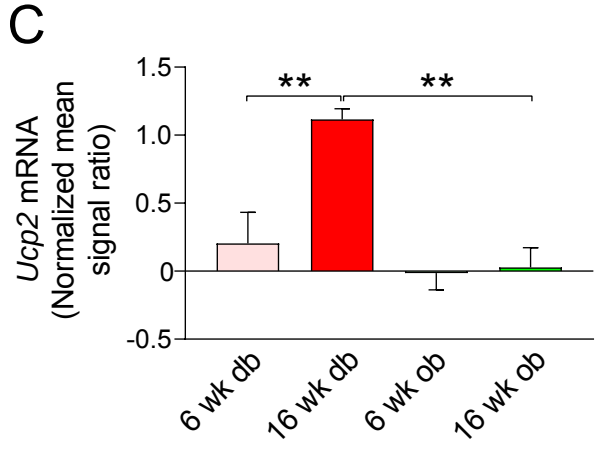
C
Ucp2 mRNA (Normalized mean signal ratio)
1.5
1.0
0.5
0
-0.5
**
**
6 wk db
16 wk db
6 wk ob
16 wk ob

Figure 4

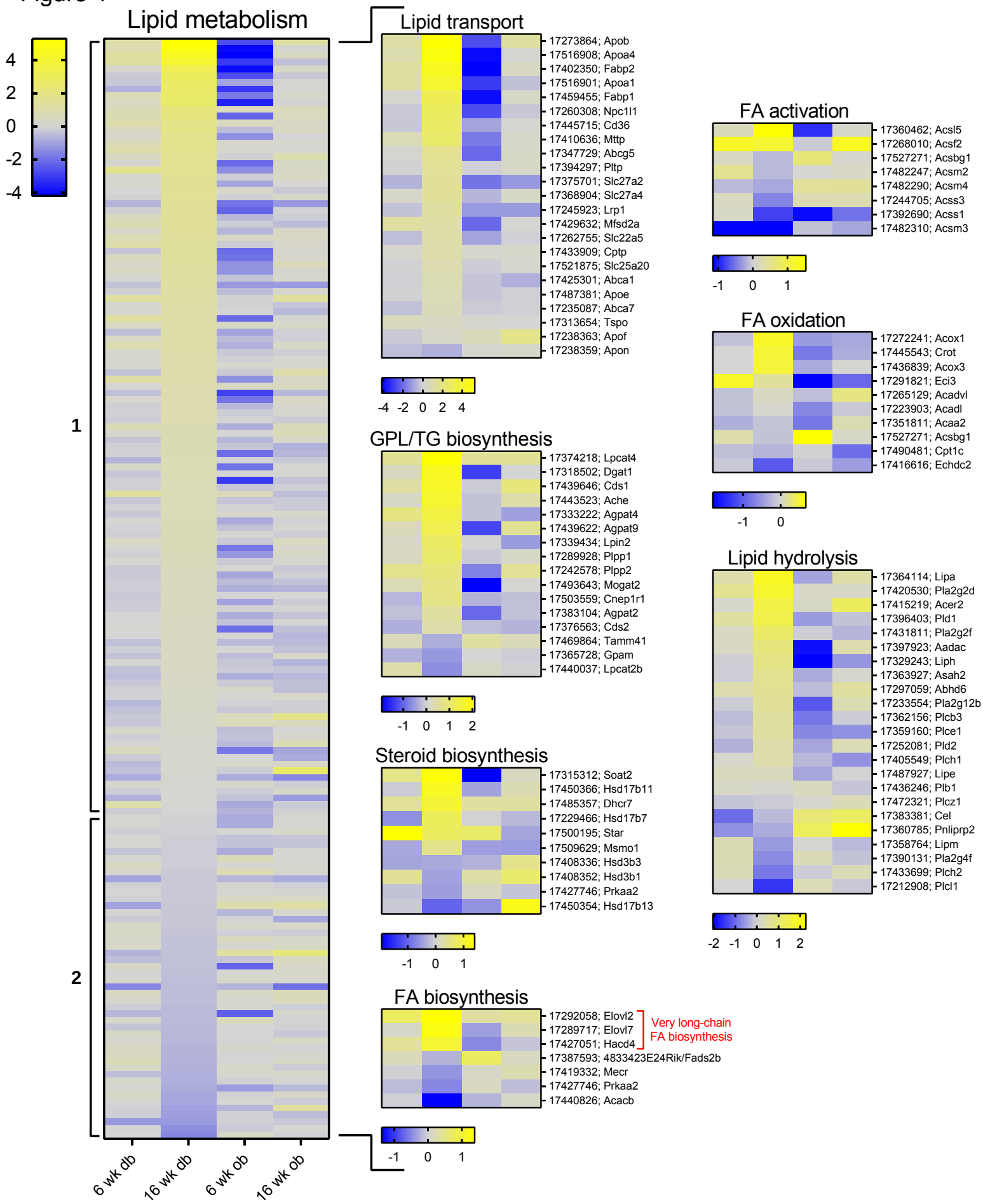
Lipid metabolism
4
2
0
-2
-4
1
2
6 wk db
16 wk db
6 wk ob
16 wk ob
Lipid transport
17273864; Apob
17516908; Apoa4
17402350; Fabp2
17516901; Apoa1
17459455; Fabp1
17260308; Npc1l1
17445715; Cd36
17410636; Mttp
17347729; Abcg5
17394297; Pltp
17375701; Slc27a2
17368904; Slc27a4
17245923; Lrp1
17429632; Mfsd2a
17262755; Slc22a5
17433909; Cptp
17521875; Slc25a20
17425301; Abca1
17487381; Apoe
17235087; Abca7
17313654; Tspo
17238363; Apof
17238359; Apon
-4 -2 0 2 4
GPL/TG biosynthesis
17374218; Lpcat4
17318502; Dgat1
17439646; Cds1
17443523; Ache
17333222; Agpat4
17439622; Agpat9
17339434; Lpin2
17289928; Plpp1
17242578; Plpp2
17493643; Mogat2
17503559; Cnep1r1
17383104; Agpat2
17376563; Cds2
17469864; Tamm41
17365728; Gpam
17440037; Lpcat2b
-1 0 1 2
Steroid biosynthesis
17315312; Soat2
17450366; Hsd17b11
17485357; Dhcr7
17229466; Hsd17b7
17500195; Star
17509629; Msmo1
17408336; Hsd3b3
17408352; Hsd3b1
17427746; Prkaa2
17450354; Hsd17b13
-1 0 1
FA biosynthesis
17292058; Elovl2
17289717; Elovl7
17427051; Hacd4
Very long-chain FA biosynthesis
17387593; 4833423E24Rik/Fads2b
17419332; Mecr
17427746; Prkaa2
17440826; Acacb
-1 0 1
FA activation
17360462; Acsl5
17268010; Acsf2
17527271; Acsbg1
17482247; Acsm2
17482290; Acsm4
17244705; Acss3
17392690; Acss1
17482310; Acsm3
-1 0 1
FA oxidation
17272241; Acox1
17445543; Crot
17436839; Acox3
17291821; Eci3
17265129; Acadvl
17223903; Acadl
17351811; Acaa2
17527271; Acsbg1
17490481; Cpt1c
17416616; Echdc2
-1 0
Lipid hydrolysis
17364114; Lipa
17420530; Pla2g2d
17415219; Acer2
17396403; Pld1
17431811; Pla2g2f
17397923; Aadac
17329243; Liph
17363927; Asah2
17297059; Abhd6
17233554; Pla2g12b
17362156; Plcb3
17359160; Plce1
17252081; Pld2
17405549; Plch1
17487927; Lipe
17436246; Plb1
17472321; Plcz1
17383381; Cel
17360785; Pnliprp2
17358764; Lipm
17390131; Pla2g4f
17433699; Plch2
17212908; Plcl1
-2 -1 0 1 2

Figure 5

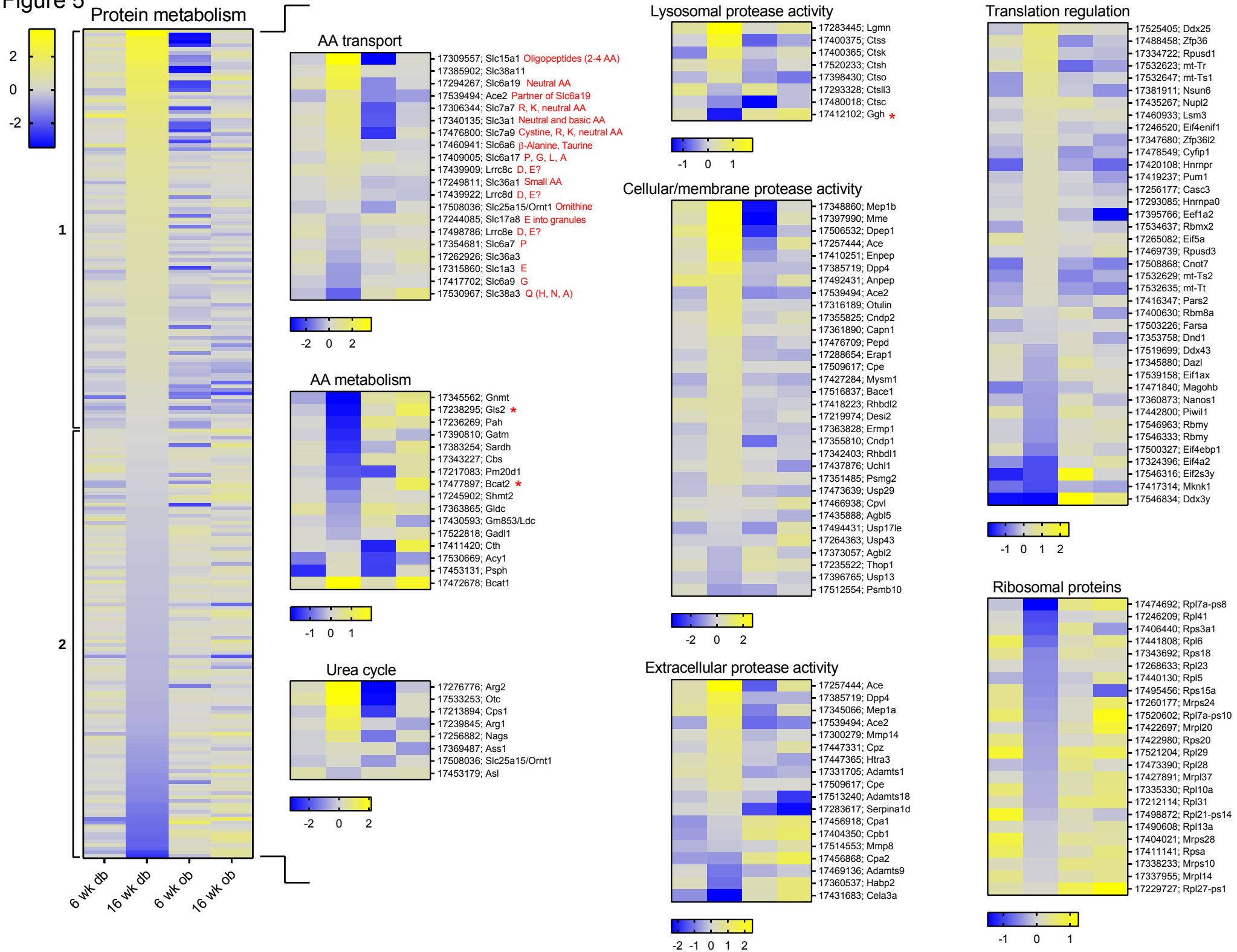
Protein metabolism
2
0
-2
1
2
6 wk db
16 wk db
6 wk ob
16 wk ob
AA transport
17309557; Slc15a1 Oligopeptides (2-4 AA)
17385902; Slc38a11
17294267; Slc6a19 Neutral AA
17539494; Ace2 Partner of Slc6a19
17306344; Slc7a7 R, K, neutral AA
17340135; Slc3a1 Neutral and basic AA
17476800; Slc7a9 Cystine, R, K, neutral AA
17460941; Slc6a6 β-Alanine, Taurine
17409005; Slc6a17 P, G, L, A
17439909; Lrrc8c D, E?
17249811; Slc36a1 Small AA
17439922; Lrrc8d D, E?
17508036; Slc25a15/Ornt1 Ornithine
17244085; Slc17a8 E into granules
17498786; Lrrc8e D, E?
17354681; Slc6a7 P
17262926; Slc36a3
17315860; Slc1a3 E
17417702; Slc6a9 G
17530967; Slc38a3 Q (H, N, A)
-2 0 2
AA metabolism
17345562; Gnmt
17238295; Gls2 *
17236269; Pah
17390810; Gatm
17383254; Sardh
17343227; Cbs
17217083; Pm20d1
17477897; Bcat2 *
17245902; Shmt2
17363865; Gldc
17430593; Gm853/Ldc
17522818; Gadl1
17411420; Cth
17530669; Acy1
17453131; Psph
17472678; Bcat1
-1 0 1
Urea cycle
17276776; Arg2
17533253; Otc
17213894; Cps1
17239845; Arg1
17256882; Nags
17369487; Ass1
17508036; Slc25a15/Ornt1
17453179; Asl
-2 0 2
Lysosomal protease activity
17283445; Lgmn
17400375; Ctss
17400365; Ctsk
17520233; Ctsh
17398430; Ctso
17293328; Ctsll3
17480018; Ctsc
17412102; Ggh *
-1 0 1
Cellular/membrane protease activity
17348860; Mep1b
17397990; Mme
17506532; Dpep1
17257444; Ace
17410251; Enpep
17385719; Dpp4
17492431; Anpep
17539494; Ace2
17316189; Otulin
17355825; Cndp2
17361890; Capn1
17476709; Pepd
17288654; Erap1
17509617; Cpe
17427284; Mysm1
17516837; Bace1
17418223; Rhbdl2
17219974; Desi2
17363828; Ermp1
17355810; Cndp1
17342403; Rhbdl1
17437876; Uchl1
17351485; Psmg2
17473639; Usp29
17466938; Cpvl
17435888; Agbl5
17494431; Usp17le
17264363; Usp43
17373057; Agbl2
17235522; Thop1
17396765; Usp13
17512554; Psmb10
-2 0 2
Extracellular protease activity
17257444; Ace
17385719; Dpp4
17345066; Mep1a
17539494; Ace2
17300279; Mmp14
17447331; Cpz
17447365; Htra3
17331705; Adamts1
17509617; Cpe
17513240; Adamts18
17283617; Serpina1d
17456918; Cpa1
17404350; Cpb1
17514553; Mmp8
17456868; Cpa2
17469136; Adamts9
17360537; Habp2
17431683; Cela3a
-2 -1 0 1 2
Translation regulation
17525405; Ddx25
17488458; Zfp36
17334722; Rpusd1
17532623; mt-Tr
17532647; mt-Ts1
17381911; Nsun6
17435267; Nupl2
17460933; Lsm3
17246520; Eif4enif1
17347680; Zfp36l2
17478549; Cyfip1
17420108; Hnrnpr
17419237; Pum1
17256177; Casc3
17293085; Hnrnpa0
17395766; Eef1a2
17534637; Rbmx2
17265082; Eif5a
17469739; Rpusd3
17508868; Cnot7
17532629; mt-Ts2
17532635; mt-Tt
17416347; Pars2
17400630; Rbm8a
17503226; Farsa
17353758; Dnd1
17519699; Ddx43
17345880; Dazl
17539158; Eif1ax
17471840; Magohb
17360873; Nanos1
17442800; Piwil1
17546963; Rbmy
17546333; Rbmy
17500327; Eif4ebp1
17324396; Eif4a2
17546316; Eif2s3y
17417314; Mknk1
17546834; Ddx3y
-1 0 1 2
Ribosomal proteins
17474692; Rpl7a-ps8
17246209; Rpl41
17406440; Rps3a1
17441808; Rpl6
17343692; Rps18
17268633; Rpl23
17440130; Rpl5
17495456; Rps15a
17260177; Mrps24
17520602; Rpl7a-ps10
17422697; Mrpl20
17422980; Rps20
17521204; Rpl29
17473390; Rpl28
17427891; Mrpl37
17335330; Rpl10a
17212114; Rpl31
17498872; Rpl21-ps14
17490608; Rpl13a
17404021; Mrps28
17411141; Rpsa
17338233; Mrps10
17337955; Mrpl14
17229727; Rpl27-ps1
-1 0 1

Figure 6

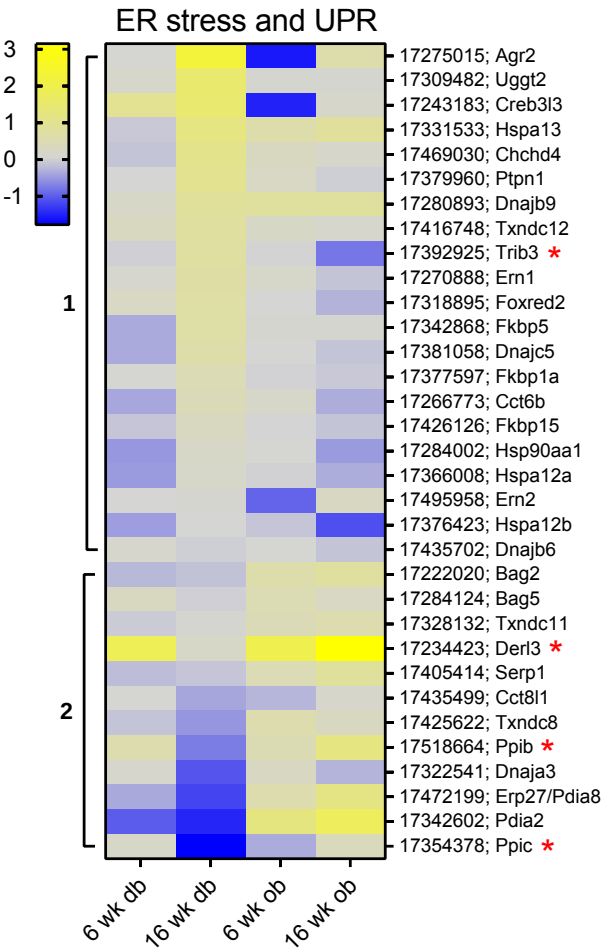
A
ER stress and UPR
3
2
1
0
-1
1
2
17275015; Agr2
17309482; Uggt2
17243183; Creb3l3
17331533; Hspa13
17469030; Chchd4
17379960; Ptpn1
17280893; Dnajb9
17416748; Txndc12
17392925; Trib3 *
17270888; Ern1
17318895; Foxred2
17342868; Fkbp5
17381058; Dnajc5
17377597; Fkbp1a
17266773; Cct6b
17426126; Fkbp15
17284002; Hsp90aa1
17366008; Hspa12a
17495958; Ern2
17376423; Hspa12b
17435702; Dnajb6
17222020; Bag2
17284124; Bag5
17328132; Txndc11
17234423; Derl3 *
17405414; Serp1
17435499; Cct8l1
17425622; Txndc8
17518664; Ppib *
17322541; Dnaja3
17472199; Erp27/Pdia8
17342602; Pdia2
17354378; Ppic *
6 wk db
16 wk db
6 wk ob
16 wk ob

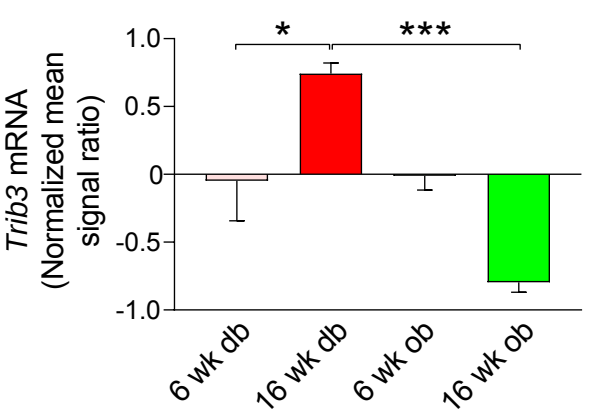
B
Trib3 mRNA (Normalized mean signal ratio)
1.0
0.5
0
-0.5
-1.0
*
***
6 wk db
16 wk db
6 wk ob
16 wk ob

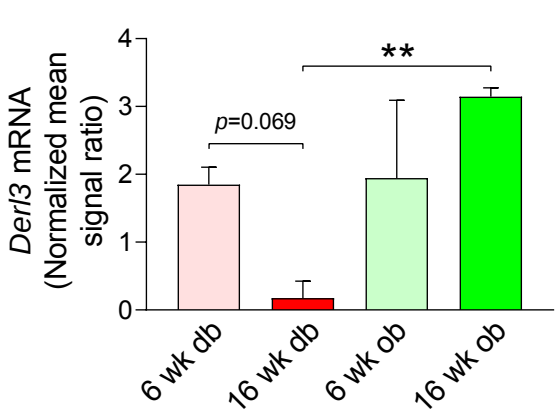
C
Derl3 mRNA (Normalized mean signal ratio)
4
3
2
1
0
p=0.069
**
6 wk db
16 wk db
6 wk ob
16 wk ob

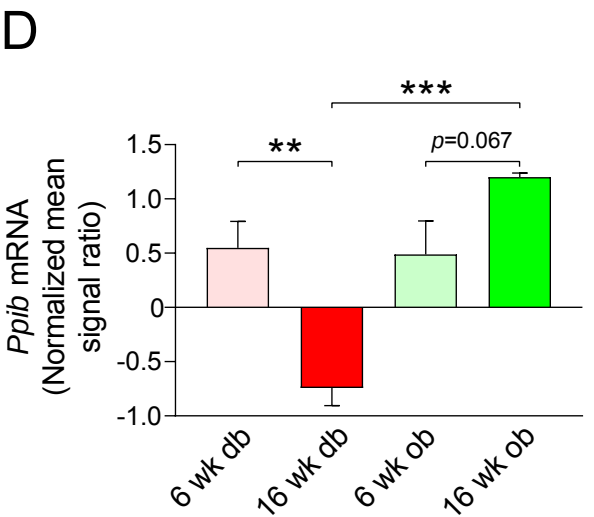
D
Ppib mRNA (Normalized mean signal ratio)
1.5
1.0
0.5
0
-0.5
-1.0
**
***
p=0.067
6 wk db
16 wk db
6 wk ob
16 wk ob

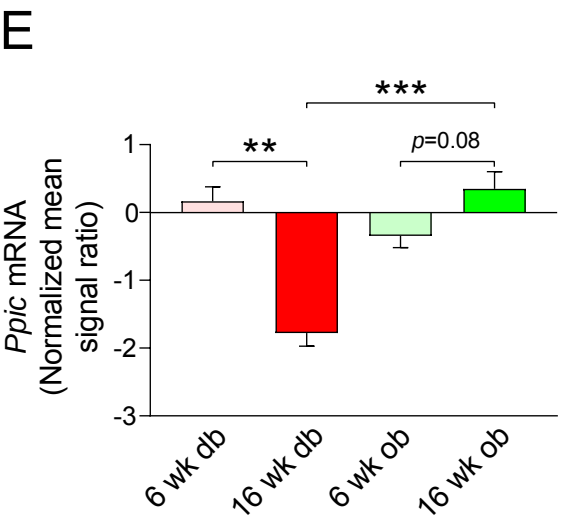
E
Ppic mRNA (Normalized mean signal ratio)
1
0
-1
-2
-3
**
***
p=0.08
6 wk db
16 wk db
6 wk ob
16 wk ob

Figure 7

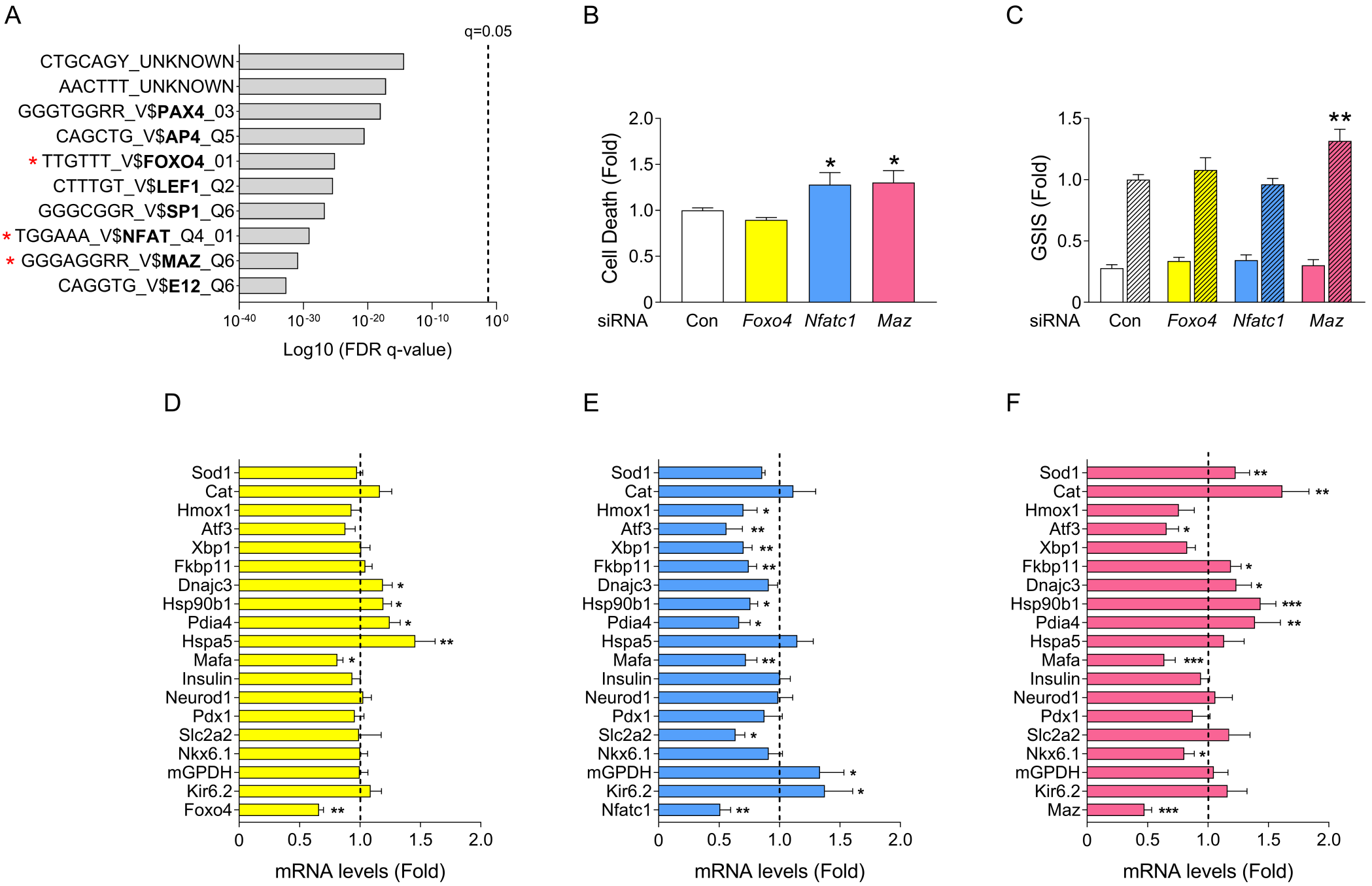
A
q=0.05
CTGCAGY_UNKNOWN
AACTTT_UNKNOWN
GGGTGGRR_V$PAX4_03
CAGCTG_V$AP4_Q5
* TTGTTT_V$FOXO4_01
CTTTGT_V$LEF1_Q2
GGGCGGR_V$SP1_Q6
* TGGAAA_V$NFAT_Q4_01
* GGGAGGRR_V$MAZ_Q6
CAGGTG_V$E12_Q6
10-40 10-30 10-20 10-10 100
Log10 (FDR q-value)
B
Cell Death (Fold)
2.0
1.5
1.0
0.5
0
siRNA Con Foxo4 Nfatc1 Maz
C
GSIS (Fold)
1.5
1.0
0.5
0
siRNA Con Foxo4 Nfatc1 Maz
D
Sod1 Cat Hmox1 Atf3 Xbp1 Fkbp11 Dnajc3 Hsp90b1 Pdia4 Hspa5 Mafa Insulin Neurod1 Pdx1 Slc2a2 Nkx6.1 mGPDH Kir6.2 Foxo4
0 0.5 1.0 1.5 2.0
mRNA levels (Fold)
E
Sod1 Cat Hmox1 Atf3 Xbp1 Fkbp11 Dnajc3 Hsp90b1 Pdia4 Hspa5 Mafa Insulin Neurod1 Pdx1 Slc2a2 Nkx6.1 mGPDH Kir6.2 Nfatc1
0 0.5 1.0 1.5 2.0
mRNA levels (Fold)
F
Sod1 Cat Hmox1 Atf3 Xbp1 Fkbp11 Dnajc3 Hsp90b1 Pdia4 Hspa5 Mafa Insulin Neurod1 Pdx1 Slc2a2 Nkx6.1 mGPDH Kir6.2 Maz
0 0.5 1.0 1.5 2.0
mRNA levels (Fold)

Figure 8

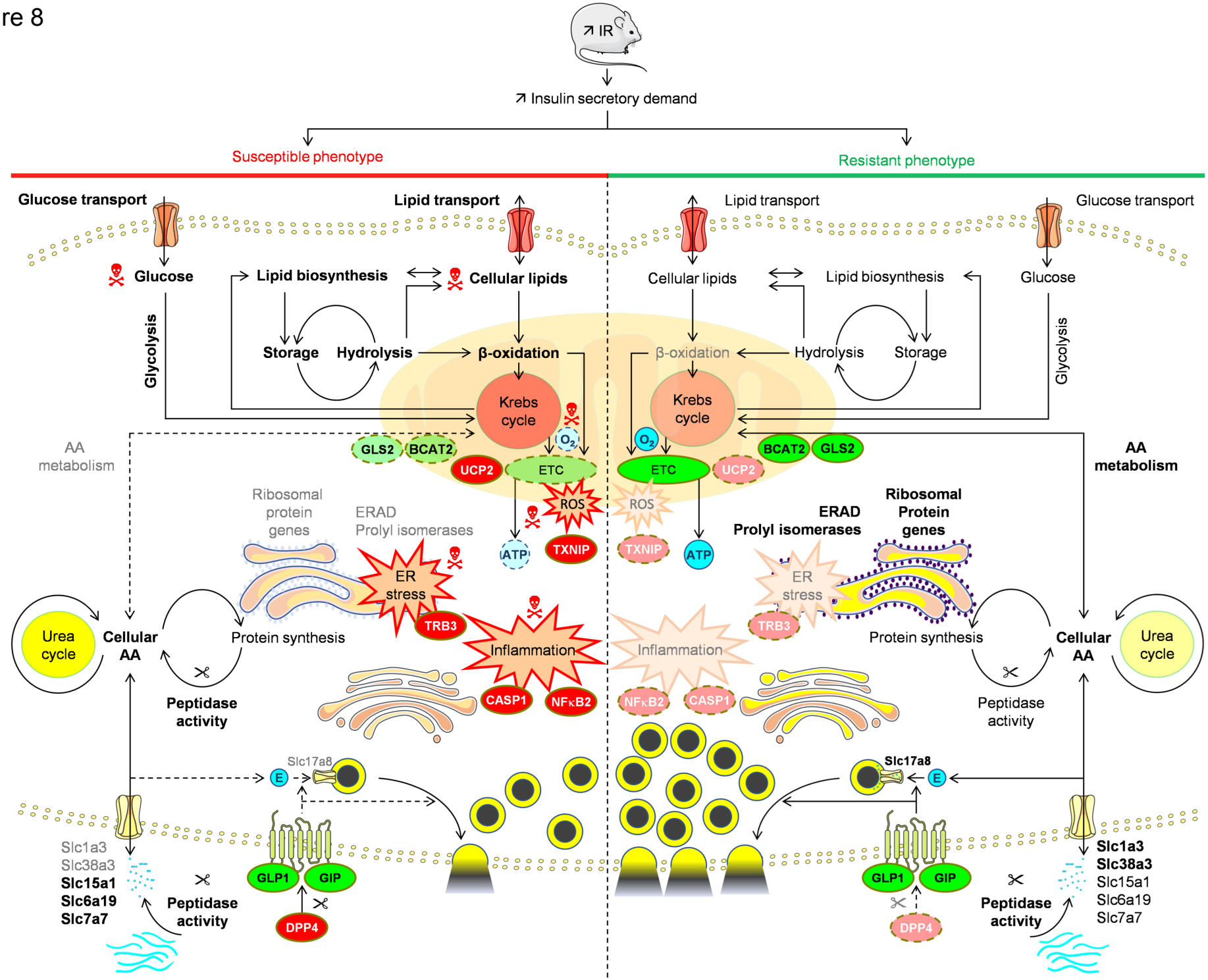
↗ IR
↗ Insulin secretory demand
Susceptible phenotype
Resistant phenotype
Glucose transport
Lipid transport
Glucose
Lipid biosynthesis
Cellular lipids
Glycolysis
Storage
Hydrolysis
β-oxidation
Krebs cycle
AA metabolism
GLS2
BCAT2
UCP2
ETC
ROS
ATP
TXNIP
Ribosomal protein genes
ERAD
Prolyl isomerases
ER stress
TRB3
Inflammation
CASP1
NFκB2
Urea cycle
Cellular AA
Protein synthesis
Peptidase activity
Slc17a8
E
Slc1a3
Slc38a3
Slc15a1
Slc6a19
Slc7a7
GLP1
GIP
DPP4

Supplementary Figure 1

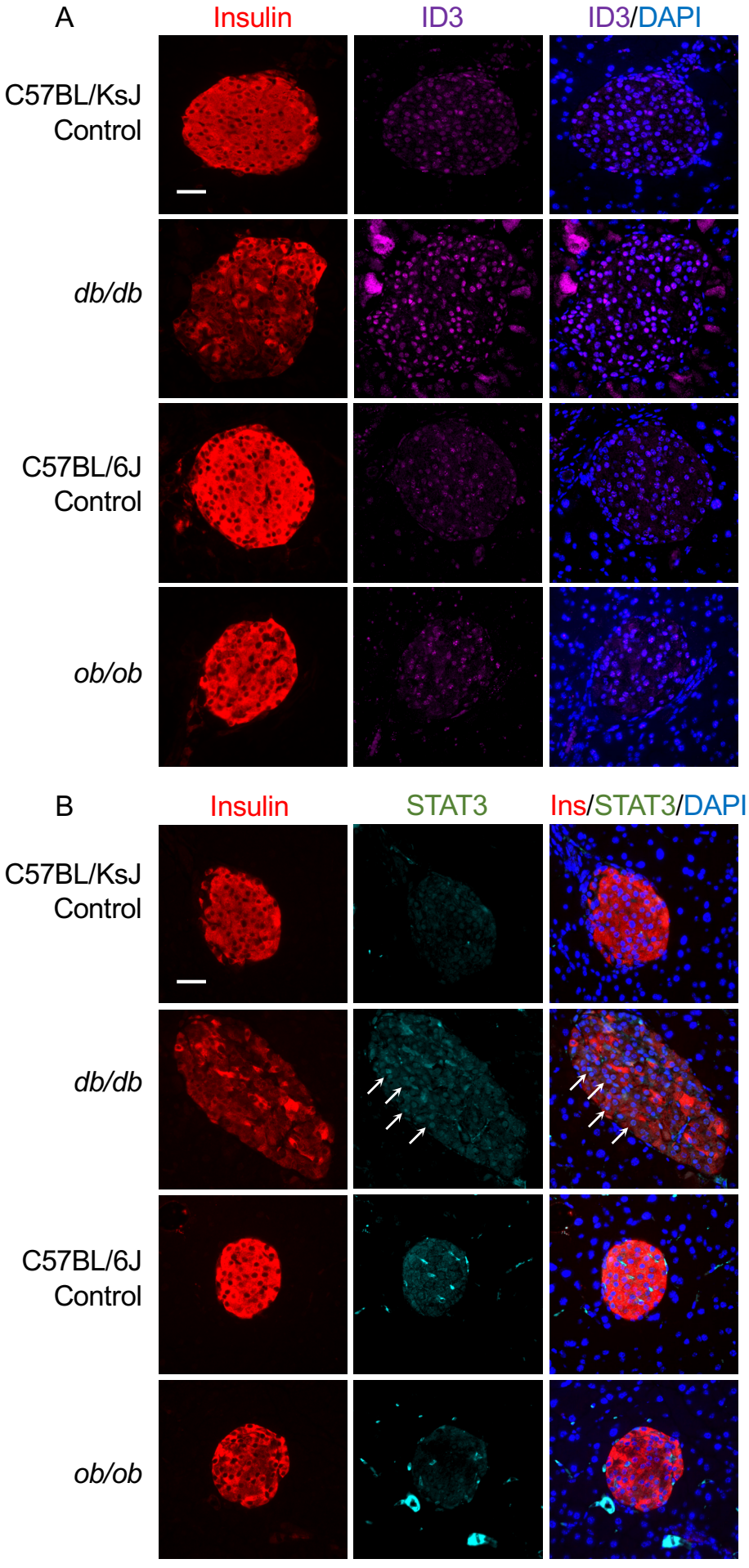

A

Supplementary Figure 2

Signaling

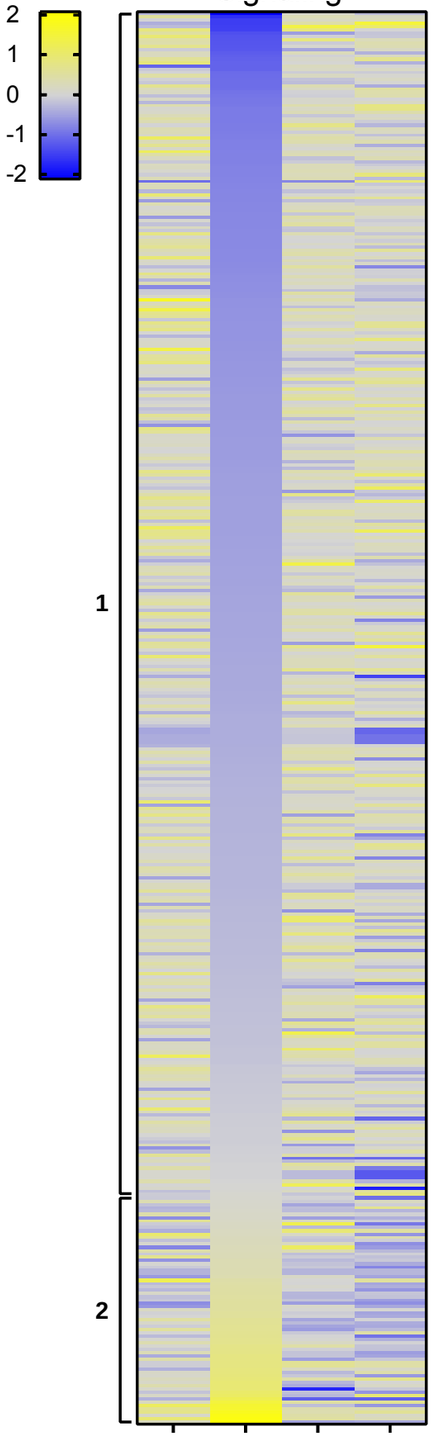

Olfactory transduction

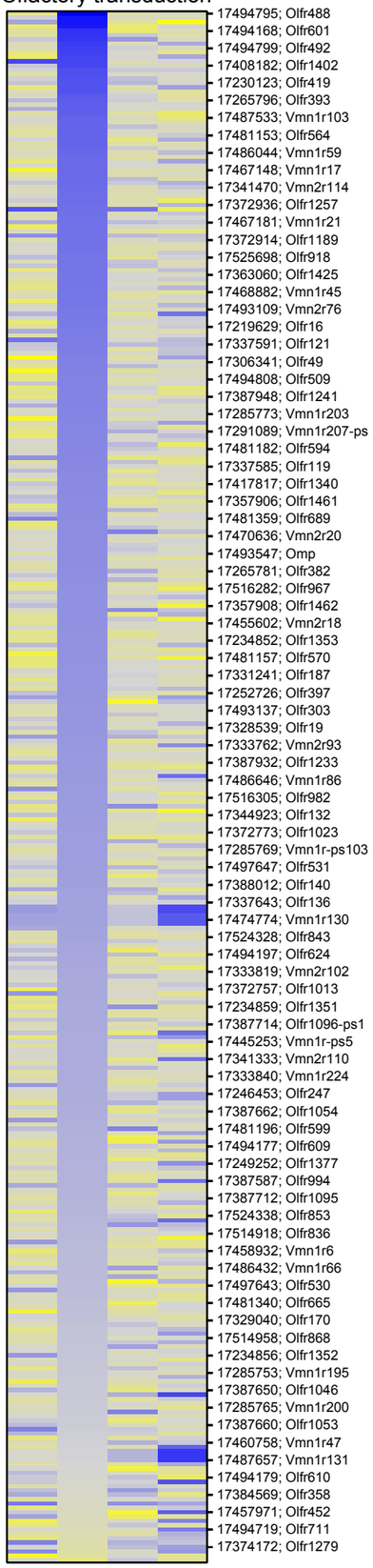

Wnt pathway

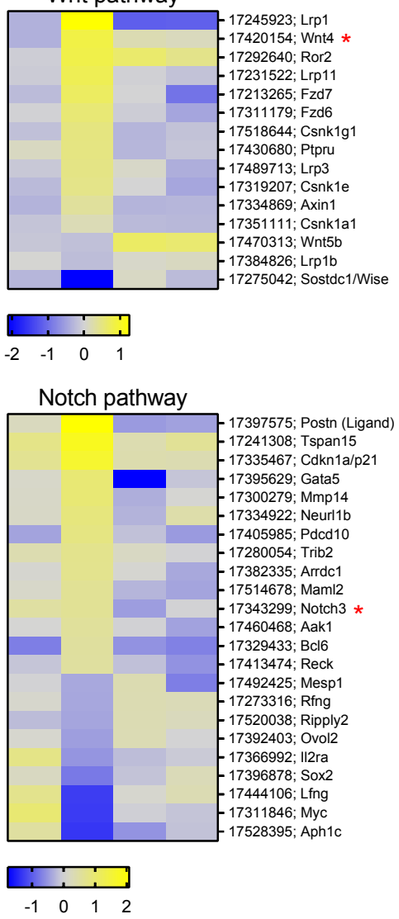

Notch pathway

BMP/TGFβ pathway

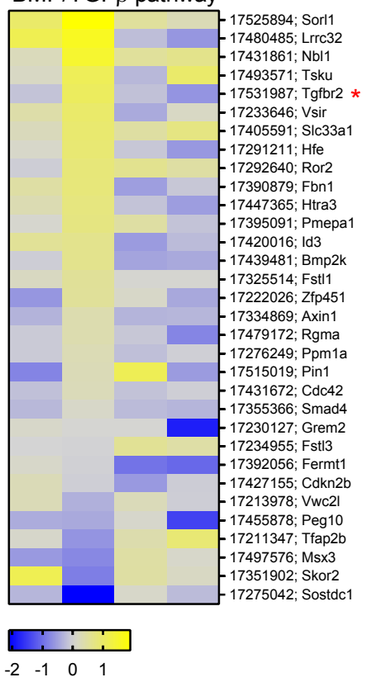

Circadian rhythm pathway

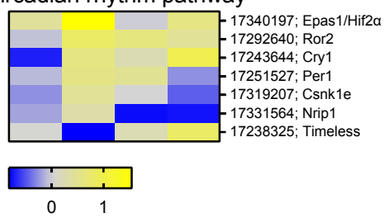

Other GPCR signaling

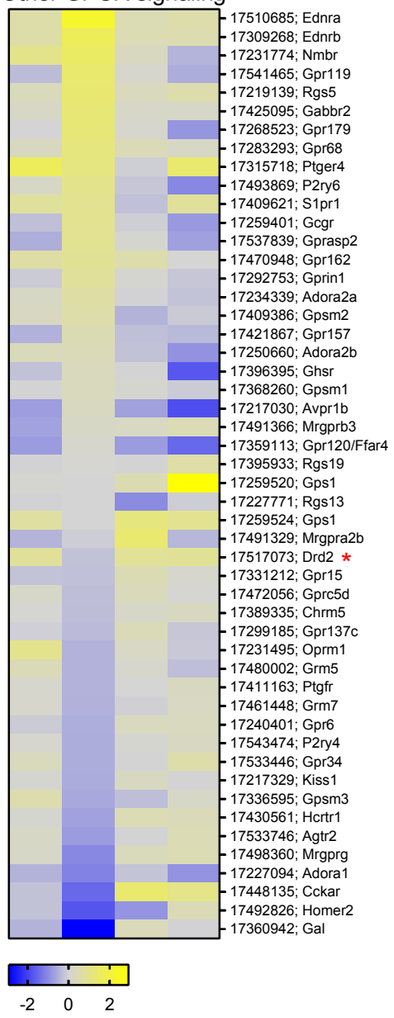

B

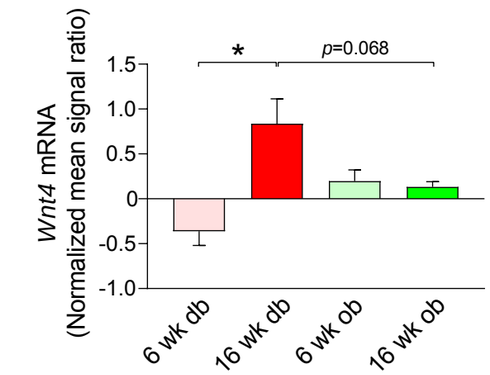

C

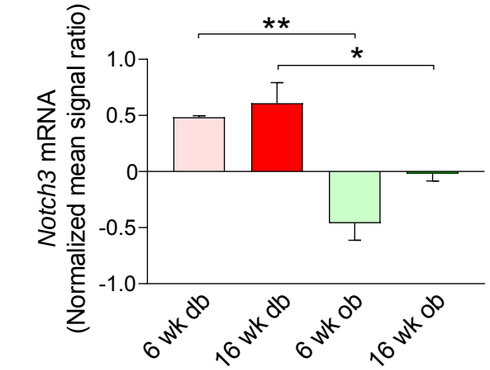

D

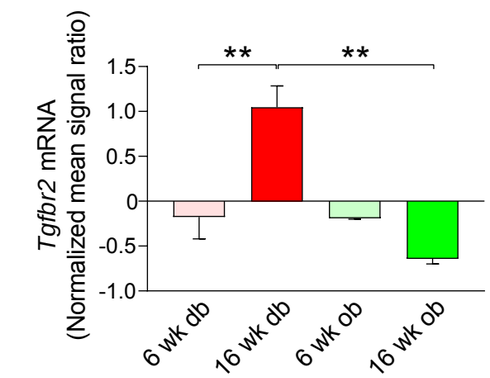

E

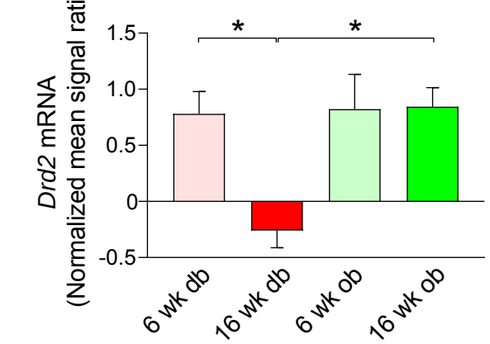

Supplementary Figure 3

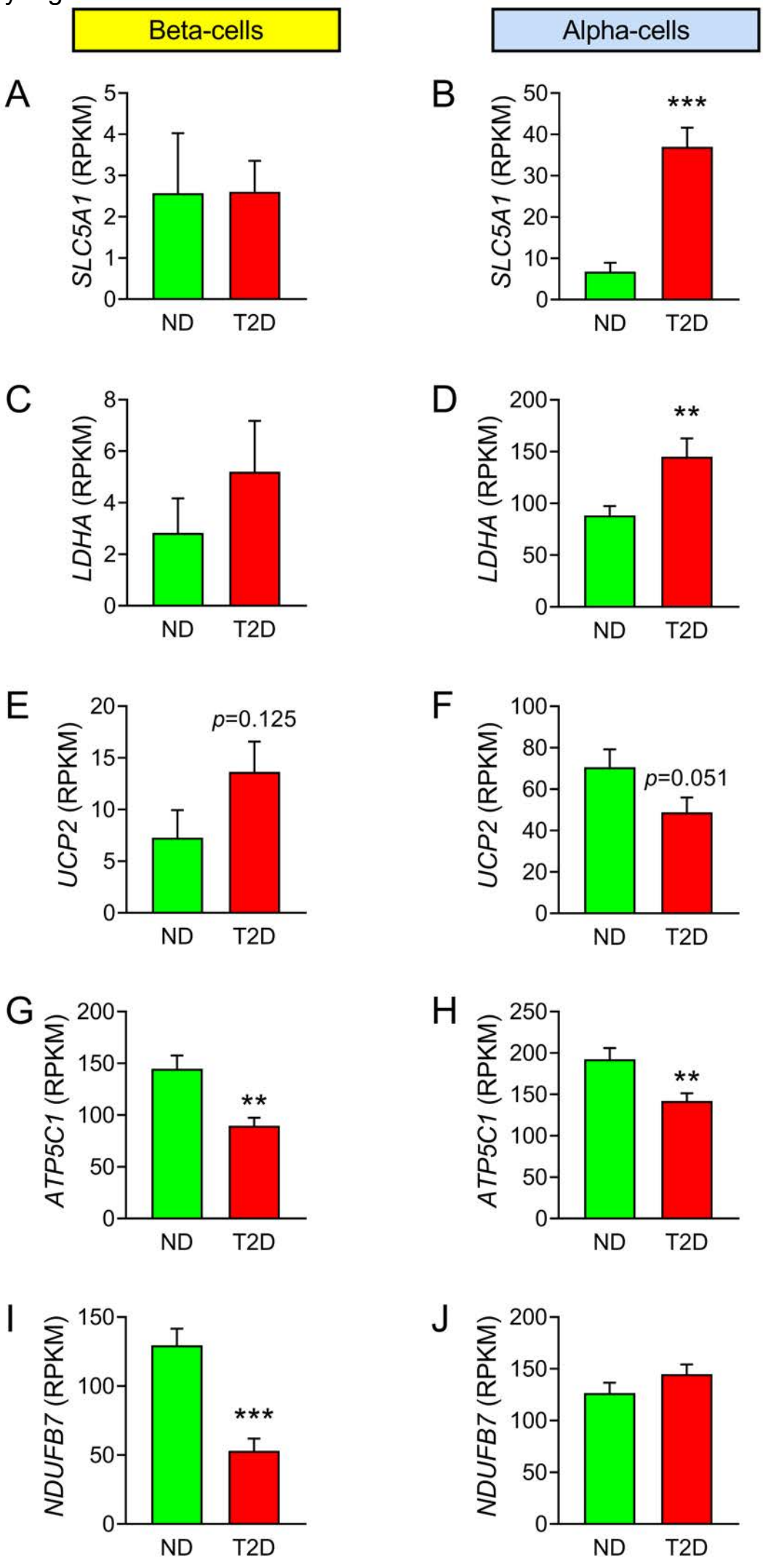

Supplementary Figure 4

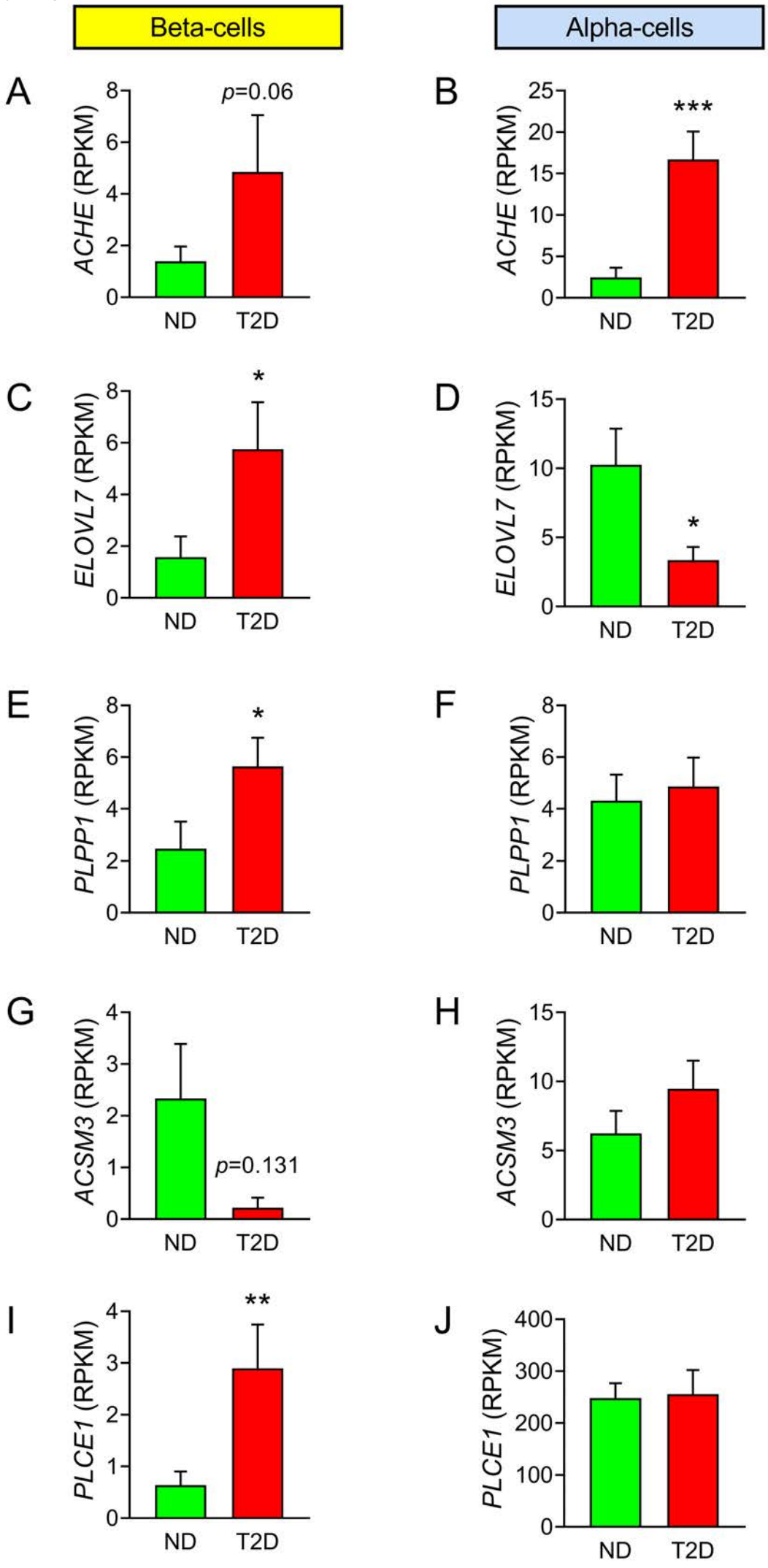

Supplementary Figure 5

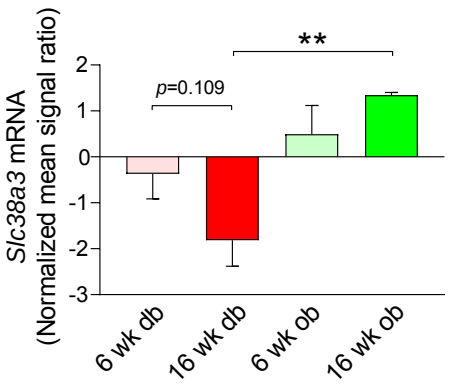

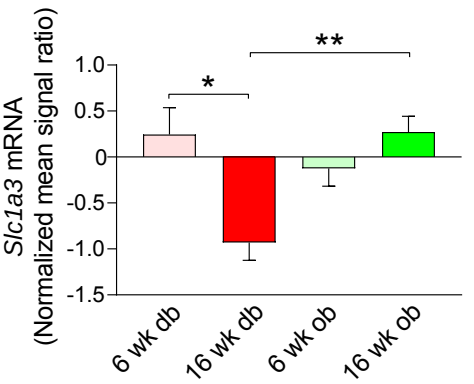

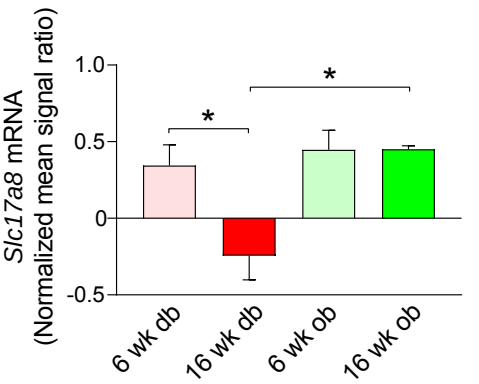

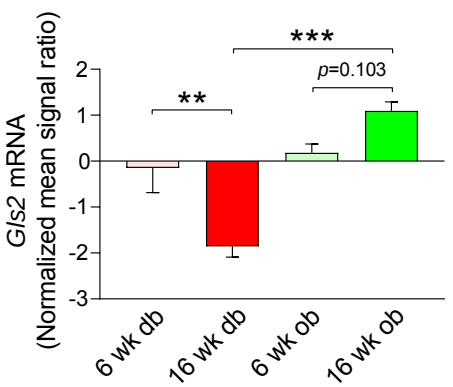

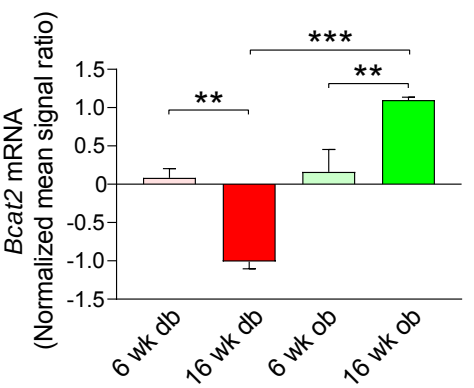

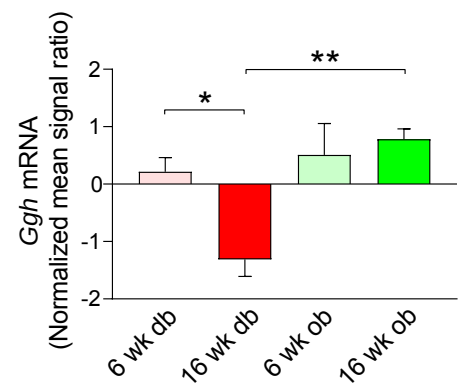

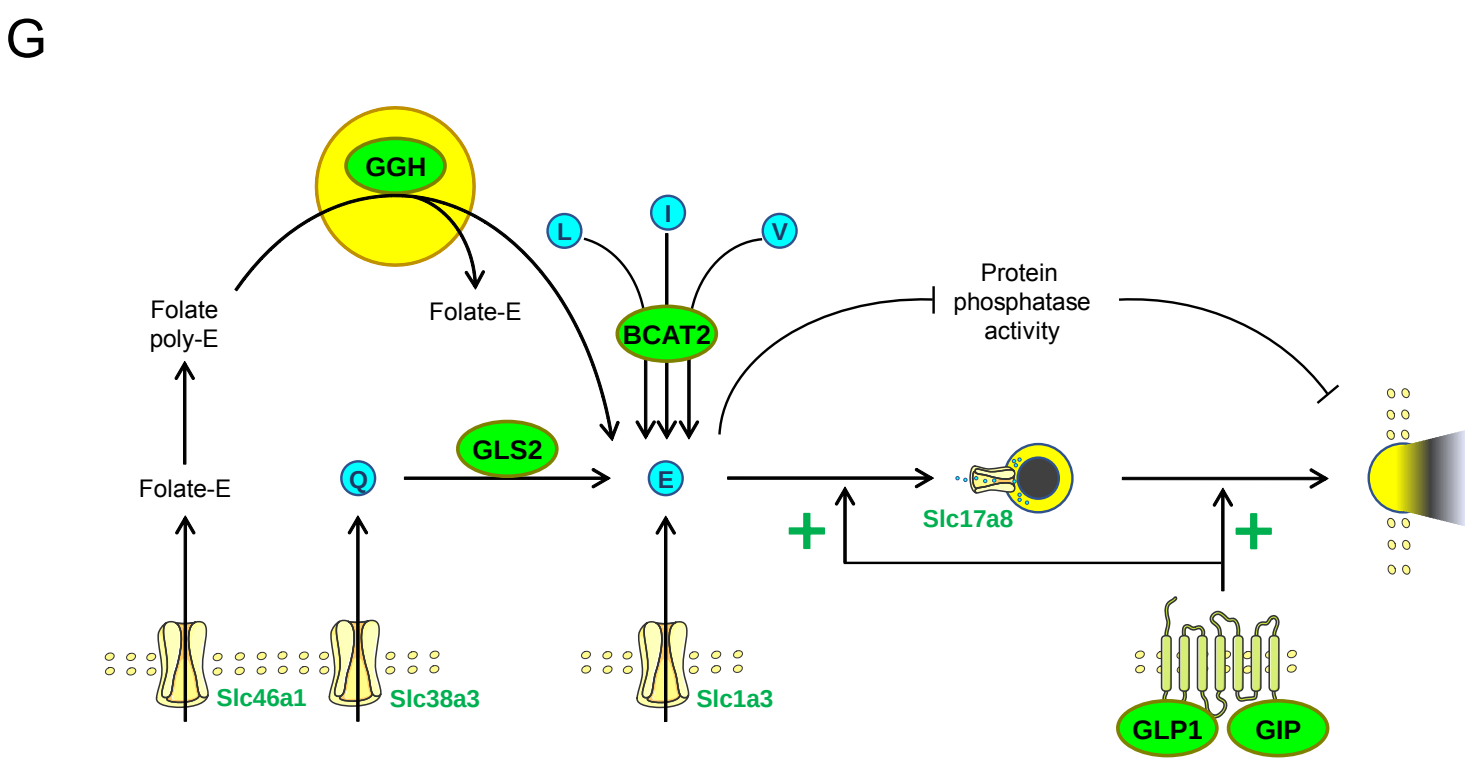

Supplementary Figure 6

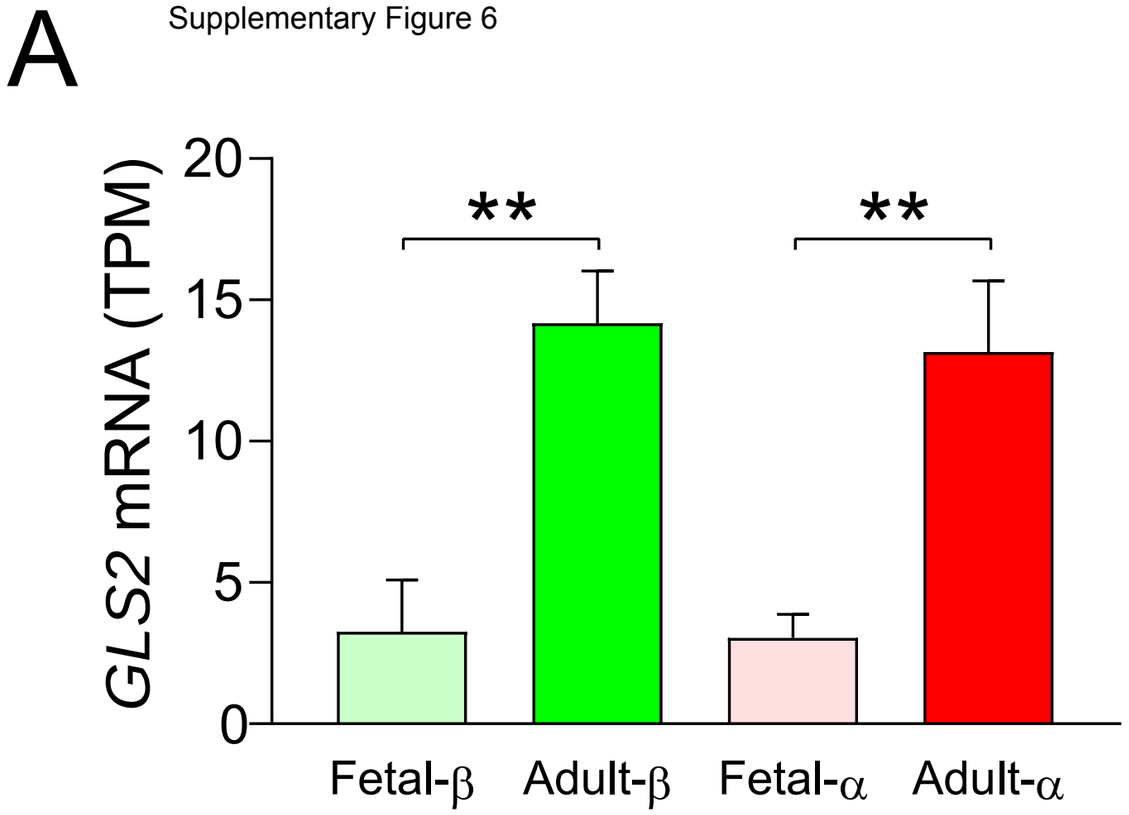

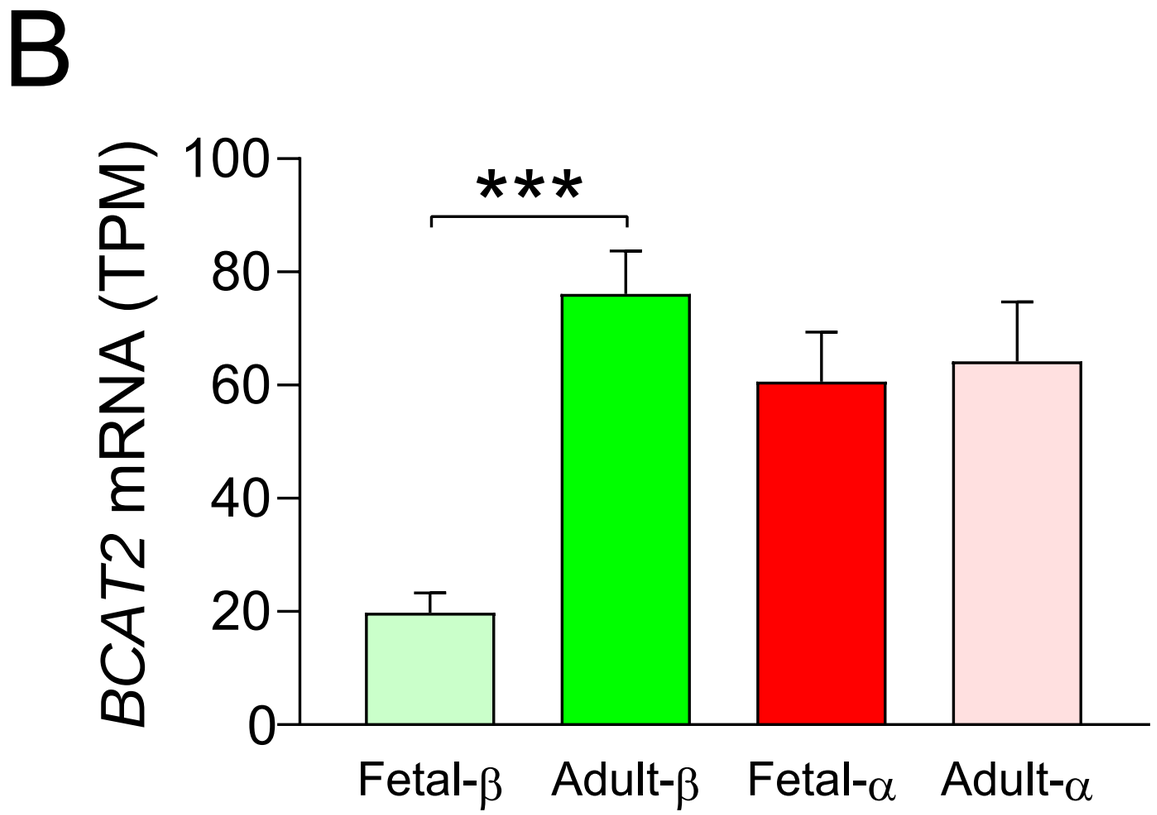

Supplementary Figure 7

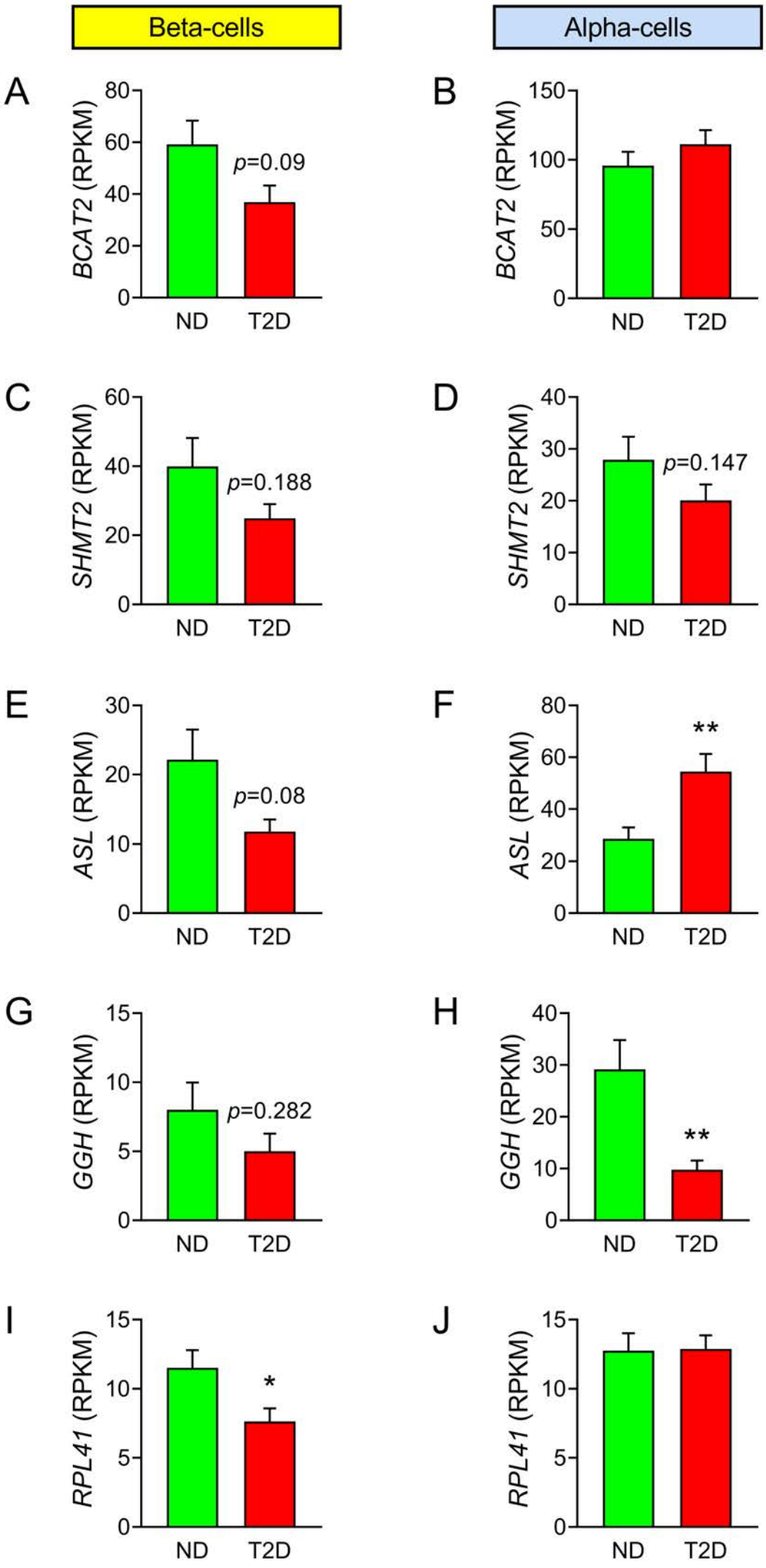

Supplementary Figure 8

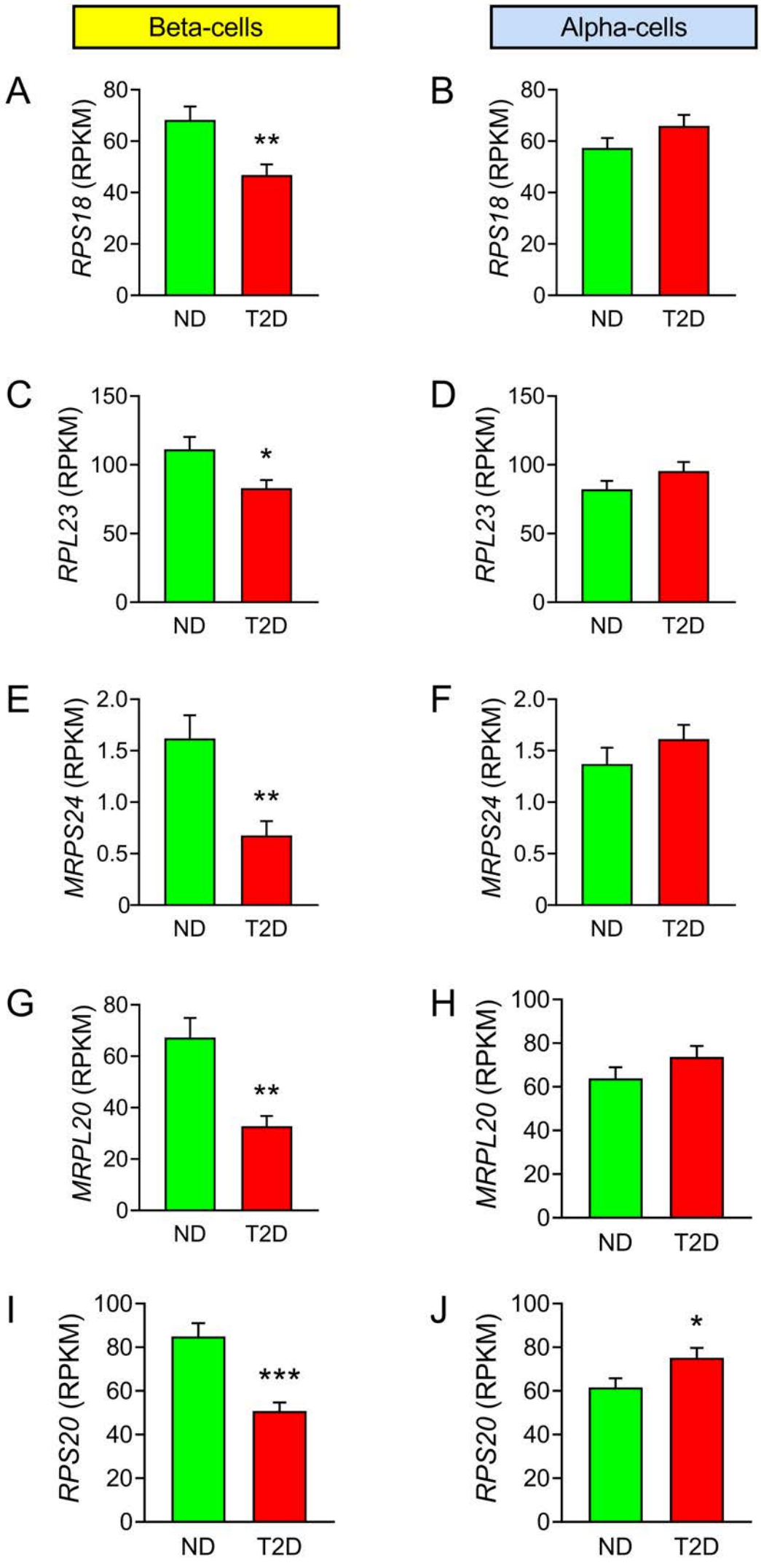

Supplementary Figure 9

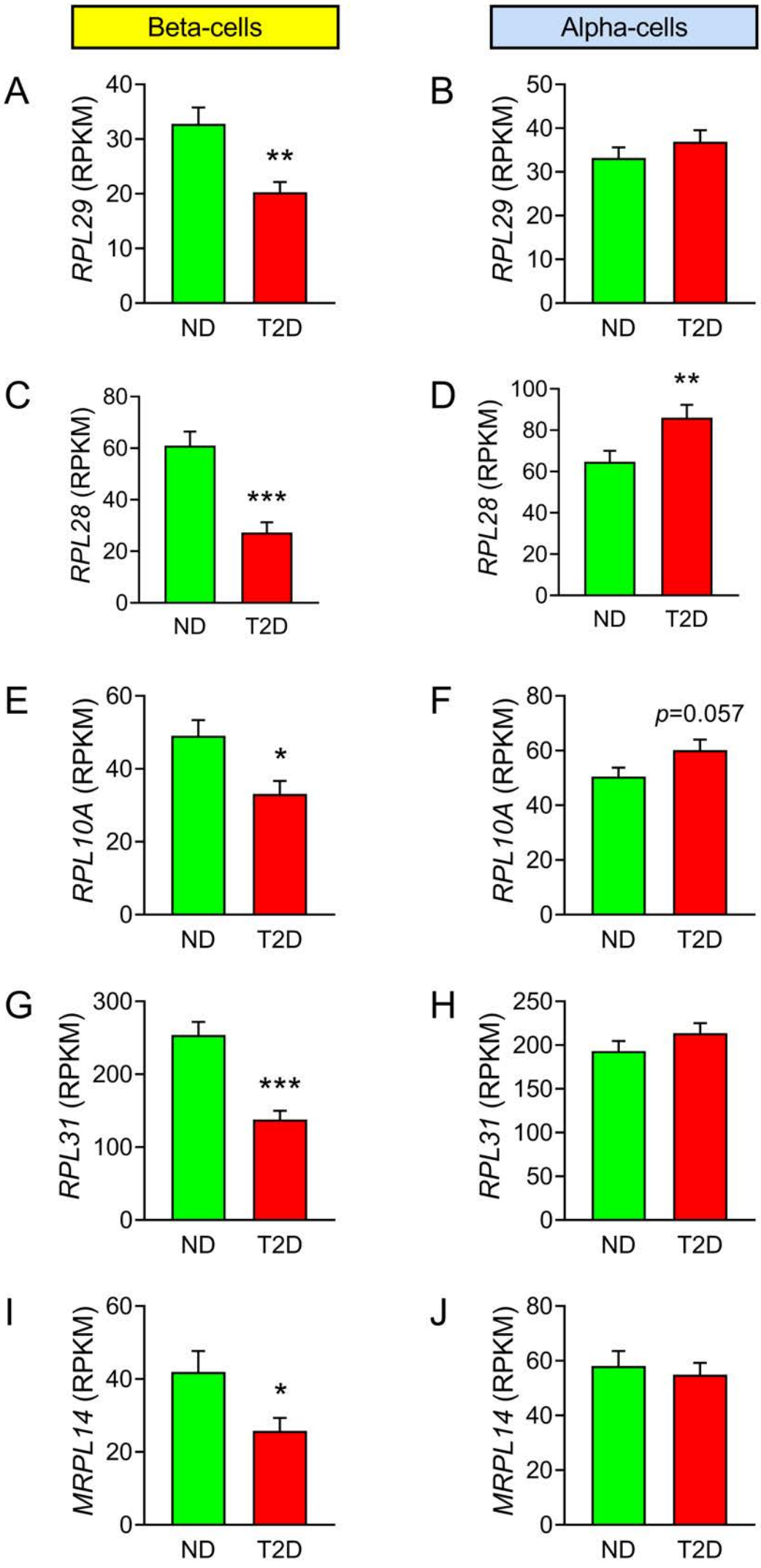

A

Suppl Figure 10

Response to stress

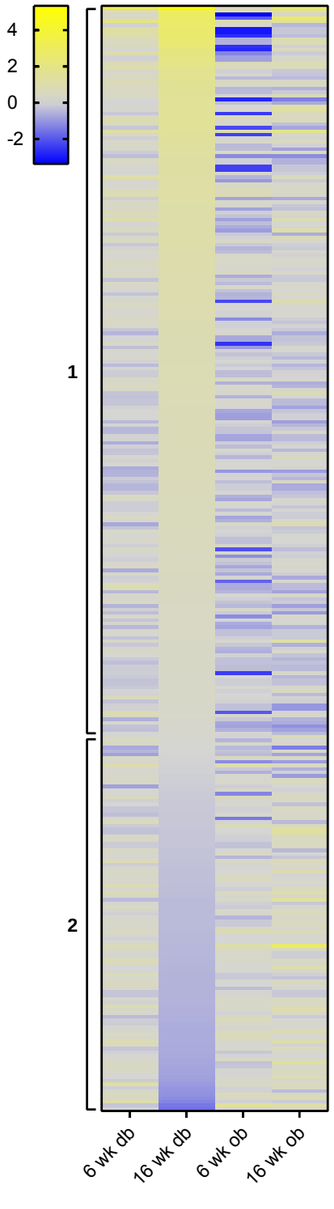

Inflammatory signaling

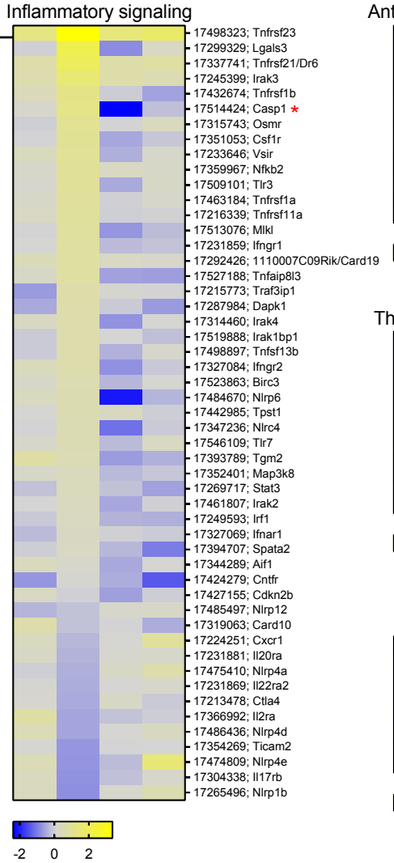

Cytokines/chemokines

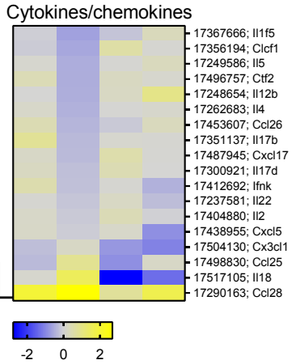

Anti-inflammatory signaling

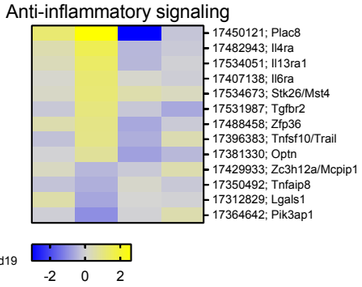

The complement pathway

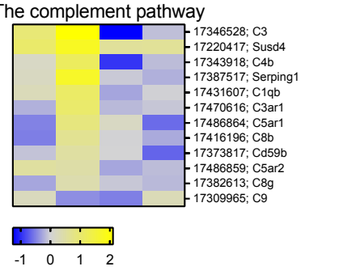

MHC

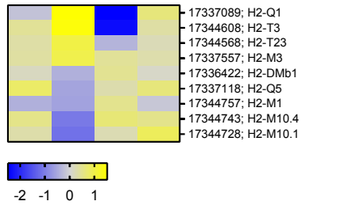

Hypoxia

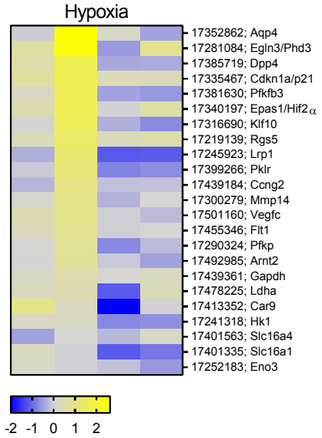

Oxidative stress

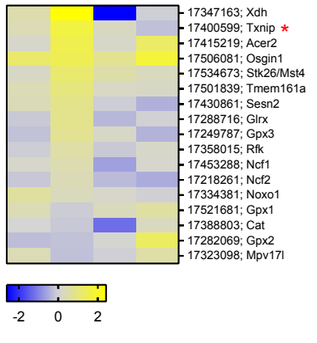

Glutathione metabolism

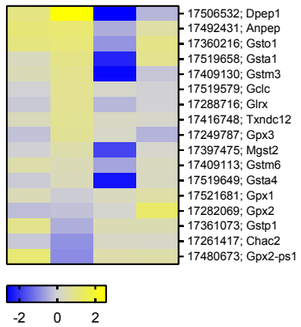

DNA damage

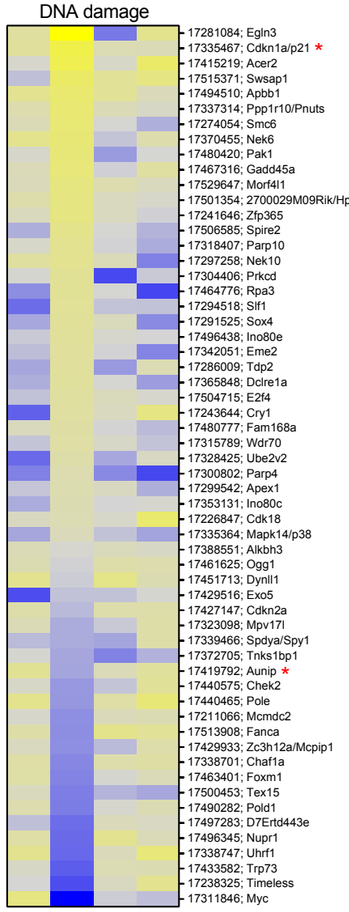

Positive regulation of cell death

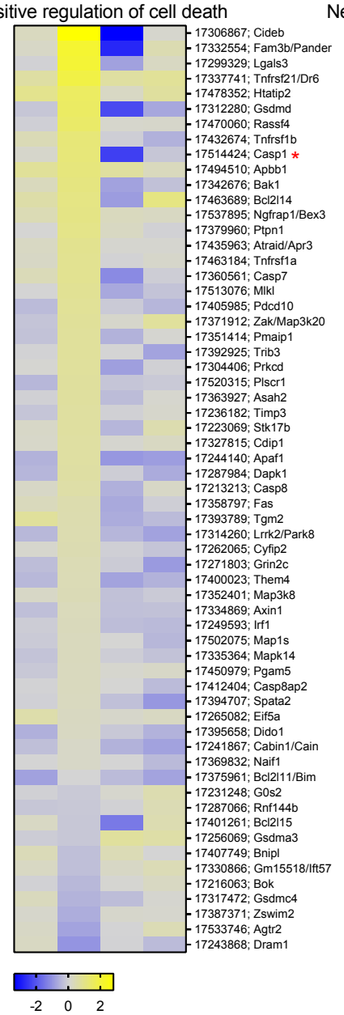

Negative regulation of cell death

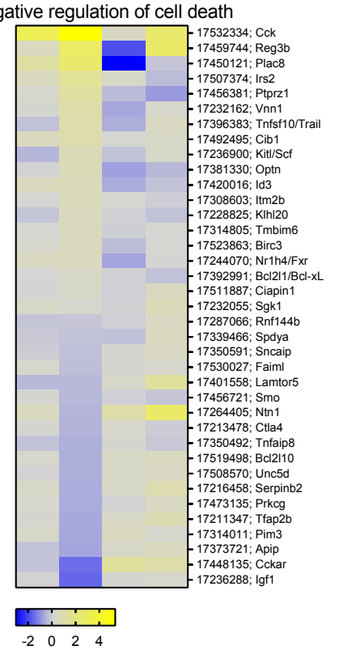

B

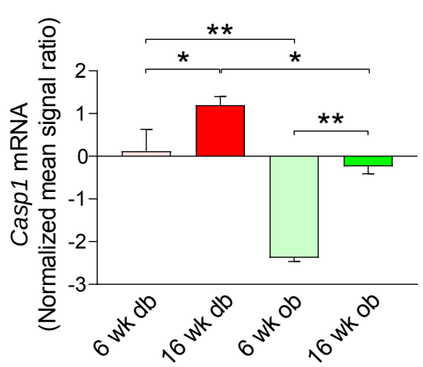

C

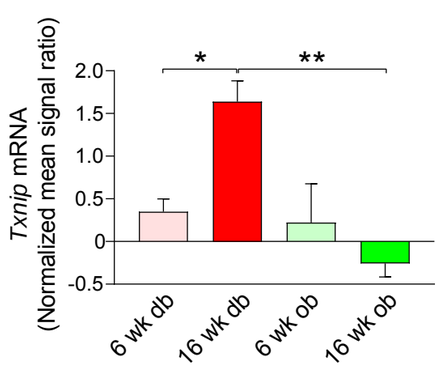

D

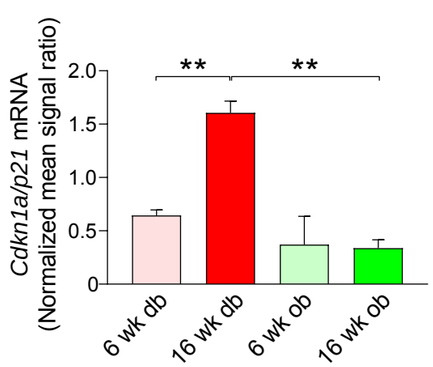

E

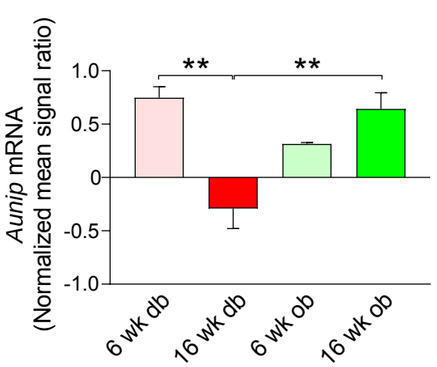

Supplementary Figure 11

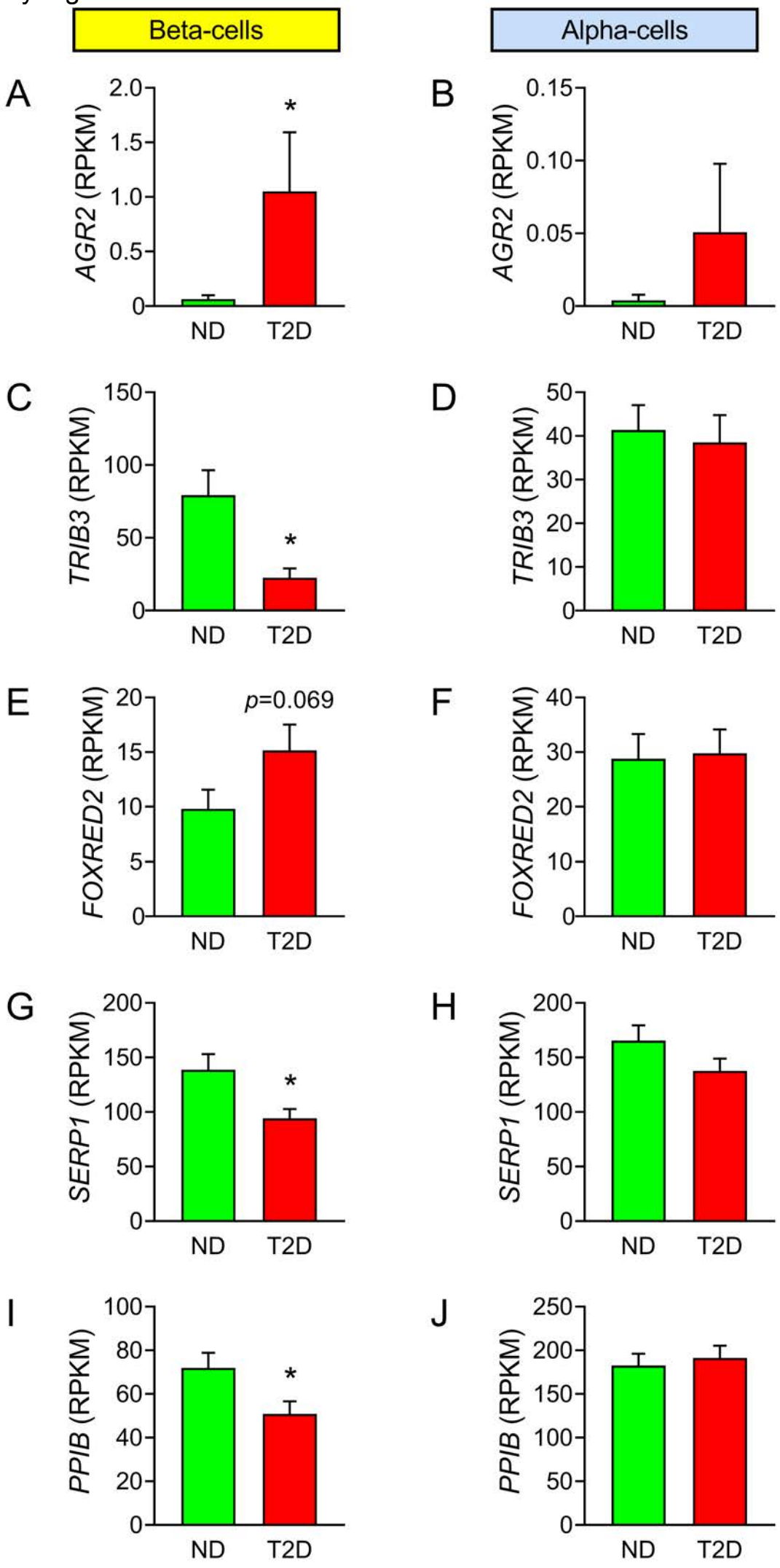

Supplementary Table 1. Real-time PCR Primer Sets.

Gene symbol	5’ Oligonucleotide	3’ Oligonucleotide
Cyclophilin A	TGTGCCAGGGTGGTGACTTTAC	TGGGAACCGTTTGTGTTTGG
Foxo4	ACTTTGAGCCAGATCCCTGAGTCAC	TAAGGACAGGCCTGGCTCCACC
Nfatc1	TGCCTTTTGCGAGCAGTATCT	CAGGCAAGGATGGGCTCATAT
Maz	CTGCCGCCATTGGACAAAC	TCCGACCACATGAAGGTGC
Sod1	ATGGGGACAATACACAAGGCTG	CAATGATGGAATGCTCTCCTGAG
Cat	ATGAAGCAGTGGAAGGAGCAGC	CTGTCAAAGTGTGCCATCTCGTC
Hmox1	CCACACAGCACTATGTAAAGCGTC	GTTCGGGAAGGTAAAAAAAGCC
Atf3	GCTGCCAAGTGTCGAAACAAG	CAGTTTTCCAATGGCTTCAGG
Xbp1	AAACAGAGTAGCAGCGCAGACTGC	GGATCTCTAAAACTAGAGGCTTGGTG
Fkbp11	ACACGCTCCACATACACTACACGG	ATGACTGCTCTTCGCTTCTCTCCC
Dnajc3	AAGCCCGTGGAAGCCATTAG	GGTCATTTTCATTGTGCTCCTGAG
Hsp90b1	AAACGGCAACACTTCGGTCAG	GCATCCATCTCTTCTCCCTCATC
Pdia4	AGTCAAGGTGGTGGTGGGAAAG	TGGGAGCAAAATAGATGGTAGGG
Hspa5	AGGACAAGAAGGAGGATGTGGG	ACCGAAGGGTCATTCCAAGTG
Mafa	CGGGAACGGTGATTGCTTAG	GGAGGTTGGGACGCAGAA
Insulin	TCTTCTACACACCCATGTCCC	GGTGCAGCACTGATCTAC
Neurod1	ACTCCAAGACCCAGAAACTGTC	ACTGGTAGGAGTAGGGATGCAC
Pdx1	CGGACATCTCCCCATACG	AAAGGGAGCTGGACGCGG
Slc2a2	CATTCTTTGGTGGGTGGC	CCTGAGTGTGTTTGGAGCG
Nkx6.1	GGACCAGAGAGAGCACGC	TTCGGGTCCAGAGGTTTG
mGPDH	AAAGACTGGAGCCCCACACTCTAC	ATCCCGTATTTCACCTCTGCTTC
Kir6.2	TCGTGTCCAAGAAAGGCAACTG	GGAAGGCAGATGAAAAGGAGTGG

Supplementary Table 2.
Pathway Enrichment Analysis
6 wk *db/db* vs 16 wk *db/db*

Pathway Name	**Database**	**Enrichment Score**	**Enrichment p-value**
Olfactory transduction	kegg	34.0811	1.58E-15
ABC transporters	kegg	5.76682	0.00312969
Fat digestion and absorption	kegg	4.74584	0.00868777
Circadian rhythm	kegg	4.4757	0.0113823
Glycosphingolipid biosynthesis - lacto and neolacto series	kegg	3.68267	0.0251558
Fc gamma R-mediated phagocytosis	kegg	3.64556	0.0261068
Glycosphingolipid biosynthesis - globo series	kegg	3.44442	0.0319232
Glutamatergic synapse	kegg	3.4295	0.0324031
Ovarian steroidogenesis	kegg	3.41083	0.0330137
Hedgehog signaling pathway	kegg	3.39459	0.0335543
Arginine and proline metabolism	kegg	3.23243	0.0394616
Glycine, serine and threonine metabolism	kegg	2.96936	0.0513363
Jak-STAT signaling pathway	kegg	2.9675	0.0514318
Biosynthesis of amino acids	kegg	2.92229	0.0538104

Supplementary Table 3.
Pathway Enrichment Analysis
16 wk *db/db* vs 16 wk *ob/ob*

Pathway Name	**Database**	**Enrichment Score**	**Enrichment p-value**
Olfactory transduction	kegg	8.14598	0.000289897
Glycerolipid metabolism	kegg	6.95917	0.000949882
Arginine and proline metabolism	kegg	6.70195	0.00122852
Dorso-ventral axis formation	kegg	6.25359	0.00192353
GnRH signaling pathway	kegg	6.24343	0.00194317
Fat digestion and absorption	kegg	6.22558	0.00197817
Glycerophospholipid metabolism	kegg	5.3305	0.00484164
Glycine, serine and threonine metabolism	kegg	5.1766	0.00564716
Glutamatergic synapse	kegg	4.93806	0.00716851
Regulation of actin cytoskeleton	kegg	4.93092	0.00721984
Long-term depression	kegg	4.86292	0.00772785
Pancreatic secretion	kegg	4.79719	0.00825293
Proteoglycans in cancer	kegg	4.77208	0.00846279
Vascular smooth muscle contraction	kegg	4.67228	0.00935092
Fc gamma R-mediated phagocytosis	kegg	4.66253	0.00944251
Oocyte meiosis	kegg	4.49795	0.0111318
Glycosaminoglycan degradation	kegg	4.45597	0.011609
Complement and coagulation cascades	kegg	4.40323	0.0122378
ABC transporters	kegg	4.07763	0.0169475
Salmonella infection	kegg	4.04886	0.0174422
Pertussis	kegg	3.90226	0.0201962
Leukocyte transendothelial migration	kegg	3.84749	0.0213333
Axon guidance	kegg	3.76561	0.0231535
Vitamin digestion and absorption	kegg	3.461	0.0313984
Gastric acid secretion	kegg	3.43118	0.0323489
Circadian entrainment	kegg	3.37009	0.0343866
Amoebiasis	kegg	3.35668	0.0348509
ECM-receptor interaction	kegg	3.3211	0.0361131
Ovarian steroidogenesis	kegg	3.2726	0.0379078
Biosynthesis of amino acids	kegg	3.13337	0.0435705
FoxO signaling pathway	kegg	3.01687	0.048954

Supplementary Table 4.
Pathway Enrichment Analysis
6 wk *ob/ob* vs 16 wk *ob/ob*

Pathway Name	**Database**	**Enrichment Score**	**Enrichment p-value**
Mineral absorption	kegg	13.1567	1.93E-06
Chemical carcinogenesis	kegg	10.9148	1.82E-05
Nitrogen metabolism	kegg	8.86086	0.000141833
Bile secretion	kegg	8.20142	0.000274265
Arginine and proline metabolism	kegg	8.17867	0.000280576
Fat digestion and absorption	kegg	7.80813	0.000406417
Arachidonic acid metabolism	kegg	7.74423	0.000433236
Metabolism of xenobiotics by cytochrome P450	kegg	7.34001	0.000649044
Glutathione metabolism	kegg	6.64121	0.00130545
2-Oxocarboxylic acid metabolism	kegg	6.44006	0.00159631
Retinol metabolism	kegg	6.37874	0.00169726
Fatty acid degradation	kegg	5.87189	0.00281754
Drug metabolism - cytochrome P450	kegg	5.86097	0.00284848
Metabolic pathways	kegg	5.38541	0.00458298
Graft-versus-host disease	kegg	5.11495	0.00600625
Allograft rejection	kegg	5.11495	0.00600625
Cardiac muscle contraction	kegg	5.07366	0.00625945
PPAR signaling pathway	kegg	4.86085	0.00774391
NOD-like receptor signaling pathway	kegg	4.60152	0.0100366
Drug metabolism - other enzymes	kegg	4.41443	0.0121014
Olfactory transduction	kegg	4.32086	0.0132884
Histidine metabolism	kegg	3.91378	0.0199649
Parkinson's disease	kegg	3.67839	0.0252636
Vitamin digestion and absorption	kegg	3.61699	0.0268634
Legionellosis	kegg	3.60723	0.027127
Autoimmune thyroid disease	kegg	3.50559	0.030029
Sulfur relay system	kegg	3.34639	0.0352111
Fc gamma R-mediated phagocytosis	kegg	3.30756	0.0366053
Type I diabetes mellitus	kegg	3.28543	0.0374245
Intestinal immune network for IgA production	kegg	3.28378	0.0374864
Biosynthesis of amino acids	kegg	3.18118	0.0415366
Caffeine metabolism	kegg	3.00337	0.0496194